The official bi-monthly publication of Bhabha Atomic Research Centre

BARC newsletter

July-August 2024

ISSN: 0976-2108

PLATINUM JUBILEE YEAR 70 Glorious Years 1954-2024

- Particle Accelerator
- Tech Spin-offs
- Quantum Technologies

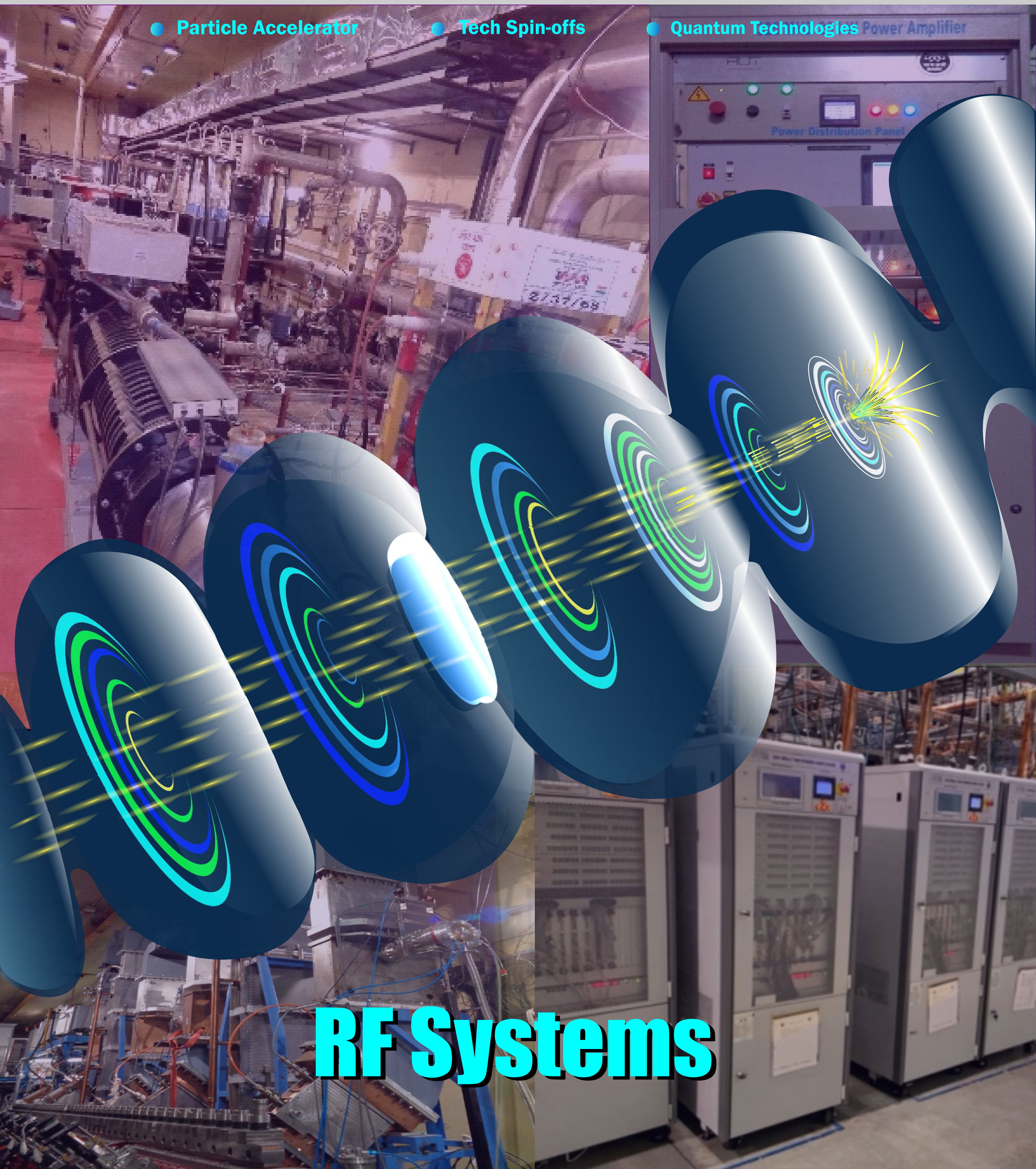

RF Systems

BARC Newsletter
July-August 2024
ISSN: 0976-2108

foreword

Radio-Frequency Technology

Radio Frequency Technology for Accelerators and Spin-offs

One of the Amritkaal targets is indigenous development of GeV range, high current proton accelerator. Globally, such accelerators employ high power RF sources, along with associated RF control and instrumentation systems, to set-up and stabilize oscillating electromagnetic fields in resonant cavities used for acceleration. Accelerator Control Division (ACnD) is developing Radio Frequency (RF) Systems for different types of accelerators.

Meeting the challenges in RF power systems catering to high power demands, both peak and average, necessitates focus on high efficiency. Development of indigenous, robust, reliable, and high efficiency solid-state amplifiers (SSA) by ACnD is an important milestone achieved, which will play a major role in self-reliance in this area. Significant efforts are being made by the division to meet future requirements using the latest technology.

Development of an integrated RF control solution (IRFCS), comprising of low-level RF control system, resonance control System, RF phase distribution system, and RF protection & interlock system is necessary for successful, smooth and reliable operation of high intensity proton accelerator. ACnD has developed and deployed IRFCS for a variety of accelerators associated with the Indian accelerator program. Starting from primarily analog based systems, the present day RF control and instrumentation systems take advantages of the advancement in digital technology. This has enabled achieving better speed of response with the flexibility of implementing the sophisticated algorithms and features with better accuracy and precision.

Apart from developing RF systems for variety of accelerators associated with the Indian accelerator program, ACnD has also been developing and delivering RF systems to Fermi National Accelerator Laboratory, USA.

Application of machine learning for optimal and adaptive control of accelerator for efficient operation is also becoming feasible. Use of a real time emulator of high-power RF system, incorporating a cavity, for the development of RF control system, is also becoming a reality.

Spin-off of this work on accelerator RF has been very useful in applications like RF-plasma based disinfection and quantum computing initiative.

This thematic issue of BARC Newsletter is a collection of articles on RF systems for accelerators and other applications. I sincerely hope that this newsletter will provide an insight into the expertise and experience available within ACnD for utilizing it for future accelerator development plans.

As the thematic issue of BARC Newsletter on Radio Frequency Technology for Accelerators and Spin-offs is being published for the first time, I take this opportunity to thank all the authors and associate editors for their time and efforts in preparing this issue.

U. D. Malshe
Director, Multidisciplinary Research Group
Bhabha Atomic Research Centre

This page intentionally left blank

Self-reliance in critical RF Systems *for* Accelerators and Spin-offs

It provides us immense pleasure to bring out this thematic issue of BARC Newsletter on important developments at Accelerator Control Division (ACnD) associated with radio frequency (RF) technology. The Division has been contributing towards RF systems for accelerators, plasma-based applications, quantum computing initiative etc.

This theme-based newsletter issue is a compendium of fifteen articles. Six articles explain indigenous development of RF systems for accelerators at BARC. Of these, one article provides a quick glance on very critical and challenging MW level solid state RF systems envisaged in the incoming decade. Two articles are dedicated to on-going developments in the cavity emulator to serve as a test bed for RF control system, and application of artificial intelligence in RF systems of accelerators, respectively.

Four articles pen the developments carried out under international collaborations, which are also very useful for upcoming Indian accelerators.

The remaining five articles present spin-offs. Two of these articles elaborate on developmental aspects of the RF systems for pulse positron spectrometer, and hollow cathode atmospheric pressure cold plasma device, respectively. Remaining three articles are devoted to superconducting qubit-based quantum computing initiative.

We sincerely hope that this issue of newsletter will enrich the scientific community at large towards development of state-of-the-art RF systems developed indigenously in line with the broader spirit of 'Atma Nirbhar Bharat'.

We take this opportunity to acknowledge all the authors for their valuable contributions. We are thankful to Director, Multidisciplinary Research Group, BARC and Director, BARC for their constant support and guidance. We sincerely appreciate and acknowledge the hard work and efforts of the newsletter editorial team of SIRD for the composition of the articles, creative and artistic work in designing the cover page, and for their dedicated efforts in bringing out this BARC Newsletter issue in a time-bound manner.

Dr. Manjiri Pande
Head, RFSS, ACnD

M. Y. Dixit
ACSS, ACnD

Dr. Gopal Joshi
Head, ACnD

9

RF System for
Positron Annihilation Spectrometer
69

53

CONTENTS

FORTHCOMING ISSUE

- Fluorescence Up-Conversion Technique in Investigating Mechanistic & Kinetic Details of Ultrafast Photoinduced Processes
- Hot Carriers in Halide Perovskites and how to follow them with Femtosecond Transient Absorption Spectroscopy?
- 2D Infrared Spectroscopy: An Innovative Technique for Probing Molecular Dynamics in Ultrafast Time Scale
- Interface-Selective Nonlinear Spectroscopy at Soft Interfaces using Ultrafast Laser
- Femtosecond Laser-Induced Breakdown Spectroscopy: Advancing Analysis of Complex Materials

This page intentionally left blank

BARC Q&A

Tête-à-tête with Dr. Sumit Som

Director
Variable Energy Cyclotron Centre (VECC), Kolkata

Dr. Manjiri Pande:* **DAE has been launching accelerator programs in a very big way. Your view on Indian ADS program, DAE accelerator program and its role in progress of India**

Dr. Sumit Som: The Indian accelerator driven sub critical reactor system (ADS) program is an ambitious and very useful program of DAE. ADS has attracted worldwide attention for its superior safety feature, incineration of minor actinides and transmutation of long lived fission products. From Indian perspective, it has additional and very important dimension of nuclear energy generation utilizing thorium as fuel. The major systems of ADS are sub critical core, spallation target and power accelerator.

DAE has made significant progress in accelerators and related technologies. Among the others, recently, low energy high intensity proton accelerator (LEHIPA) has accelerated proton beam up to 20 MeV energy.

Under in-kind international collaborations, DAE has delivered and deployed many indigenous accelerator technologies. Under Indian Institutes and Fermilab Collaboration (IIFC), for Proton Improvement Plan-II Injector Test facility (PIP2IT), BARC has delivered nine 325 MHz solid state RF amplifiers, magnets accelerator and RRCAT has delivered 650 MHz solid state RF amplifiers and high beta elliptical cavities. Along with this, VECC has delivered two numbers of 650MHz low beta (LB650) single-cell SRF cavities that have achieved the high accelerating gradient.

Under Facility for Antiproton and Ion Research (FAIR) project in Germany, DST & DAE jointly have delivered ultra-high vacuum (UHV) chambers, power converters via Indian industries and development of high energy detectors is in progress under the leadership of VECC. This definitely establishes the competence of DAE laboratories and local industries in accelerator field. These accomplishments have generated a lot of confidence on the proposed energy frontier future accelerators.

The journey of achieving 1GeV accelerator is going to give rise to a lot of exciting spin-offs in the uses of low and medium energy beam from intermediate accelerators. This will immensely help and open the doors of wide opportunities for Indian Micro, Small and Medium Enterprises (MSME) or Small and Medium Enterprises (SME) in both domestic and international markets.

Dr. Manjiri Pande: **Accelerators are increasingly being used for medical and societal applications. How do you envisage indigenous accelerators making significant contributions in these fields?**

Dr. Sumit Som: India is a populous country. It is envisaged that the percentage of cancer inflicted population will increase multi-fold in near future.

As per information published in Indian Journal of Med Research (IJMR) in its Oct-Nov 2022, issue (DOI: 10.4103/ijmr.ijmr_1821_22), the estimated number of cases of cancer in India for the year 2022 was found to be 14,61,427 (approximate rate:100.4 per 100,000). The incidence of cancer cases is estimated to increase by 12.8 per cent in 2025 as compared to 2020.

DAE is developing a number of indigenous medical cyclotrons and electron accelerators. These accelerators, especially medical cyclotrons will be critically useful, especially in cancer scenario. These will be immensely beneficial in every aspect of the cancer scenario i.e. starting from its early detection and diagnostics to cure by generation of radio isotopes for treatment. This will be greatly valuable in increasing the quality of life and life expectancy of cancer afflicted patients.

...The journey of achieving 1GeV accelerator will give rise to exciting spin-offs in the use of low and medium energy beam from intermediate accelerators. This will immensely help and also open new and prospective avenues for Indian industry ...

Dr. Sumit Som

Dr. Manjiri Pande: **How participation of Indian Micro, Small and Medium Enterprises (MSME) or small and medium enterprises (SME) can be increased substantially in accelerator technology?**

Dr. Sumit Som: The Indian MSME and SME are already contributing in the accelerator sector. Their footprint in accelerator domain can be increased substantially in quality and quantity. Their participation will improve significantly by handholding between the accelerator scientists, technologists, engineers and their industry counterparts. This will assist in transferring indigenously developed technologies into deployable engineering products. MSME and SME should join hands with accelerator community in participating in flagship initiative of Government of India like public private partnership (PPP), Atal Innovation Mission (AIM) etc. to promote the culture of innovation and entrepreneurship in India. This will further establish the requisite infrastructure and skilled manpower or human resources in the country. All these amalgamated efforts may converge in opening the doors of international accelerator market for these SME and MSMEs. This would lead to extra drive towards 'Make in India', under 'Atmanirbhar Bharat' initiative and substantial import substitute.

Dr. Manjiri Pande: **Today, Artificial Intelligence (AI) is a buzz word. AI is making inroads in every field. What will be the role and usefulness of AI in accelerators and in related technology?**

Dr. Sumit Som: Particle accelerator is a complex machine. It's a combination of a variety of subsystems and components related to different technological domains. An accelerator has to operate cohesively with a huge number of sensors and considerable number of subsystems to deliver the required beam. An artificial intelligence (AI) based algorithm(s) can aid to monitor the performance of accelerator, to perform automated beam tuning of the machine, to detect the operational concerns or issues, to identify the faults w.r.t. specific subsystem etc. This would enhance the reliability of particle accelerator and hence availability of the accelerated beam. The AI approach can further be configured to analyse the available operational data that can predict most probable failure scenarios. This will help the scientists in improvisation and enhancement in accelerator operation and also can assist in advance planning and maintenance of the accelerator inventory.

Dr. Manjiri Pande: **RF systems play a very significant part in accelerators as well in other fields and many other scientific applications. What are the futuristic options for RF Technology?**

Dr. Sumit Som: Radio-frequency (RF) systems are critical and integral part of linear and circular accelerators and deliver the power to attain and change the energy of a charged particle beam. RF Accelerators are large users of energy, mostly RF power.

In accelerator, the RF system is the key element that provides RF power for generation of electric field for beam acceleration. Integrated RF system drives the major part of the accelerator performance. Many state-of-the-art technologies are used in design and development of the RF systems, such as vacuum science, high-voltage / high current technology, surface physics, advanced materials, high speed controls, protections, advanced mechanical fabrication and processing etc.

In addition to particle accelerators, RF systems or technologies are used in broadcasting, communications, wireless power, medicine etc. Very high frequency (VHF) and ultra-high frequency (UHF) are used in the communication systems by military and industry sectors.

VHF frequencies are able to penetrate walls and •••

...AI based algorithm(s) can aid the accelerator development community in a variety of functions, including monitoring the performance of accelerator, performing automated beam tuning and several others thereby contributing to enhancing the reliability of particle accelerator as well as availability of the accelerated beam...

Dr. Sumit Som

other structures. It can also enter deep into the human body without causing any damage and hence, medical devices use VHF for deep penetration in human body. UHF penetrates at further deeper level. Medical institutions or medical fraternity use these properties to monitor internal organs and their respectively functions in a patient. In remote surgery, higher-frequency mm - wave based technology can be used by enabling precision operations with ultra-reliable data connections and with extremely low latency (lag).

Smart RF-systems comprising of RF transmitters, receivers, and transceivers send / receive data over the air. These are used in satellite communication, in defence for securing critical communications, to provide reliable Wi-Fi on trains and for high-performance private wireless networks.

Very high reliable data connectivity can be ensured using mm - wave frequencies in driverless car technology, intelligent traffic light controls and traffic-management etc. The high end RF / MW technologies are being developed for quantum technologies.

To summarize, RF technology is used in a variety of important fields and hence, will always remain in high demand and has a very promising future. Globally, it will experience significant growth and innovation in the coming years.

Dr. Manjiri Pande: **Globally, food security is an important topic. How RF systems can participate in such a prominent domain?**

Dr. Sumit Som: Food security, as defined by the United Nations' Committee on world food security, means that all people, at all times, have physical, social, and economic access to sufficient, safe, and nutritious food that meets their food preferences and dietary needs for an active and healthy life.

Food security is an important global need. Safe and nutritious food can be achieved by customizing RF as an innovative technology, in numerous food processing and preservation purposes like inactivation of pathogens, pasteurization, fungi inactivation, and disinfestation etc. RF drying technology for food and agricultural products have characteristics like fast, steady, and volumetric heating, high energy efficiency and moisture reduction. However, the RF drying as a single stage method may be insufficient or can have drawbacks. Utilizing multi-stage drying approach in conjunction with RF technology can effectively address the limitations of one-stage strategy using diligently the combination of other drying methods.

DAE has designed and developed a variety of matured indigenous RF technologies, which can be customized for RF drying of food and agricultural produce for our domestic purposes. This will enhance the quality and storage life of these items and thereby will contribute to food security.

Dr. Manjiri Pande: **World is transitioning towards Green Energy. How the upcoming technology initiative of 'Radio Frequency Energy Harvesting' can contribute towards this?**

Dr. Sumit Som: In today's modern era, most miniature electronic devices are being used in automation, medical treatment, environmental monitoring etc. In these applications, electronic devices are conventionally battery-powered to ensure their operation. But, as power source, these batteries impose serious limitations because of their size, lifespan, bio-compatibility etc. Consequently, electronic device gets affected in their weight, portability, miniaturization, lifetime etc.

Additionally, limited battery life and need for regular replacement greatly limits the performance and reduce the quality of service. In some special implanted electronic devices, the replacement and maintenance cost of the battery is very expensive.

In recent years in particular, the disposal of

...RF technologies can play a crucial role in addressing food security. The bouquet of DAE RF technologies can be customized to meet the challenges faced in food preservation chain, particularly for maintaining high quality and safe post-harvest storage...

Dr. Sumit Som

battery waste has become a significant environment issue. Battery waste is primarily disposed off in landfills that contribute to land pollution and the contamination of underground water due to the harmful chemical contents of the battery. This problem is more aggravated with Lithium batteries, as they are considered hazardous and their safe disposal poses a huge challenge.

Therefore, moving towards green energy, it is meaningful and very natural to develop the low-cost and pollution-free energy resource to replace the battery.

Our mother earth's natural environment, have abundant energy resources in the form of solar energy, motion/vibration energy, thermal energy, wind energy, tidal energy and man-made RF energy.

Globally, huge interest is generated in energy-harvesting technologies that use ambient power sources such as heat, vibration, and electromagnetic waves. Radio frequency energy harvesting (RF-EH) is a promising technology that operates using electromagnetic waves. This advanced RF-EH technology proposes the supply of wireless power to battery-free devices, thus making it a potential and strong alternative energy source for future applications.

In addition to the dynamic energy recharging of wireless devices and a wide range of environmentally friendly energy source options, the RF-EH technology is advantageous in facilitating various applications that require quality of service.

The proposed RF-EH technology possesses numerous distinctive advantages such as, it can function in any location with a strong radio frequency signal, including areas with no sunlight or indoor spaces with specialized transmitters. As RF energy is not much influenced by weather and location, it can be effectively used by RF-EH system. It is an alternative method to reduce the cost of regular maintenance in terms of device improvement. It will be cheaper and eco-friendly. Thus, RF energy harvesting proposes a very worthwhile and workable substitute that circumvents some of the environmental issues or limitations.

Dr. Manjiri Pande: **Nationally and internationally, large accelerator programs with latest science and technology are either being commissioned or are upcoming. What is your advice to the young budding engineers, scientists on having a career interwoven with accelerator and RF?**

Dr. Sumit Som: Accelerator is an ever developing field and is progressively attaining higher energy frontiers. Ambitious accelerator programs are being launched both nationally and internationally. Science and technology of accelerators is growing very fast, which gives opportunity to learn many new and advance technologies and do the scientific researches as well. Working in accelerator and in RF is a very challenging job.

The young budding engineers and scientists will gain multi-disciplinary knowledge and exposure while working in accelerators. The knowledge gained in these RF and accelerators field will be at par with international laboratories. The young scientists and engineers should utilize this perfect opportunity and give their valuable contribution for our motherland.

**Dr. Manjiri Pande is currently heading Radio Frequency System Section of Accelerator Control Division in BARC. Dr. Manjiri specializes in diversified areas that include particle accelerators, klystrons, Solid State RF technology, RF breakdown and multipacting, high power RF systems etc. She is a recipient of DAE Scientific and Technical Excellence Award, DAE Group Achievement Awards, S.N. Seshadri Award and VEDA award.*

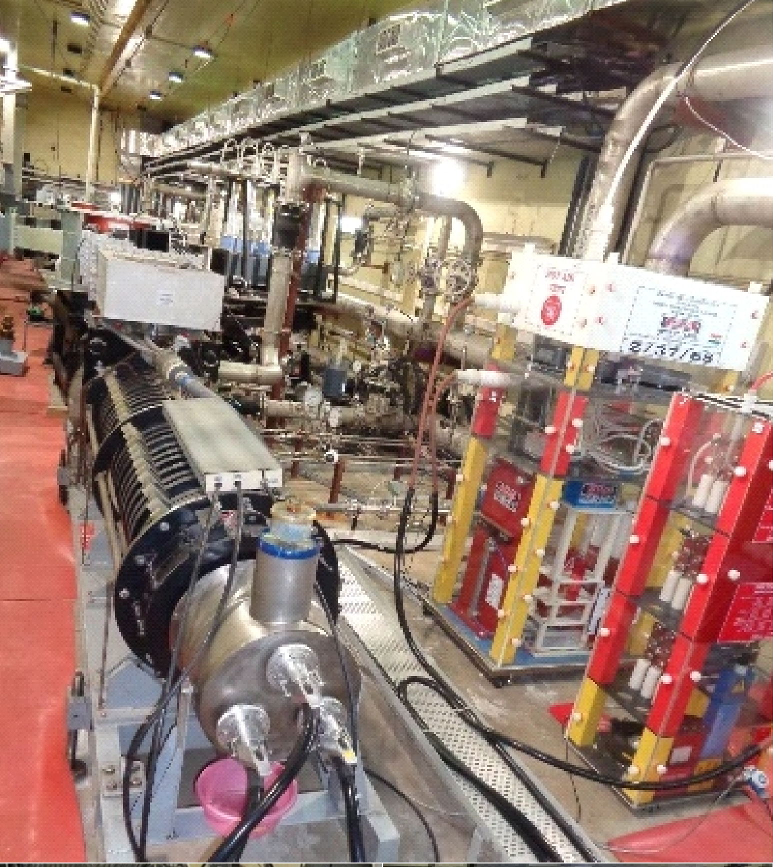

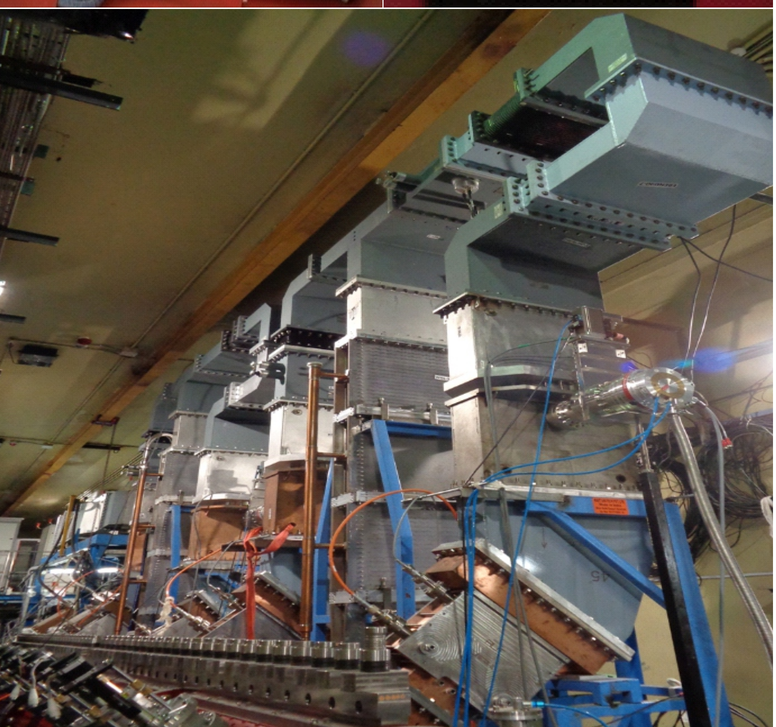

INTEGRATED RADIO FREQUENCY (RF) SYSTEMS FOR PARTICLE ACCELERATOR

Integrated RF systems are crucial for the performance of an accelerator.
The state-of-the art RF systems are equipped with advanced control features to enable acceleration of charged particles effectively within the structural framework of the accelerator

This page intentionally left blank

उच्च तीव्रता प्रोटॉन त्वरक

1

LEHIPA के लिए उच्च शक्ति वाली रेडियो आवृत्ति प्रणालियां

*मंजिरी पांडे, संदीप श्रोत्रिया, रामाराव बी.वी.एन., आर.पटेल, शिजू ए., जे.के.मिश्रा, स्निग्धा एस., श्याम सुदर जेना, मुथु एस. और गोपाल जोशी

त्वरक नियंत्रण प्रभाग, भाभा परमाणु अनुसंधान केंद्र (भापअ केंद्र), ट्रांबे-400085, भारत

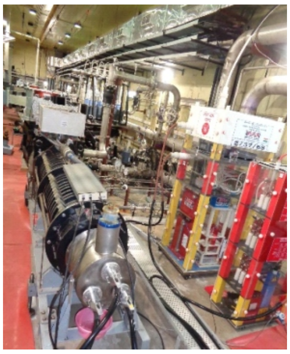

क्लाइस्ट्रॉन एच.पी.आर.एफ. प्रणाली

सारांश

निम्न ऊर्जा उच्च तीव्रता प्रोटॉन त्वरक (एल.ई.एच.आई.पी.ए) को स्वदेशी रूप से निर्मित किया गया है और प्रोटॉन किरण के त्वरण को 20 MeV की ऊर्जा स्तर तक बढ़ाया गया है। इस तीन त्वरक गुहाओं के सोपानी संचालन द्वार प्राप्त किया गया है; रेडियो आवृत्ति चतुर्द्ध्रुवी (आर.एफ.क्यू) और दो चरण अपवाह नालिका रैख़ित त्वरक (ड्रिफ्ट ट्यूब लिनक्स - डी.टी.एल) को तीन क्लाइस्ट्रॉन आधारित उच्च शक्ति 352 MHz प्रणालीयो द्वारा, प्रत्येक 1 मेगावाट प्रणाली से संचालित किया गया है। पूर्ण रूप से परीक्षित किए गए रेडियो आवृत्ति (आर.एफ.) और डीसी घटकों और/या उप प्रणालियों, शक्ति आपूर्ति, मापन और नैदानिकी अंतर्बद्ध और सुरक्षा प्रणालि को एकीकृत, परीक्षण किया गया और एक समेकित उच्च शक्ति रेडियो आवृत्ति (एच.पी.आर.एफ) प्रणाली के रूप में स्थापित किया गया है। 10 किलोवाट का एक ठोस अवस्था शक्ति प्रवर्धक विकसित किया गया है बंचर गुहिका को शक्ति प्रदान करता है।

High Intensity Proton Accelerator

1

High Power Radio Frequency Systems for LEHIPA

***Manjiri Pande, Sandip Shrotriya, Ramarao B. V. N., R Patel, Shiju A., J. K. Mishra, Snigdha S., Shyam sunder Jena, Muthu S., and Gopal Joshi**

Accelerator Control Division, Bhabha Atomic Research Centre (BARC), Trombay-400085, INDIA

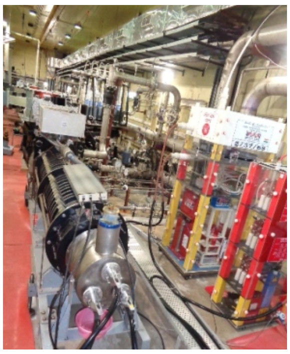

Klystron HPRF system

ABSTRACT

The Low Energy High Intensity Proton Accelerator (LEHIPA) has been indigenously built and proton beam has been accelerated to an energy of 20 MeV. This has been achieved by driving a cascade of three accelerator cavities; Radio frequency quadrupoles (RFQ) and two stages of Drift Tube Linacs (DTL) i.e. 10 MeV DTL and 20 MeV DTL by each of the three klystron based high power 1 MW at 352 MHz systems. The thoroughly tested radio frequency (RF) and DC components and/or sub systems, power supplies, measurement and diagnostics, interlock and protection systems were integrated, tested and commissioned as a consolidated high power RF (HPRF) system. The RF power from klystron RF system is transmitted through high power rectangular waveguide WR2300 systems towards accelerating cavity. A solid-state power amplifier of 10 kW has been developed and powers the buncher cavity.

KEYWORDS: *Accelerator, Buncher, Interlock and protection, RF, Klystron, LEHIPA, Proton, Waveguide*

*Author for Correspondence: Manjiri Pande
E-mail: manjiri@barc.gov.in

Introduction

High energy proton accelerators have applications in the areas of scientific, medical etc. BARC is embarked upon the development of high energy proton accelerator for its ambitious program of Accelerator Driven Sub-critical reactor (ADS). In ADS [1], proton beam from proton accelerator is coupled to a sub critical reactor, which can be operated in sub-critical mode and have inherent safety features. As a front end of a high energy proton accelerator development, LEHIPA has been developed and commissioned at BARC and accelerated the proton beam up to 20 MeV. LEHIPA has three accelerator cavities viz., 3 MeV Radio frequency quadrupole (RFQ), 10 MeV and 20 MeV Drift Tube Linacs (DTL) that are powered by each of Klystron based high power radio frequency (HPRF) system. The article describes details of klystron based HPRF system, its wave guide (WG) based transmission system and a solid state amplifier (SSA) for buncher cavity.

Klystron Based MW Level HPRF Systems

Radio frequency (RF) particle accelerators use RF fields in the accelerator cavities for particle acceleration, which is generated by RF power. The HPRF system is an important critical system that generates electric field across the cavity for beam acceleration.

LEHIPA (20 MeV) - a front end of ADS, uses three 352 MHz, 1 MW klystron (TH2089) based HPRF systems [2] to power its three accelerating sections viz. 3 MeV RFQ, 10 MeV DTL and 20 MeV DTL. These three accelerating sections are coupled in series via their respective beam transport lines viz. low energy beam transport (LEBT) between ion source and RFQ, and medium energy beam transport (MEBT) between RFQ and 10 MeV DTL. The MEBT section includes a buncher cavity, which is powered by a 10 kW solid state RF power amplifier. The three klystron RF systems have been successfully designed, developed, tested and then, integrated with RFQ and both the DTLs to accelerate the proton beam to 20 MeV energy.

HPRF systems are complex and comprise of a variety of sub-systems. These systems incorporate high voltage and high current subsystems in addition to RF Power components, measurement & diagnostics and interlock & protection sub systems. All these except klystron and circulator are indigenous including high efficiency & compact-bias supplies, waveguide components with reduced insertion losses, fast protection system against arcing & other fault conditions [2]. Mitigation of RF radiated & conducted emission [3] and proper thermal management has ensured the reliable operation of HPRF system.

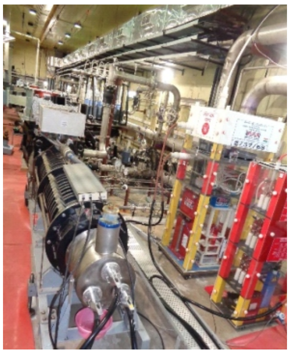

Fig.1: Klystron HPRF system.

Fig.2: Klystron HPRF with WG line.

Each of the 1 MW at 352 MHz RF system (Fig.1 & 2) comprises of 1 MW klystron, RF components like harmonic filter, directional coupler, circulator, RF loads, interlock and protection system (Fig.3), eight low voltage (LV) and high voltage (HV) bias supplies, wave-guide window, and WR2300 wave-guide components, like straight sections, magic tees, bends etc. Except klystron and circulator, all the sub systems and components of 1 MW RF system [4] are indigenously developed by Micro, Small & Medium Enterprises(MSME) i.e local industries based on BARC design. Fast acting Interlock and Protection system (IPS) (Fig.3) [5] is used for safe and reliable operation of high power RF system. All the bias supplies of the HPRF system are controlled by IPS, which have to function satisfactorily in RF interference (RFI) environment. Each RF system is cooled by low conductivity water (LCW) having total inventory of almost 2000 lpm per system

HPRF systems of LEHIPA are physically spread over three floors or levels of the building. In its basement, there are klystron gallery and Linac gallery housed in two parallel tunnels. Linac gallery houses three accelerating cavities. Klystron gallery (Fig.1 and 2) houses the major RF components like klystron, circulator, RF Load (Fig.4), Harmonic filter etc. handling 1 MW RF power [6]. It also houses major part of HV sub-systems of all the three HPRF systems. RF power from each of the three HPRF systems is coupled to each of the (resp.) three accelerating sections via a long wave-guide WR 2300 based transmission line. The mezzanine floor accommodates IPS and LV bias supplies (Fig.3) of the three HPRF systems. The regulated high voltage power supply (RHVPS) (100 kV, 25 A) is used for biasing cathode of each klystron and is physically located on the ground floor. Each of the three HPRF systems that is spread over large area, is expected to operate and perform at design parameters while overcoming on-field challenges.

Table 1: Parameters of Klystron HPRF system.

Parameter	Klystrons HPRF System		
	I	II	III
Frequency	352.21 MHz	352.21 MHz	352.21 MHz
RF Power	750 kW	830 kW	850 kW
Gain	41 dB	39 dB	40.2 dB
Efficiency	60 %	54.8 %	57.4 %
2nd & 3rd Harmonics	-25 dBc & -30 dBc	-25 dBc & -30 dBc	-25 dBc & -30 dBc

Fig.3: Interlock and protections systems and LV supplies.

Fig.4: Circulator (1 MW) and 0.8 MW RF Load.

HPRF system may cause radiated emissions (RE) and conducted emissions (CE). Hence its constituent components and sub systems that are spread over large space may get exposed to conducted and radiated emissions. So, electromagnetic compatibility (EMC) of IPS and other subsystems has been ensured. The techniques of filtering, glavanic isolation, effective grounding topology, shielding, EM suppression practices have been followed to achieve EMC. By integrating the multi-disciplinary sub-systems/components and techniques in the domains of RF, HV, high current, low level signal instrumentation, RFI suppression, vacuum, thermal management etc., each of the three 1 MW klystron-based HPRF systems has been designed, developed and tested independently on RF load. Each HPRF system then, separately integrated and tested with 3 MeV RFQ, 10 MeV DTL and 20 MeV DTL sections. Using these RF power systems LEHIPA has been successfully tested and proton beam accelerated to 20 MeV energy.

Indigenous Waveguide Transmission Systems

The three independent WR2300 based waveguide (WG) systems [7] have been designed, developed and commissioned for three accelerating sections for 20 MeV accelerator [4]. One WG line is for RFQ and one each for 10 and 20 MeV DTL. These WG systems constituting various types of waveguide components, like, straight sections, tapers, directional couplers, 30 and 45-degree bends, phase shifters, water-based WG RF loads, windows etc. and having both half height and full height structures, have been designed and developed using local MSME parties and commissioned with the respective accelerating cavities.

Waveguide system for 3 MeV *RFQ*

The RFQ required more than 600 kW RF power at 352 MHz to be coupled across its two ports for proton acceleration from 50 keV to 3 MeV energy. RF power from HPRF system is divided in two parts and coupled to each of the two ports of 3 MeV RFQ. The waveguide transmission line (Fig.5) involves various components like E-plane and H-plane bends to rotate the polarisation, Magic Tee to divide and generate two RF power outputs with equal amplitude and phase, water cooled RF loads at various locations to dissipate the unwanted and unbalanced reflected power from RFQ, directional couplers to measure the RF power in both forward and reverse modes at various locations across WG line, RF windows to transmit RF power while simultaneously providing isolation between air and vacuum inside the RFQ. All these waveguide components were designed with stringent specifications at 352 MHz and were fabricated with local Indian industries. These were characterised for their RF performance parameters, and then installed and commissioned with RFQ for 3 MeV operation.

Waveguide system for 10 MeV DTL-1

The 10 MeV DTL-1 accelerator section required a total RF power of ~800 kW at 352 MHz and has four coupling ports for coupling the RF power. Hence, the RF power from HPRF system has been split into 1: 4 by two successive stages of 1:2 power dividers i.e., using a two-stage binary divider into two sets of in-phase and anti-phase vectors. The anti-phase vectors are

Fig.5: Waveguide transmission line from Klystron HPRF to 3 MeV RFQ.

Fig.6: Installed and commissioned waveguide systems of 10 MeV DTL.

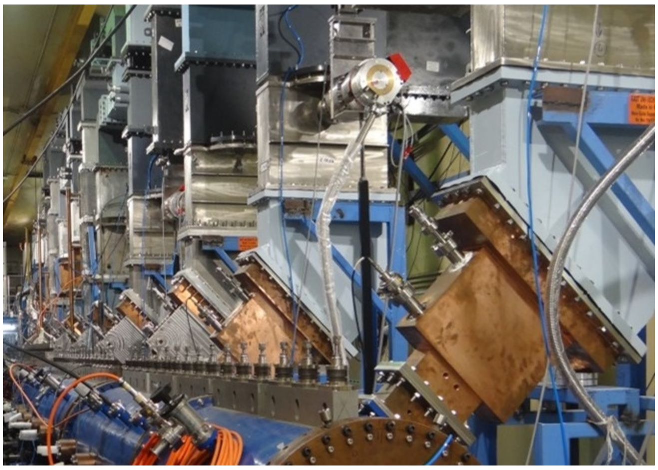

Fig.7: Installed and commissioned waveguide systems of 20 MeV.

again rotated using an additional path length of waveguides to feed in phase power into four ports of DTL-1. Each waveguide line (Fig.6) has directional couplers at various locations to measure both forward and reflected power for diagnostics and in some cases for protection against faults. A total of eight directional couplers are used in the system. The water-based WG RF loads located at the centre of magic tees are used to dissipate the unbalanced reflected power from the DTL side.

Waveguide system for 20 MeV DTL -2

Almost similar waveguide system (Fig.7) with similar layout as that of 10 MeV DTL -1 has been tested, installed and commissioned for 20 MeV DTL-2 accelerator. All the three waveguide systems for 3 MeV RFQ, 10 MeV DTL-1, 20 MeV DTL-2 have been commissioned with their respective accelerator section.

Solid-state RF power amplifier for buncher cavity

LEHIPA uses buncher cavity between RFQ and 10 MeV DTL to bunch the incoming protons from RFQ using RF power from a solid-state RF power amplifier. Indigenous 10 kW, 352.21 MHz Solid-State Amplifier (SSA) [8] (Fig.8), housed in the klystron gallary, has been designed and developed along with coaxial transmission line for coupling the RF power to the buncher cavity of MEBT (Fig.8).

This SSA has been designed using the solid-state transistor technology. It consists of 16 power amplifier modules, two 8-way power combiners, a two-way combiner, a two-way divider, two 8-way dividers, pre-driver, driver modules, DC power supplies, sensors, and an interlock and protection system. The output of the RF power amplifier is coupled to the buncher cavity using 3-1/8", 50 Ohm coaxial transmission system. This transmission system incorporates directional couplers for power measurement, bends for rotation of wave front, and straight sections. All these are made in rigid 3-1/8 inch transmission line. The salient technical specifications of SSA are given in Table 2.

The RF power waveform during testing and after coupling to Buncher cavity are shown in Fig.9. The RF power waveforms of 3 MeV RFQ and 10 MeV DTL during proton beam acceleration are shown in Fig.10.

Fig.8: SSA (10 kW at 352.21 MHz) (in klystron gallary) for Buncher cavity (on the left) and its coaxial transmission line in Linac gallary(on the right).

Table 2: Salient technical specifications of SSA

Sr. No.	Parameters	Values
1.	Centre Frequency	352 MHz
2.	Bandwidth (3 dB)	>30 MHz
3.	Max. power output	12 kW
4.	Harmonics	<-25 dBC
5.	Coolant	water
6.	Output Connector	3-1/8" EIA Flange
7.	Efficiency	>60% both pulse and CW
8.	Power gain	>70 dB

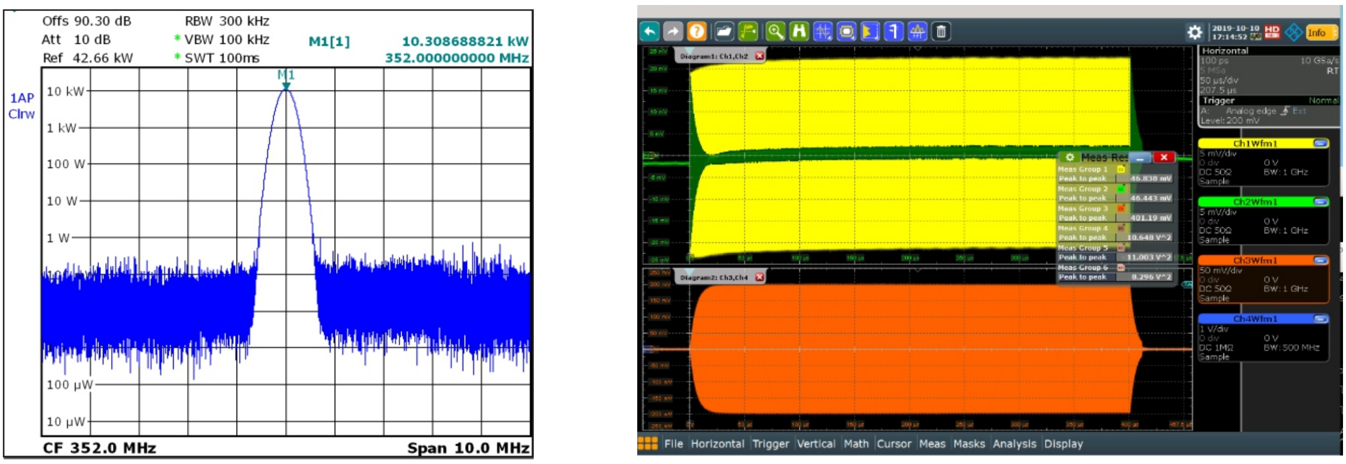

Fig.9: RF Power Waveform of SSA and RF waveforms recorded after RF amplifier was integrated with buncher.

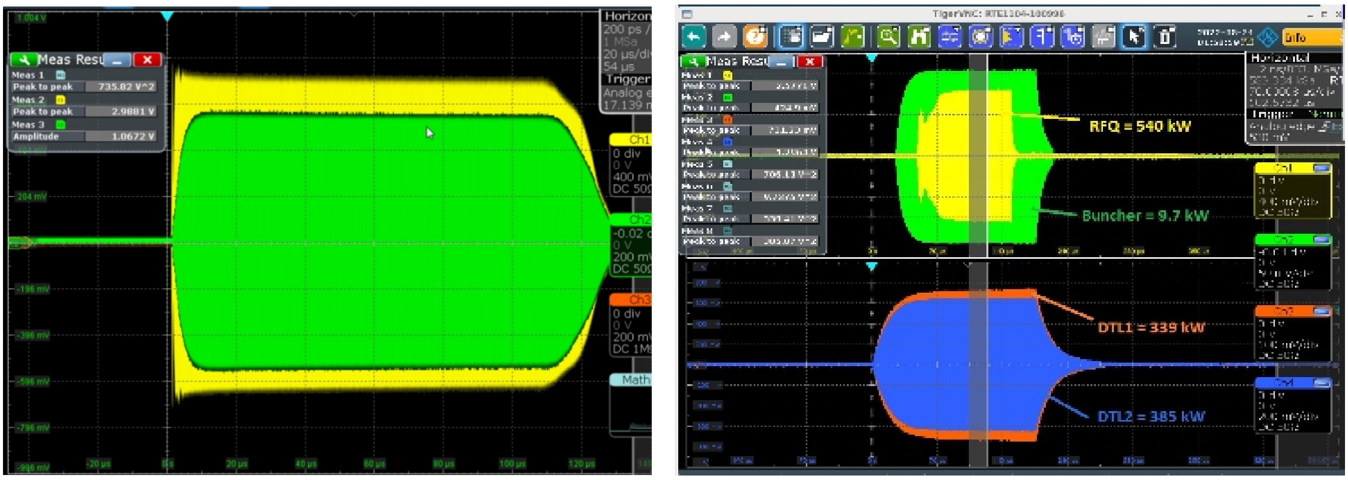

Fig.10: RF Power Waveforms across 3 MeV RFQ and 10 MeV DTL.

Conclusions

In LEHIPA, three klystron based HPRF systems along with WG transmission lines have been successfully operating with 3 MeV RFQ, 10 MeV DTL1, 20 MeV DTL2 respectively for 20 MeV proton beam acceleration. RF power waveforms recorded across 3 MeV RFQ & 10 MeV DTL operation are shown in Fig.10. All these RF systems have been locally designed, tested and commissioned.

Acknowledgements

The authors are very much thankful to Shri U. D. Malshe, Director, MRG and Shri Vivek Bhasin, Director, BARC for their constant encouragement and continued support for such a valuable BARC program.

The authors acknowledge for the huge technical help and efforts provided by Shri Hitesh Kadam and Shri Jagdish Bowlekar. The authors would like to sincerely thank the IADD team for their excellent support and collaboration.

References

[1] S.S. Kapoor, Accelerator-driven sub-critical reactor system (ADS) for nuclear energy generation, PRAMANA journal of physics, Vol. 59, No.6, December 2002, pp. 941–950, Indian Academy of Sciences.

[2] Manjiri Pande, S.D. Shrotriya, Shiju A, N. R. Patel, S.S. Jena, Gopal Joshi, High Power RF Systems of LEHIPA - Technology Development", IEEE Explorer proceedings of IEEE MTT & APS joint conference on 'Microwaves, Antennas and Propagation Conference (MAPCON), December 2023, Ahmedabad.

DOI: 10.1109/MAPCON58678.2023.10464048

[3] Manjiri Pande, S.D. Shrotriya, Shiju A, N. R. Patel, S.S. Jena, EMC and protection of 1 MW klystron RF system for proton accelerator. The proceedings of Joint Asia Pacific Symposium on Electromagnetic Compatibility (APEMC) 2023 and International Conference on Electromagnetic Interference and Compatibility (INCEMIC) 2023, DOI: 10.1109/APEMC57782.2023.10217762.

[4] Sandip Shrotriya, Niranjan Patel, Shiju A, S.S. Jena, Manjiri Pande and Gopal Joshi, Testing and commissioning of 1 MW, 352 MHz klystron system for 10 MeV DTL of LEHIPA, Proc. of InPAC-2022.

[5] Sandip Shrotriya, N.R. Patel, Shiju A, S.S. Jena, Manjiri Pande and Gopal Joshi, Interlock and Protection System of 1 MW Klystron RF System for 20 Mev DTL of LEHIPA, Proc. of InPAC-2022.

[6] Snigdha Singh, J.K. Mishra, Muthu S., Manjiri Pande, P.V. Bhagwat, High power circulator testing and design of its bias control circuit, Proc. of InPAC-2019.

[7] B.V. Ramarao, Muthu S., J.K. Mishra, Manjiri Pande, and Gopal Joshi, Status of Commissioning of the High-Power Waveguide Systems for LEHIPA", Proc. of InPAC-2022, paper no.22.

[8] B.V. Ramarao, S. Muthu, J.K. Mishra, Manjiri Pande, Gopal Joshi, M.R. Mishra, V.M. Jose, S.V.L.S. Rao, Rajesh Kumar, and S. Krishna Gopal, Coupling and energising of 10 kW, 352 MHz solid-state RF power amplifier for buncher cavity of proton accelerator, Proc. InPAC-2019.

उच्च तीव्रता प्रोटॉन त्वरक

2

निम्न ऊर्जा उच्च तीव्रता प्रोटॉन त्वरक (LEHIPA) के लिए निम्न–स्तर आरआफ नियंत्रण प्रणालियां

*आलोक आगाशे, पी.डी. मोतीवाला, राधिका नासेरी, श्याम मोहन, ज्योति पी. और गोपाल जोशी
त्वरक नियंत्रण प्रभाग, भाभा परमाणु अनुसंधान केंद्र (भापअ केंद्र), ट्रांबे-400085, भारत

एल. एल. आर. एफ प्रणाली

सारांश

भाभा परमाणु अनुसंधान केंद्र,मुंबई के निम्न ऊर्जा उच्च-तीव्रता प्रोटॉन त्वरक (LEHIPA) के लिए एक डिजिटल निम्न स्तरीय रेडियो आवृत्ति नियंत्रण प्रणाली (LLRF) के स्वदेशी डिज़ाइन और कार्यान्वयन को प्रस्तुत किया गया है। निम्न स्तरीय रेडियो आवृत्ति नियंत्रण प्रणाली, आरएफक्यू, बंचर, डीटीएल1 और डीटीएल2 कैविटी में आरएफ क्षेत्र के आयाम और चरण पर सटीक नियंत्रण को सक्षम बनाती है। एडीसी, डीएसी, एफपीजीए, और क्लॉक संश्लेषक से सुसज्जित सीपीसीआई (cPCI) आधारित डिजिटल बोर्ड का लाभ उठाते हुए, प्रणाली आवश्यक सिग्नल प्रसंस्करण और नियंत्रण को लागू करती है। विलंबता को न्यूनतम करने के लिए फर्मवेयर को अनुकूलित किया गया है और इसमें प्रभावी एलएलआरएफ संचालन के लिए विविध प्रसंस्करण मॉड्यूल शामिल हैं।। एलएलआरएफ प्रणालियों की सफल तैनाती कई कैविटीज़ की समवर्ती लॉकिंग को सक्षम बनाती है, जिसके परिणामस्वरूप लेहिपा में 20MeV प्रोटॉन बीम की त्वरण प्राप्त होती है।

High Intensity Proton Accelerator

2

Low Level RF Systems for LEHIPA

***Alok Agashe, P. D. Motiwala, Radhika Nasery, Shyam Mohan, Jyothi P. and Gopal Joshi**
Accelerator Control Division, Bhabha Atomic Research Centre (BARC), Trombay-400085, INDIA

LLRF system

ABSTRACT

The indigenous design and implementation of a digital Low-Level RF (LLRF) control system for the Low Energy High-Intensity Proton Accelerator (LEHIPA) at BARC, Mumbai is presented. The LLRF system facilitates precise control over the amplitude and phase of RF field in RFQ, Buncher, DTL1 and DTL2 cavities. Leveraging a cPCI based digital board equipped with ADCs, DACs, FPGAs, and clock synthesizers, the system implements required signal processing and control. The firmware is optimized to minimize latency and includes diverse processing modules for effective LLRF operation. Successful commissioning of the LLRF systems enables simultaneous locking of multiple cavities, resulting in the attainment of 20MeV proton beam acceleration in LEHIPA.

KEYWORDS: *Accelerator, Buncher,* cPCI, *RF, Klystron, LEHIPA, Proton,* LLRF

**Author for Correspondence: Alok Agashe*
E-mail: aagashe@barc.gov.in

Introduction

A carefully and judiciously designed LLRF system based on digital techniques and incorporating FPGA offers unique advantages of precision, improved digital signal processing capabilities, possibility of implementing complex algorithms in FPGA, flexibility, programmability, repeatability and powerful diagnostic capabilities.

LLRF control system is one of the key subsystems in RF accelerator. Accelerator Control Division (ACnD), BARC has designed, developed and commissioned digital LLRF systems to control the amplitude and phase of RF field in resonant cavities in LEHIPA at BARC, Mumbai. LEHIPA consists of a 50keV ECR ion source, LEBT, 3MeV RFQ, Buncher cavity and Drift Tube Linac (DTL) section to deliver 20MeV proton beam. LEHIPA has a total of four LLRF systems for control of RF field in RFQ, Buncher, DTL1 and DTL2 as shown in Fig.1.

The LLRF system developed for LEHIPA is a compact cPCI based system, employing full digital approach, not requiring Up and Down converters. The hardware of the system consists of an Analog conditioning module (ACM) and a cPCI based digital board built around an FPGA. The ACM consists of input buffer/attenuation and the output drive amplifier sections. Pickup, Forward power and reflected power signals are digitized and processed. Windows based GUI application software has been developed for Control and display of parameters and data. The LLRF systems have been commissioned successfully for all the cavities of LEHIPA enabling extraction of 20 MeV proton beam. LLRF system has been modified for DTL so that it drives two RF Tanks (as shown in Fig.1) with single RF drive using Vector sum control method.

Hardware Description

Fig.2 shows the module level block diagram of the LLRF system. It consists of mainly two parts, namely,

a. Analog Conditioning Module (ACM), and

b. Digital Board.

RF signals from the field are received and conditioned by the ACM before feeding them to the digital board. High speed ADCs on the digital board digitizes the incoming RF signals and feeds the digital data to the FPGA for further processing. The LLRF system employs direct digitization scheme where it samples the incoming 352MHz RF signals directly without down-conversion. Feedback loop with PI controller is implemented in the FPGA for generating RF drive signal which after suitable amplification in the ACM, is fed to the Klystron through RF switch. The LLRF system supports pulsed and CW modes of operation. It is used in open loop mode during the RF cavity conditioning, and in closed loop mode during normal operation. Fig.3 is photograph of commissioned LLRF for RFQ at LEHIPA.

Analog conditioning module (ACM)

It is an FPGA based 19-inch rack mountable stand-alone module (Fig.4), remotely operated via Ethernet through Control System Studio (CSS) based application software. Analog signals are conditioned in this module to utilize the full dynamic range of the high speed multi-channel ADC's situated on the digital board. One ACM contains nine buffer channels and two

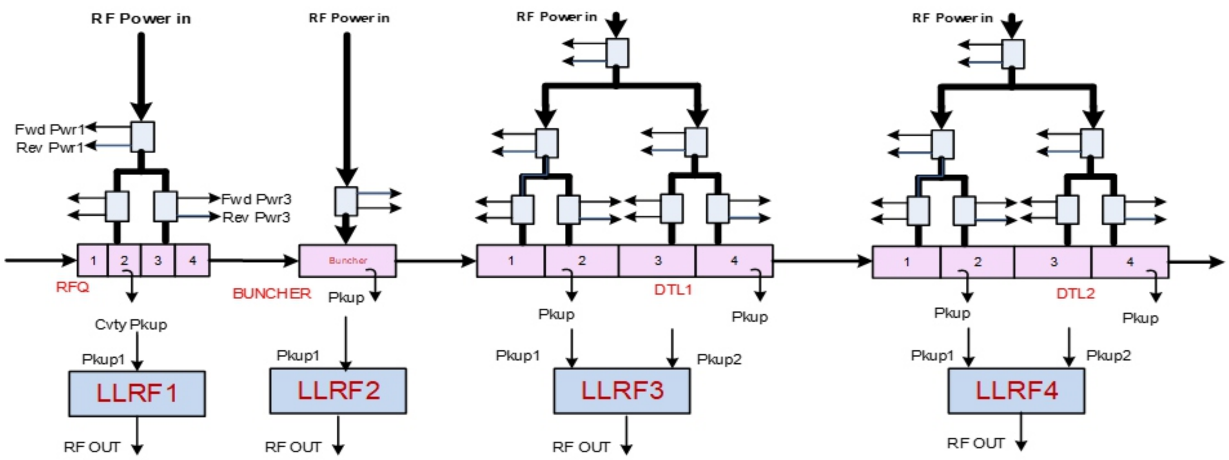

Fig.1: LLRF Systems for 20 MeV LEHIPA

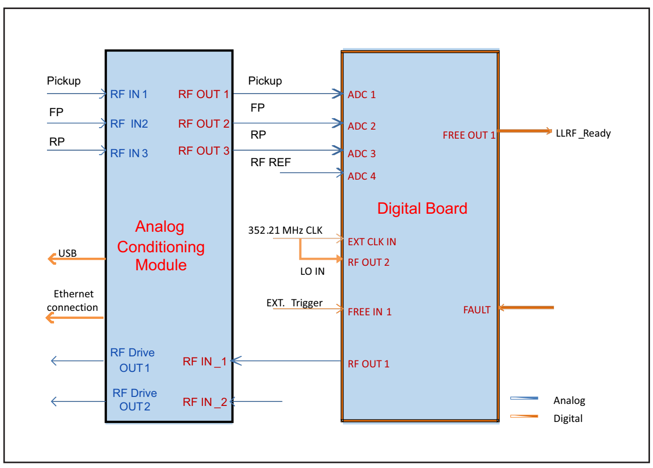

Fig.2: Modules in the LLRF System

Fig.3: LLRF system for RFQ, commissioned at LEHIPA

Fig.4:Analog conditioning Module

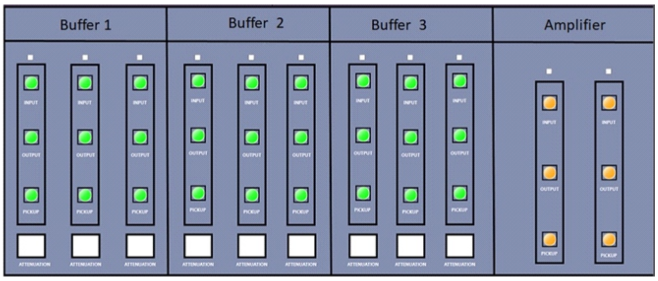

Fig.5: Analog Conditioning Module EPICS CSS GUI

amplifier channels and it can cater to two cavities. Buffer channel provides buffering and suitable programmable attenuation (0 to 15 dB) along with band-pass filtering to cavity RF signals. It protects Digital board from High levels of RF field signals. ACM also processes the RF drive out signal produced in the digital board. It buffers, filters and amplifies the drive out signal by 30db, which is further connected to the cavity via high power RF Amplifier. Fig.5 Shows the CSS GUI for ACM.

Fig.6: cPCI based Digital Board

Digital Board

The cPCI-based digital board, shown in Fig.6, includes an eight-channel ADC of suitable resolution for RF signal digitization, a high-density FPGA for data processing, and sufficient SRAM for storage, three low-speed DACs for tuner output and diagnostics, clock synthesizers for synchronized clock generation, and a dedicated cPCI controller for interface management. External 352 MHz RF signal, serves as the reference clock input. On board programmable clock synthesizers produce stable sampling clocks for ADCs and DACs. The digital board can simultaneously acquire and process eight analog signals, enabling control of two RF cavities. The firmware, optimized for minimal latency, includes

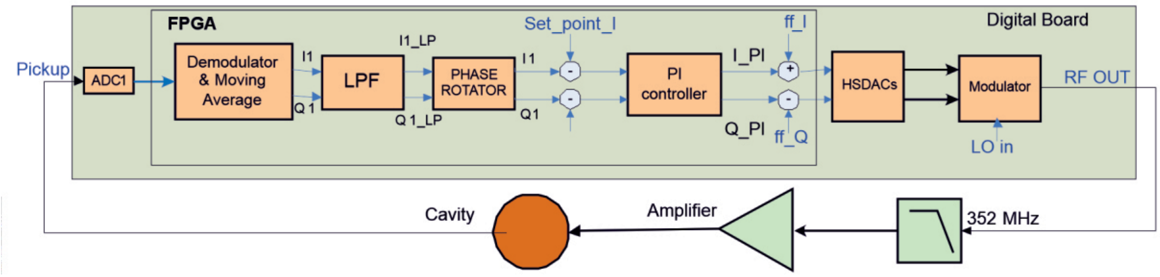

Fig.7: Implementation of feedback loop in digital board.

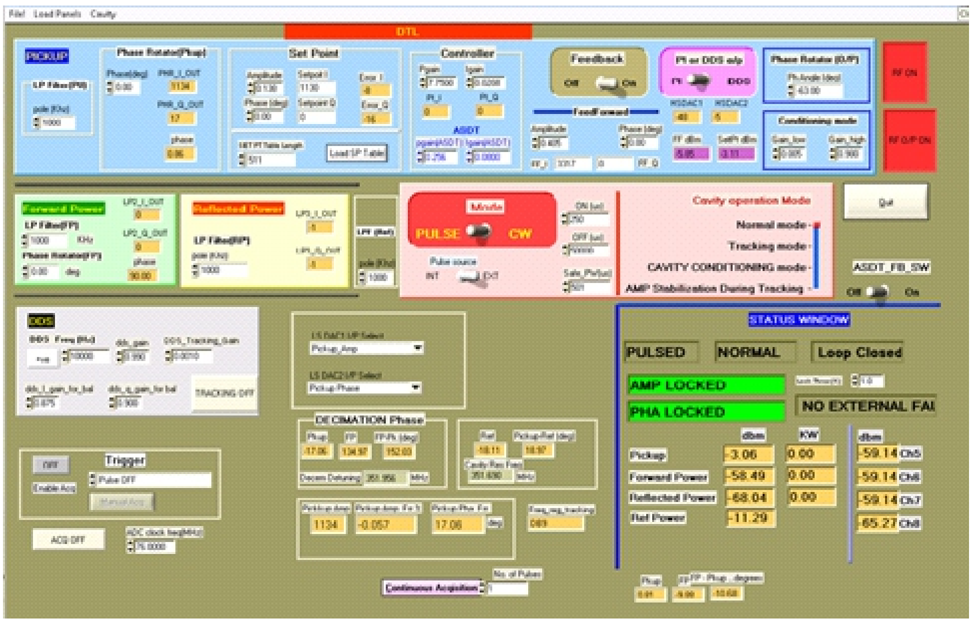

Fig.8: LLRF GUI in Amplitude and phase loop in lock condition for DTL.

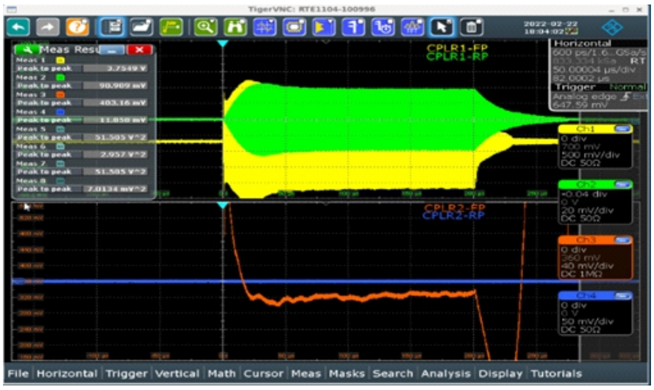

Fig.9: DTL forward power and pickup signals

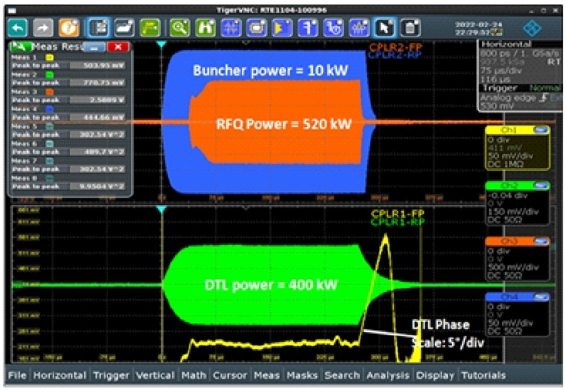

Fig.10: RFQ, Buncher and DTL1 locked at LEHIPA

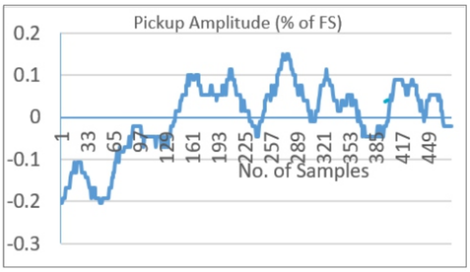

Fig.11: Pickup Amplitude for DTL1

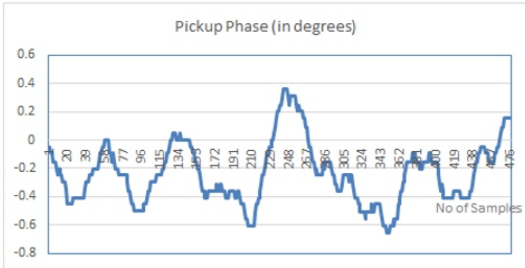

Fig.12: Pickup Phase for DTL1

various processing modules like quadrature demodulators, PI controllers, and data acquisition modules, ensuring smooth LLRF system functioning. The software facilitates communication with hardware for control diagnostics and data retrieval.

Feedback Control Loop

The pickup signal undergoes necessary signal conditioning and processing, as illustrated in the block diagram in Fig.7. The programmable gains in digital controller is useful in attaining optimal response for stabilizing the RF field within the cavity. Subsequently the on-board analog modulator generates the RF OUT which is conditioned and amplified by ACM for feeding to the klystron.

Software

The LLRF software controls all four LLRF systems at LEHIPA. Fig.8 shows main GUI of the system for DTL. It shows the amplitude and phase in DTL in locked condition.

Results

Fig.9 shows a screenshot of the oscilloscope, showing forward power and pickup signal for following conditions

DTL: 400kW Power, Pulse-Width =200us, Repetition rate=2Hz.

Fig.10 shows the pickup signals from RFQ, Buncher, and DTL1 under locked condition for 6.8 MeV operation. The yellow trace represents the phase of the DTL1 pickup, which falls within acceptable limits. Data for pickup amplitude (Fig.11) and phase (Fig. 12) for DTL1 has been acquired and amp and phase jitters have been found to be less than 0.2% and 0.2 degrees rms, respectively.

Acknowledgements

Authors sincerely thank LEHIPA team IADD, BARC for all the support in performing experiments, and providing results.

References

[1] Alok Agashe, P.D. Motiwala, S.K. Bharade, Shyam Mohan and Gopal Joshi, "Digital LLRF System for RFQ" InPac2015, Mumbai, India.

[2] Gopal Joshi, Shyam Mohan, Sandeep Kashinath Bharade, Motiwala Paresh, C.I.Sujo, T.S.Anantkrishnan, Chandrakant Pithawa, "RF Control System For 400 keV RFQ", in PCaPAC2012.

[3] Paresh D. Motiwala, Gopal Joshi, C.I. Sujo, "Development of Hardware for Digital Low Level RF (DLLRF) Control System", NSNI 2010, BARC.

[4] S.V.L.S. Rao, Jose V Mathew, S.K. Singh, M.R. Mishra, Rajesh Kumar, Mentes Jose, Hitesh Kewlani, Sandip Shrotriya, B V Rama Rao, Rajni Pande, Shweta Roy, Roushan Abhishek, Piyush Jain,Alok Ghosh, Deepak Mathad, Sumit Garg, Aman Bajaj, P Bhumeshwar, A Shiju, Pallavi Priyadarshini, Sonal Sharma, A Basu, Sherry Rosily, V K Kotak, N R Patel, Laxman Tayade, Pravin Parate, G N Singh,S K Bharade, C I Sujo, H Shukla, R T Keshwani, M M Pande, Paresh Motiwala, Alok Agashe,Gopal Joshi,Srinivas Krishnagopal , "Commissioning of the LEHIPA 3 MeV RFQ" , INPAC 2019; IUAC.

उच्च तीव्रता प्रोटोन त्वरक

3

त्वरकों के लिए आरएफ प्रोटेक्शन इंटरलॉक एवं मॉनिटरिंग प्रणालियां

*सुजो सी.आई., आर.टी. केशवानी, संदीप भराडे, मयूर एम. सुतार, गोपाल जोशी
त्वरक नियंत्रण प्रभाग, भाभा परमाणु अनुसंधान केंद्र (भापअ केंद्र), ट्रांबे-400085, भारत

चार वीएमई मॉड्यूल युक्त आरएफपीआई प्रणाली

सारांश

त्वरक नियंत्रण प्रभाग, भाभा परमाणु अनुसंधान केंद्र (भा.प.अ.कें.), ने वीएमई 64x आधारित रेडियो आवृत्ति सुरक्षा इंटरलॉक (आरएफपीआई) और निगरानी प्रणाली विकसित की है, जो वर्तमान में कार्यरत है। यह प्रणाली भा.प.अ.कें में निम्न-ऊर्जा उच्च-तीव्रता वाले प्रोटॉन त्वरक (एलईएचआईपीए), आरआरकेट में क्षैतिज परीक्षण स्टैंड (एचटीएस), और फर्मीलैब में पीआईपी2आईटी सहित विभिन्न त्वरक केंद्र में स्थापित की गई है। आरएफपीआई प्रणालियाँ त्वरक केंद्रों में स्थापित विभिन्न संवेदकों, जैसे कि दिशात्मक युग्मक, फोटो गुणक ट्यूब (पी. एम. टी.), क्षेत्र उत्सर्जन जांच, रेडियो आवृत्ति एंटीना, तापमान संवेदक आदि की निगरानी करता है, और यदि निगरानी किया गया कोई भी सिग्नल निर्धारित सीमा से अधिक है, तो 1-2 माइक्रोसेकंड के भीतर केविटी में रेडियो आवृत्ति तरंगों को बंद कर देता हैं। इन संकेतों को डिजिटल रूप में मेमोरी में संग्रहीत किया जाता है, जो बाद में दोष विश्लेषण के लिए उपयोगी होता है। भारतीय संस्थानों फर्मीलाब के बीच विज्ञान और प्रौद्योगिकी सहयोग के तहत विकसित 325 मेगाहट्र्ज, 7 किलोवाट रेडियो आवृत्ति पावर एम्प्लीफायरों की सुरक्षा के लिए इंटरलॉक सुरक्षा और निगरानी प्रणाली को साकार करने के लिए आरएफपीआई की डिजाइन संरचना का विस्तार किया गया है।

High Intensity Proton Accelerator

3

RF Protection Interlock and Monitoring Systems for Accelerators

***Sujo C. I., R. T. Keshwani, Sandeep Bharade, Mayur M. Sutar and Gopal Joshi**
Accelerator Control Division, Bhabha Atomic Research Centre (BARC), Trombay-400085, INDIA

One RFPI system with four VME modules

ABSTRACT

Accelerator Control Division, Bhabha Atomic Research Centre has developed VME64x based RF Protection Interlock (RFPI) and monitoring systems presently functional and installed at different accelerator facilities including Low Energy High Intensity Proton Accelerator (LEHIPA) at BARC, Horizontal Test Stand (HTS) at RRCAT and PIP2IT at Fermilab. RFPI systems monitor different outputs of different sensors such as Directional Couplers, Photo Multiplier Tube (PMT), Field Emission Probes, RF antenna, Temperature Sensors etc. installed in an accelerator facility and if any of the monitored signals exceeds the set limit, switches OFF RF power to the RF cavity within 1-2us. All the monitored signals are digitised and stored in memory, which is available for post fault analysis. The design architecture followed for RFPI has been extended to realize Interlock Protection and Monitoring system for protection of 325 MHz,7 KW RF power amplifiers developed under IIFC.

KEYWORDS: *Accelerator, EPICS, fast protection and interlock, RF, VME64X*

*Author for Correspondence: Sujo C. I.
E-mail: sujo@barc.gov.in

Introduction

ACnD has designed, developed and installed RF Protection and Interlock system which protects high power RF components, such as, RF windows, Couplers, RF power sources, waveguide, RF cavity etc. of an accelerator facility. RFPI system monitors sensor outputs installed in these sub-systems as well as status signals from other sub-systems, such as vaccum and cooling in an accelerator. Upon detecting a fault, it switches OFF RF input to the RF power source within 1-2us. RFPI system has been installed at LEHIPA, BARC and at HTS, RRCAT. Two RFPI systems have been delivered to Fermilab, USA under IIFC.

RFPI Architecture

The RFPI system has been designed based on VME protocol and is modular and scalable in nature. 6U, single width modules have been fabricated and the system is easily expandable depending on the number of signals to be monitored. Each module has a VME carrier board and a rear carrier board which are same for all the modules and function specific mezzanine cards have been placed on the carrier boards.

Each mezzanine card (Fig.1) on the front carrier card can monitor four input signals on SMA connectors. RF signals, PMT signals, Field Emission Probe signals can be interfaced on the front mezzanine cards. Analog/digital/contact signals can be processed by RFPI system in the mezzanine cards placed on the rear carrier card. Analog and TTL outputs are available from these cards.

The RF signals have a dynamic range of 70 dB and the maximum RF input signal to the module is configured to be 0 dBm so that the sensor is in linear region of operation. Analog input/output signal level and digital input/output levels from the field are 5V to the module. The system is configurable for a particular accelerator facility depending on parameters and number of sensors to be monitored. The modules are connected to the master module through Inter Card Communication Bus and it is the master module which takes decision of switching off of the RF signal, by operating the RF switch, based on the firmware logic programmed. Four TTL output signals are available on the rear carrier card at LEMO connectors which can be interfaced to other sub-systems and also to control the RF switch which will control the RF power input to the high power RF system.

The RFPI system has been developed and realized using in-house expertise in hardware, firmware and software and have undergone significant quality assurance stages.

Function and Interfaces of RFPI system

As shown in Fig.2, RFPI system can be interfaced with signals from cavity, other subsystems such as Low Level RF (LLRF), RF power source, cryogenics, vaccum system, machine protection system etc. and also with sensors such as thermocouples, Resistance Temperature Detectors, water flow/airflow meters etc.

Fig.1: One RFPI module with four mezzanine cards.

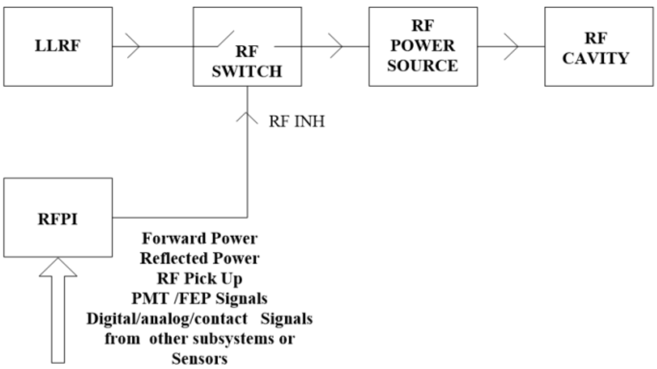

Fig.2: Interfaces of RFPI system to other systems.

If any of the monitored parameter develops a fault condition exceeding the set limit, RF switch placed at the output of LLRF is switched OFF within 1-2us, which inhibits RF signal from LLRF output to RF power source, thus protecting high power RF components (Fig.3). High isolation, absorptive type RF switch with response time better than 25ns has been selected for this purpose.

All the signals being monitored are digitised and are available for on-line monitoring at a rate of 10kS/s. All the interfaced signals are digitised at a frequency of 6.25MHz and the digitised values are continuously stored in a circular DDR3 memory. Each signal data is available for pre and post fault analysis for a duration of 1ms (Fig.4)

RFPI GUI

The operator of RFPI system has been provided with in-house developed Human Machine Interface (HMI) as shown in Fig.5. EPICS IOC is responsible for all the functionalities supported by the RFPI system including control, monitoring, data display and data collection for diagnostics. The RFPI EPICS IOC is deployed on the VME platform and interfaces to the FPGA. CSS based GUI has been developed, which provides different tabs for control, calibration and waveform data display.

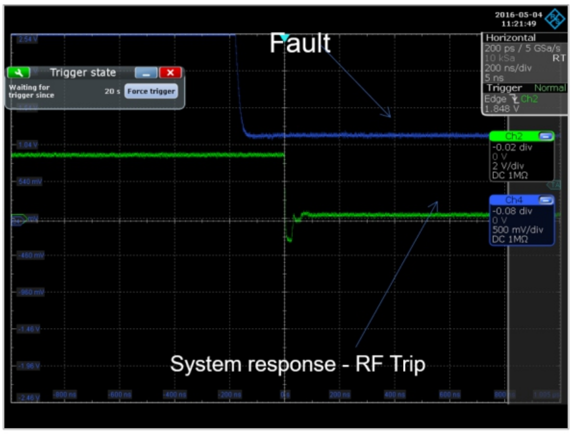

Fig.3: Time response of RFPI system < 200ns.

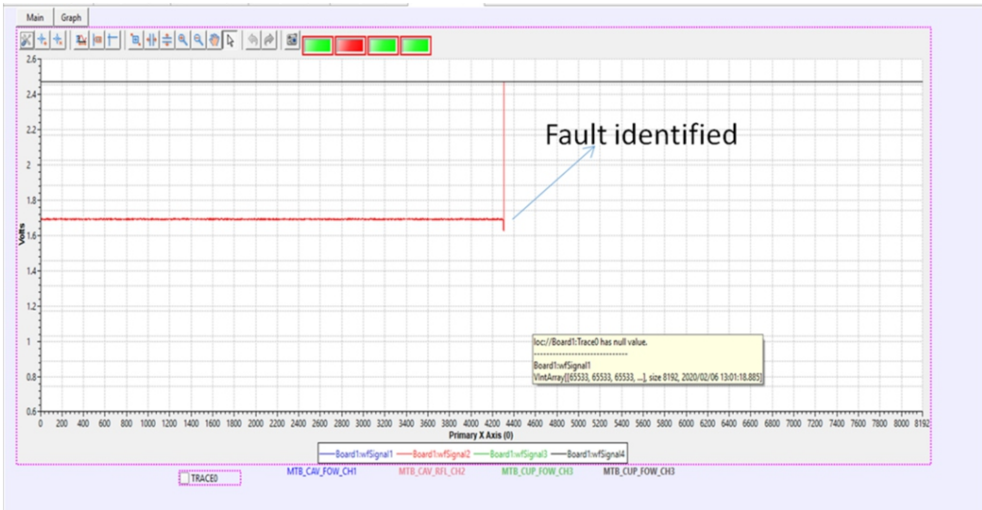

Fig.4: Pulsed RF signal data stored in DDR3 (x- axis gives number of data samples).

GUI features setting of control limit of each parameters monitored by RFPI system. The set limit can be controlled locally or remotely. The value of each parameter monitored is indicated on GUI in appropriate units. A provision has been kept in GUI to set cavity fill time which enables handling high reflected power during transient ON time in pulse mode of cavity operation. Digital inputs to RFPI are monitored and outputs under its control are also displayed. A calibration table has been provided for each monitored parameter so as to incorporate insertion loss or coupling factor of RF signals. Display of all parameters on same GUI panel eases fault diagnosis and arriving at quick conclusions in event of fault/trip. Provision to exclude a particular signal from being monitored and /or not to affect the output signal of RFPI has been implemented. The signal causing trip is also be indicated on the GUI.

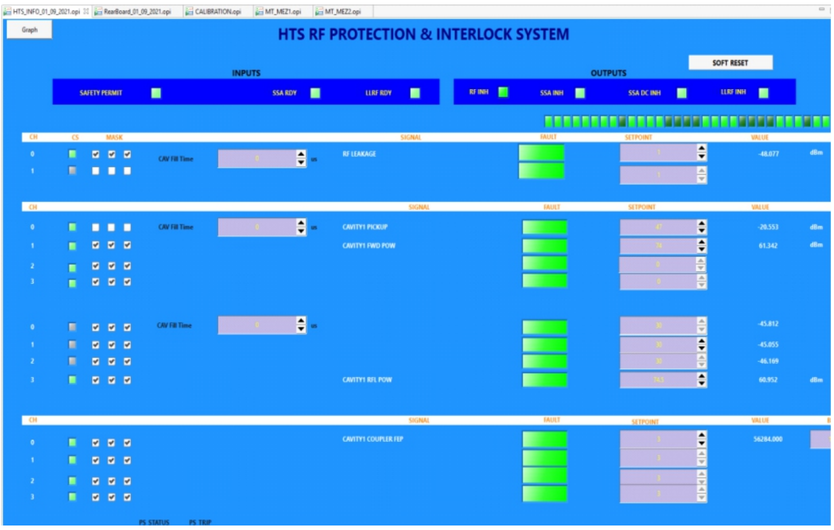

Fig.5: GUI of RFPI system.

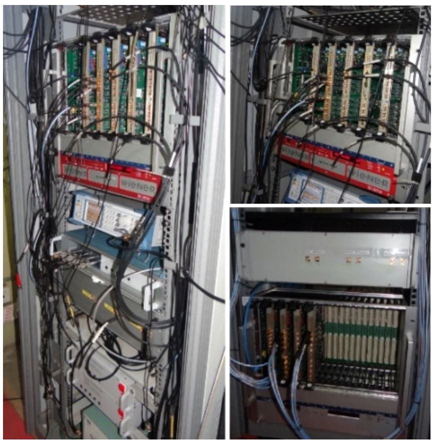

Fig.6: RFPI system for protection of RFQ, buncher and 10 MeV DTL.

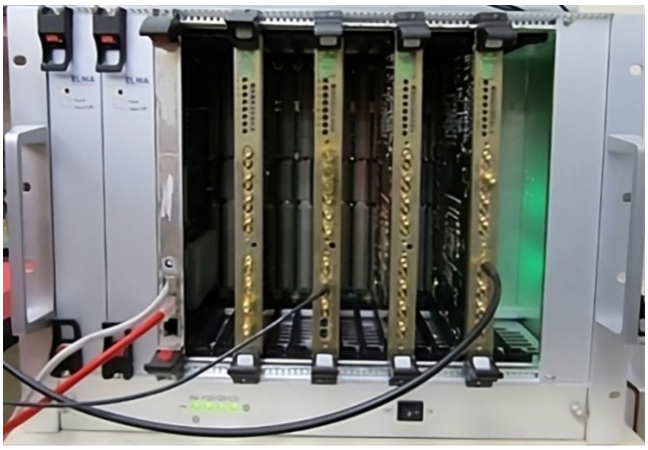

Fig.7: One RFPI system with four VME modules.

RFPI Systems at LEHIPA

RFPI system for LEHIPA has been designed such that each RF cavity is protected by one RFPI system. As LEHIPA has multiple cavities viz. Radio Frequency Quadrapole (RFQ), buncher, 10 MeV and 20MeV Drift Tube Linac (DTL)s, cascading of multiple RFPIS for multi-cavity protection is implemented. Hence, any fault arising in DTL system ceases RF input not only to DTL but also to buncher & RFQ thus avoiding possibility of damage due to beam from RFQ output to DTL.

At LEHIPA, RF signals (forward and reflected power) from directional couplers (placed at Magic Tee input and output), pick up signals from cavity, signals from PMTs mounted at RF windows, and RF load, water flow status etc. are interfaced with RFPI system. RFPI also has the capability to monitor Field Emission Probe signals, RF antenna signals, Digital input signals from other subsystems. Fig.6 shows the RFPI systems installed at LEHIPA. Identical scheme has been followed for RFQ, buncher and DTL cavities of LEHIPA.

More recent developments include addition of linear detection card which has better resolution to monitor RF signals compared to earlier versions. This card has been augmented into RFPI system for protection of 10 MeV DTL section of LEHIPA. Fig.7 shows one RFPI system housing four VME64X based modules. A fast protection action needed optimization of hardware design and firmware development for multiple modules. Modular architecture enables easy scalability to large number of different types of signals from multiple cavities in an accelerator.

Interlock Protection and Monitoring System (IPMS)

A 325 MHz, 7 kW solid state RF power amplifier has been developed and delivered by ACnD under IIFC [5] by combining power output of eight 1 kW RF power modules. An IPMS system [6] has been developed for the protection of the solid state RF amplifier, against any fault conditions. This involves monitoring RF, analog and digital signals from each 1 kW module of the amplifier. External signals such as water flow rate, ambient temperature and safety status signals are also being monitored. Logic interlocks [7] have been incorporated in the system for initialization of RF power amplifier depending on status signals from different subsystems like RFPI and

Fig.8: IPMS with controller.

personal protection system. If any of the parameter monitored exceeds or goes below the set limit, suitable protective actions are taken depending on the signal. All these objectives are achieved by integrating the high speed IPMS with RF power amplifier. IPMS is a VME64X based system which includes seven functional modules and monitors more than eighty parameters from the RF power amplifier.

Forward power, reflected power, drain current and voltage, gate voltage, status of DC power supplies, and temperature of each 1 kW module are monitored and displayed by IPMS. 14 bit ADCs are used to digitize the signals monitored, which are placed on mezzanine cards. The monitored signals are displayed continuously on a local display and also on a remote PC. If any of these parameters, deviates from the set value, corresponding power module is switched off. If more than one RF power modules deviates from set value, all the RF power modules and RF input signal to the driver amplifier are made OFF. The reasons for switching off of the power amplifier are indicated on the GUI, whereas the data acquisition continues for a pre-determined time. If the temperature of any RF module exceeds the set value, all the DC

Fig.9: In house developed GUI for IPMS.

power supplies and RF input to the driver amplifier are switched OFF. Ambient temperature, cooling water temp. and driver amplifier temp. are continuously monitored. Fig. 8 shows the IPMS system with VME controller in a 19" crate and Fig.9 shows in-house developed GUI.

Careful design, layout and component selection has been done so that the IPMS passed the qualification tests [8] such as conducted /radiated emissions and EM field immunity test (IEC 61000-4-6 & 4.3 and 6.3 &6.4), electrical fast transient/burst immunity and surge immunity (IEC 61000-4-4 and 4-5). Voltage dips, short interruptions & voltage variations as per IEC 61000-4-11, and vibration and drop tests IEC-60068-2-64 also were conducted. Industrial grade components have been selected for all the modules of IPMS so that ESS tests are passed as per standard IEC 60068-2-1, IEC 60068-2-2 and IEC 60068-2-14. Burn- in test was done at 40^{0}C for 48 hours integrated with RF power amplifier.

Acknowledgement

The authors sincerely acknowledge and appreciate the technical support received from Fermilab during design, technical discussions, and testing phases. Authors would like to acknowledge colleagues of IADD, BARC for testing of RFPI system at LEHIPA. Authors acknowledge colleagues of RRCAT, Indore for testing of system at HTS facility. In addition, authors also acknowledge Smt. C. D. Shinde, ACSS, ACnD for assistance in testing of RFPI and IPMS system. We also acknowledge colleagues of RFSS, ACnD and production team of IPMS at ECIL Hyderabad.

References

[1] Sujo. C. I., et al., "Description of RF Protection Interlock System for LEHIPA", Proceedings of Inpac2015 held at TIFR, Mumbai, 21-24th Dec 2015.

[2] Sujo. C. I., et al., "RF Protection Interlock System for Proton Linacs under Indian Institutions and Fermilab Collaboration", Proceedings of Inpac2018, RRCAT, Indore, 09th-12th Jan 2018.

[3] Rajesh Keshwani, et al., "Design Architecture of RF Interlock, Protection & Monitoring system for HTS control electronics", Proceedings of Inpac 2019 at IUAC Delhi, 18th-21st Nov, 2019.

[4] Rajesh Keshwani, et. al.,"Installation and Commissioning of RF Protection and Interlock System at HTS facility, RRCAT", Proceedings of InPac-2022 at VECC, Kolkata, 22nd-25th March 2022.

[5] Jim Steimel, et. al. "Development and Operation of PIP-II Injector Test, SSR1 Cryomodule, 325 MHz Amplifiers", JACoW SRF2021 (2022), doi: 10.18429/JACoW-SRF2021-MOPTEV01.

[6] R. T. Keshwani, et. al., "Design architecture of Interlock Protection and Monitoring System for 7KW Solid state RF power amplifier", Proceedings of Inpac2018 held at RRCAT, Indore 2018.

[7] Hitesh Shukla, et. al., "Firmware Architecture and Operational experience of Interlock Protection and Monitoring System (IPMS) for 7 KW, 352 MHz Solid State power amplifier for FNAL", Proceedings of Inpac 2019 at IUAC Delhi, 18 -21 Nov, 2019.

[8] Sujo. C. I., et al., "Features and Qualification tests of Interlock Protection and Monitoring System for 7 KW Solid state RF Power Amplifier", Proceedings of Inpac 2019 at IUAC Delhi, 18 -21 Nov, 2019.

किरणपुंज स्थिति अनुवीक्षक

4

जीएएनआईएल, फ्रांस में SPIRAL2 के रैखिक त्वरक हेतु कणपुंज स्थिति अनुवीक्षक इलेक्ट्रॉनिक्स प्रणाली का विकास एवं अधिचालन

गोपाल जोशी, *परेश डी. मोतीवाला, संदीप भराडे, जी.डी. रंदाले, आलोक आगाशे, पी. ज्योथि और श्याम मोहन

त्वरक नियंत्रण प्रभाग, भाभा परमाणु अनुसंधान केंद्र (भापअ केंद्र), ट्रांबे-400085, भारत

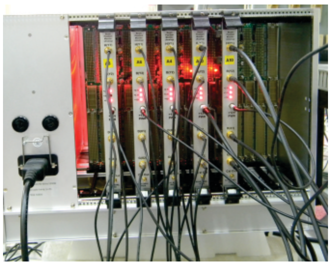

VME64 चेसीस में पांच बीपीएम मॉड्यूल

सारांश

भापअ केंद्र-टीआईएफआर और जीएएनआईएल के बीच "नाभिकीय भौतिकी, अनुसंधान और विकास सहयोग" हेतु समझौता ज्ञापन और भारतीय एवं फ्रांसीसी वैज्ञानिक संस्थानों के बीच संबद्ध अंतर्राष्ट्रीय प्रयोगशाला (एलआईए) अनुबंध के तहत त्वरक नियंत्रण प्रभाग (एसीएनडी), भापअ केंद्र में किरणपुंज स्थिति अनुवीक्षक (बीपीएम) इलेक्ट्रॉनिक्स और नियंत्रण का अभिकल्पन और विकास किया गया। प्रोटोटाइपिंग और परीक्षण के बाद, 20 बीपीएम इलेक्ट्रॉनिक सिस्टम बनाए गए और जीएएनआईएल, फ्रांस में SPIRAL2 के रैखिक त्वरक (लिनाक) में कमिशनन किया गया। बीपीएम प्रणाली न केवल बीम की स्थिति का मापन करती है, बल्कि त्वरक के प्रचालन के दौरान कणपुंज रेखा के चरण, आकार और तीव्रता का भी मापन करती है, SPIRAL2 एक उच्च तीव्रता वाला कण त्वरक है, जो दिसंबर 2021 से जीएएनआईएल में कमीशन हुआ और प्रचालनरत है।

Beam Position Monitor

4

Development & Commissioning of Beam Position Monitor Electronics Systems for LINAC of SPIRAL2 at GANIL, France

Gopal Joshi, *Paresh D. Motiwala, Sandeep Bharade, G. D. Randale, Alok Agashe, P. Jyothi and Shyam Mohan

Accelerator Control Division, Bhabha Atomic Research Centre (BARC), Trombay-400085, INDIA

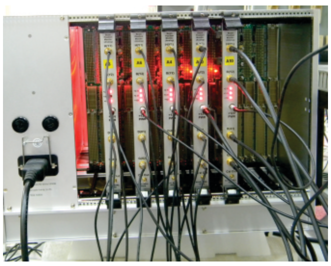

Five BPM modules in a VME64 chassis

ABSTRACT

Design and development of Beam Position Monitor (BPM) electronics and control was carried out at Accelerator Control Division (ACnD), BARC under the MOU between BARC-TIFR and GANIL for “Nuclear Physics, Research and Development Co-operation” and Associated International Laboratory (LIA) agreement between Indian and French scientific Institutes. Subsequent to prototyping and testing, 20 BPM electronic systems were fabricated and commissioned in the LINAC of SPIRAL2 at GANIL, France. BPM system performs the measurement of not only beam position, but also phase, shape and intensity of the beam line during the operation of the accelerator. SPIRAL2 is a high intensity particle accelerator commissioned and operational at GANIL since Dec 2021.

KEYWORDS: *Beam position monitor, Beam diagnostics, Auto-gain equalization.*

*Author for Correspondence: Paresh D. Motiwala
E-mail: parmot@barc.gov.in

Introduction

The LINAC of SPIRAL2 at GANIL, France uses non-intrusive, capacitive type Beam Position sensors and the related electronics. Accurate tuning of the LINAC is essential for the operation of SPIRAL2 and requires measurement of various vital beam parameters such as beam transverse (X-Y) position, phase of the beam with respect to the RF Reference, beam ellipticity, beam energy etc. with high precision and accuracy. BPM systems are being used for this purpose.

A BPM system typically consists of a sensor and associated electronics for processing these signals. BPM electronics system based on digital implementation incorporating a novel implementation of 'Auto-Gain Equalization' technique has been developed. It carries out measurement of various beam parameters over a wide dynamic range of beam current.

The electronics system has been designed, developed and commissioned at SPIRAL2 by ACnD, BARC jointly with GANIL team. The system performs processing at both the fundamental (88 MHz) and the first harmonic (176 MHZ). This article briefly discusses the system architecture, specifications and features of the BPM electronic system and results.

The Beam Position Monitor (BPM) System

SPIRAL2 at GANIL is a high intensity particle accelerator. The LINAC of SPIRAL2 is designed to accelerate 5 mA deuteron beams up to 40 MeV, proton beams up to 33 MeV and 1mA light and heavy ions up to 14.5 MeV/A. The LINAC is composed of two types of cryomodules, A and B for lower and higher energy sections, respectively. All the cavities of the LINAC operate at RF reference of 88.0525 MHz. There are twelve cryomodules of the type A and seven of type B as shown in Fig.1 [1]. One BPM sensor is placed before and after each of the cryomodules, making the total no. as twenty.

Each BPM system consists of a sensor portion and the signal readout & processing electronic module. Each BPM sensor consists of four electrode sensors that transduce the beam electromagnetic image into electrical signals. The electronics associated to each BPM sensor processes the electrical signals and enables the measurement of beam transverse position, phase, energy and transverse beam ellipticity.

The BPM electronic modules commissioned at SPIRAL2 LINAC are required to have the capability to perform the measurements using either the beam induced signal at fundamental frequency 88.052500 MHz (F) or at the first harmonic 176.1050 MHz (2F). Block diagram for the measurement principle is shown in Fig.2 [1]. The electronic processing system performs following measurements:

- Amplitude and phase w.r.t. the RF Reference.
- Amplitude and phase of the vector sum of the 4 electrode voltages of each BPM sensor.
- Phase shift between the vector sum of the four electrode voltages and the RF Reference frequency at, F and 2F.
- Horizontal and Vertical beam positions.
- Ellipticity of the beam.

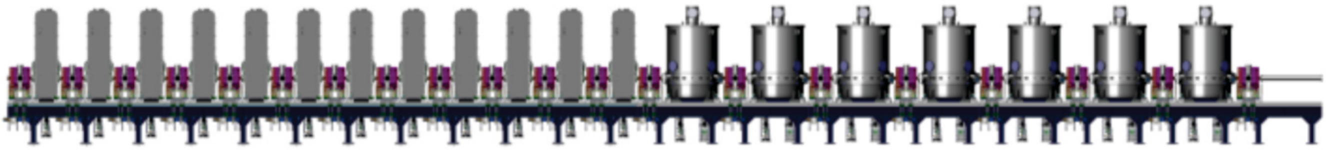
Courtesy GANIL, France

Fig.1: Layout of the 19 Cryomodules in LINAC of SPIRAL2 (12 of type A and 7 of type B).

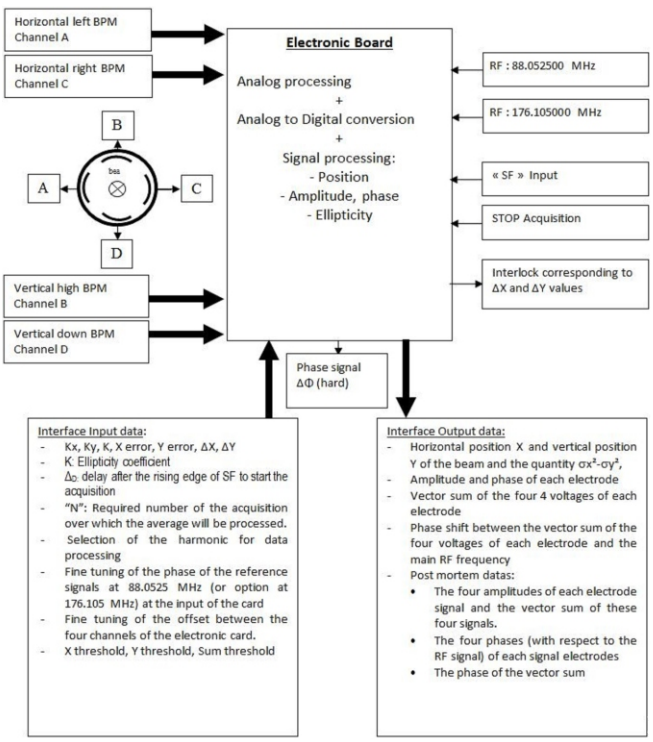

Fig.2: BPM measurement Principle.

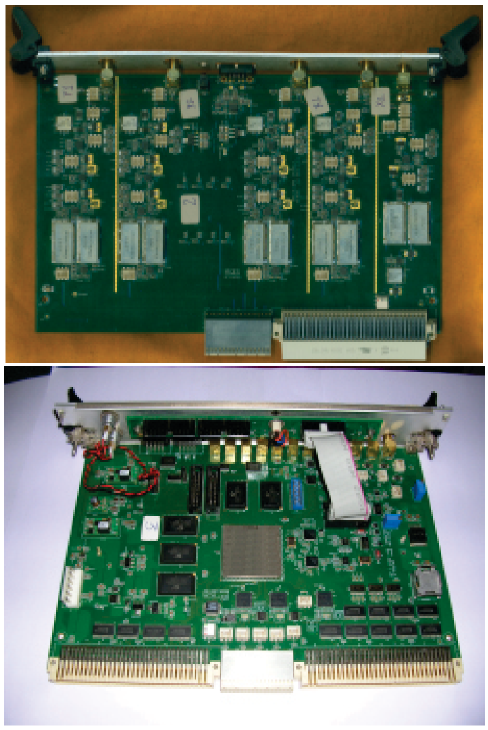

Fig.3: Analog and Digital boards comprise of one BPM electronic system.

Table 1: BPM measurement Specifications.

Parameter		
Position	± 50µm	Over ± 10 mm
Accuracy	± 150µm	Over ± 20 mm
Phase	± 0.5deg	±180 deg
Ellipticity	± 20%	-
Beam current		0.15 – 5 mA

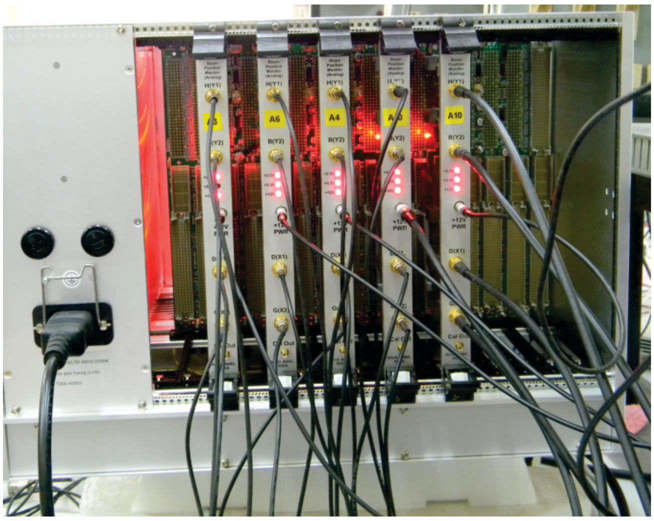

Fig.4: Five BPM modules in a VME64 chassis.

- Digital samples to reconstruct shape of the bunch from the signal received from a given electrode, over one RF Period.

General description of the BPM electronic module and sensor signal processing

The hardware of the BPM electronics system consists of a pair of VME64 based Analog and Digital boards (See Fig.3). The analog front end board conditions incoming signal from the sensors. The digital board consisting of high speed ADCs, DACs, FPGA and other devices, and processes the digitized signal and controls the overall operation of the module.

Each BPM sensor feeds an electronic module through eighty meter long coaxial cables. The electronic design is based on the novel scheme of auto-gain equalization using offset tone. The electronic module is able to work either at F or 2F frequencies to deliver the required measures. In this scheme the gain of different channels is equalized with respect to the internally generated and stabilized offset tone. This offset tone is added to each of the four incoming signals from BPM sensor and variation in the four channels compensated. The scheme of equalization is also effective in compensating the drift due temperature and ageing.

As far as electronic processing is concerned, the accuracy of position measurement is dependent on the ability to equalize the gain of the four channels. The various calculations are to be performed in the FPGA taking care that the addition of noise due to finite precision is kept low enough such that it does not degrade the signal to noise ratio significantly.

Regarding the phase measurement- the phases of both the RF reference and the electrode signals are measured with respect to a common reference signal. Even though the phase of either of these signals change, depending on the phase of

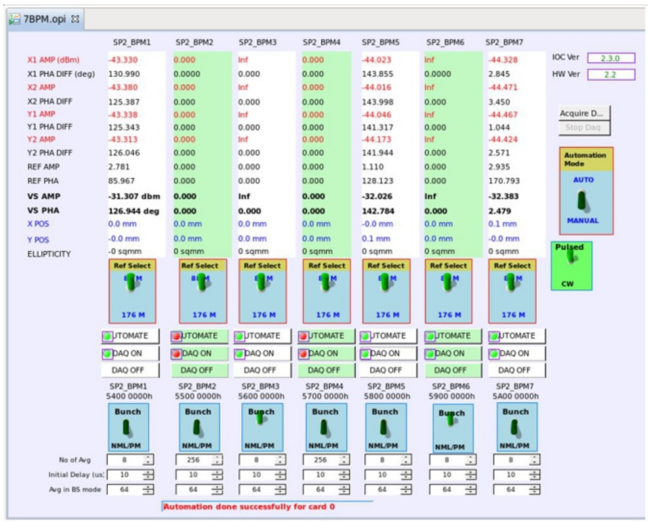

Fig.5: Command control application screen for control of 7 BPM systems.

the common reference, the difference of phase between the measured signal and the selected RF reference remains unambiguous. Fig.4 shows a VME64 chassis holding five BPM electronic modules. Fig.5 shows screen shot of the front end software application developed using EPICS platform supporting 7 BPM modules.

BPM data acquisition modes

The BPM system supports extensive data acquisition schemes viz; Normal, Post mortem & Bunch shape reconstruction for diagnostic as well as during the system operation. The Normal mode of acquisition makes available various beam parameter measures at the rate of 1 kHz to the command control via the EPICS IOC. In the Post mortem mode data acquisition is very useful in case of system malfunction. A unique acquisition mode for reconstruction of the beam bunch shape has been incorporated in the system. The BPM system is able to deliver the pulse shape of the beam bunch over one RF period (11.356 ns) by acquiring 256 samples in 345 clock cycles resulting into an effective sampling rate of 44.36 ps. These samples are arranged in the software to form one period of the bunch shape which is as narrow as 11.356 ns. See Fig.13.

BPM Tests on the SPIRAL2 Intermediate Test Bench (ITB)

Before characterizing the BPM system in the "Intermediate Tests Bench" (ITB) assembled at GANIL, the BPM

Fig.6: BPM characterization test bench at ACnD, BARC.

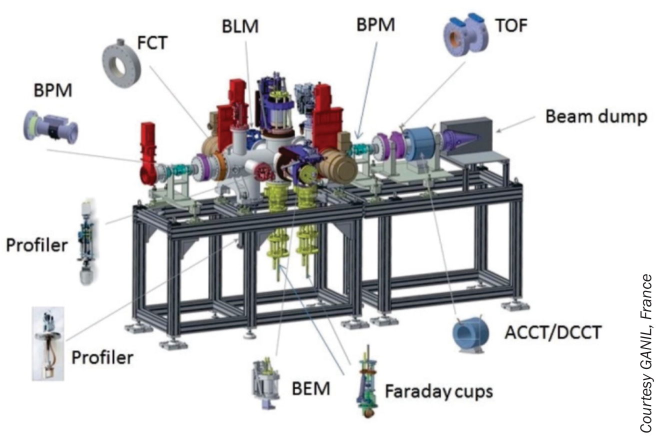

Fig.7: ITB at GAINL for testing various beam diagnostic equipment including BPM.

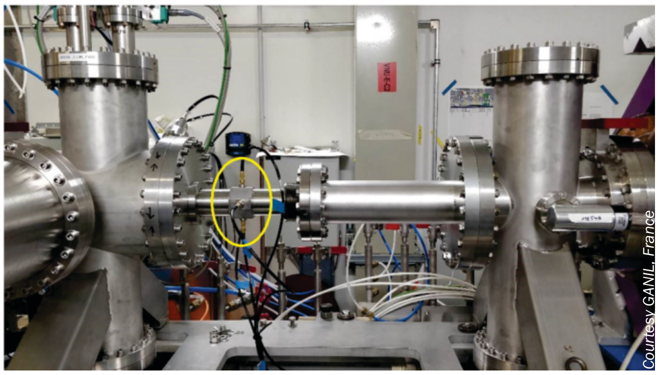

Fig.8: BPM sensor installed in MEBT line.

electronic was tested using precision test bench at ACnD. Fig.6 shows the characterization test bench having a resolution better than 25 μm. The BPM system was subsequently installed with the ITB at GANIL as a part of the injector commissioning plan. The aim of the ITB was to fully characterize the properties of the beam accelerated by the RFQ and also to study the behaviour of the diagnostic elements including the BPM developed at ACnD, BARC. All kinds of measurements were carried out; beam intensity, transverse beam position, profiles and emittance, phase and longitudinal emittance with a beam energy equal to 750KeV/A. Control command operation gathered the measurements performed by all these diagnostics almost on real time (every 200ms). Fig.7 shows the ITB.

BPM Current dynamic range

The first tests of the BPM and its associated electronics was to check the beam current dynamic range over which the BPM electronics is working properly. The dynamic range was observed to be 75μA - 5.5mA at 88MHz and 60μA – 5.5mA at 176MHz.

BPM phase measurement

The phase relative to the accelerating RF signal has been measured simultaneously by the BPM and by one of the three

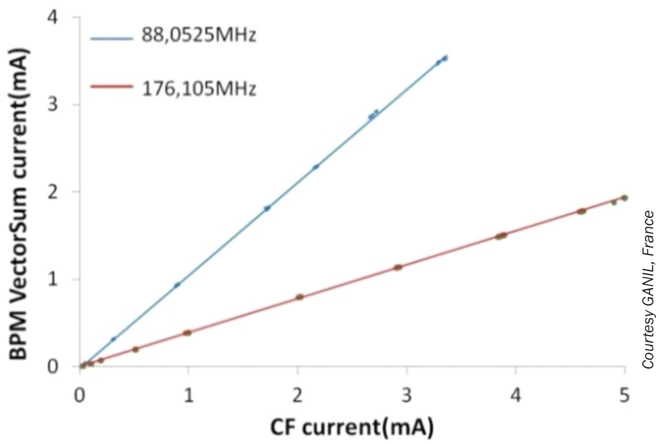

Fig.9: Beam current dynamic range.

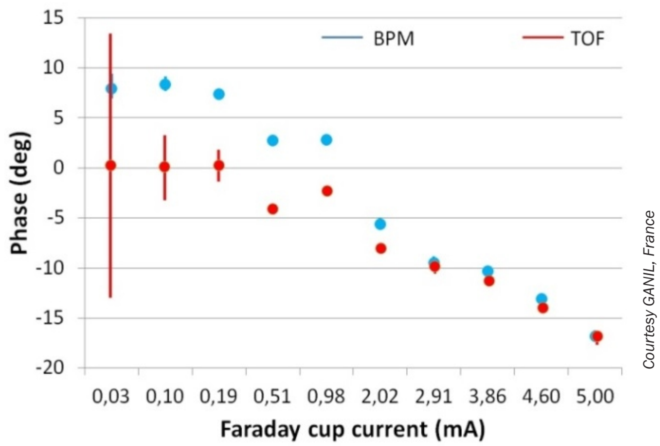

Fig.10: Beam phase measurement by a BPM and TOF probe at 88.0525MHz.

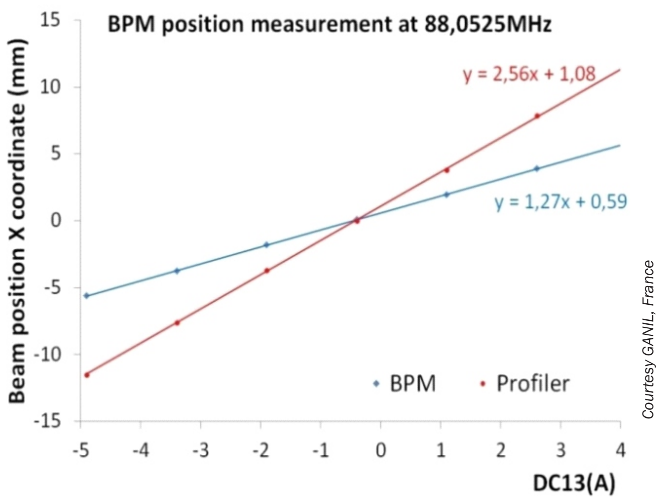

Fig.11: Beam position measurement at 88.0525MHz using BPM and beam profiler.

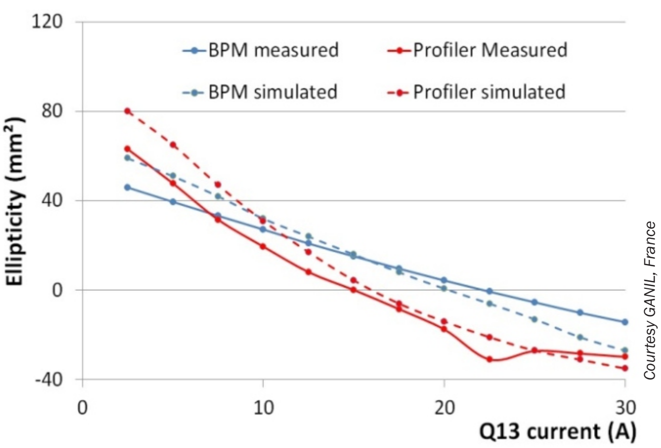

Fig.12: beam ellipticity measurement at 88.0525MHz.

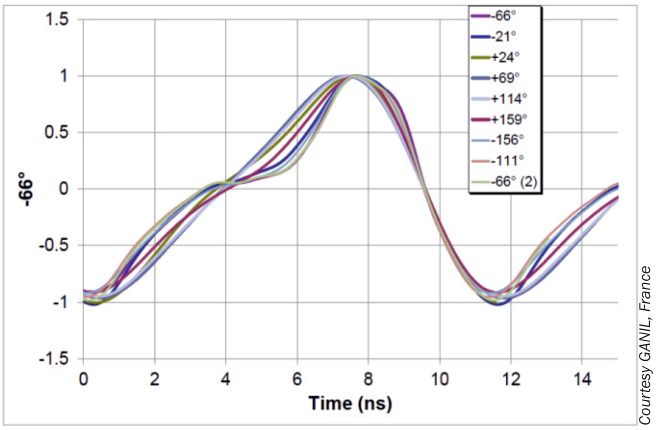

Fig.13: Reconstructed bunch shape construction at different phases for 1mA beam current.

electrostatic P.U. electrodes of the time of flight (TOF) energy measurement system mounted on the ITB. The BPM is measuring the phase at F and 2F whereas the TOF is only measuring it at F. The results showed a proper behaviour and a good agreement with the electrode of the TOF system over the measured beam current dynamic range.

Beam position measurements

The beam position measurements were simultaneously performed by the BPM and the secondary emission monitor (SEM) profiler (pulsed mode operation) located after a drift space downstream in the ITB. The results obtained with the BPM measurements at F and 2F have been compared to the profiler measurements (frequency independent). It was observed that the response of the BPM over the required range was satisfactory. The BPM position sensitivity remains roughly constant over the current dynamic range.

Fig.15: 8 of the 20 BPM modules at SPIRAL2 LINAC tunnel.

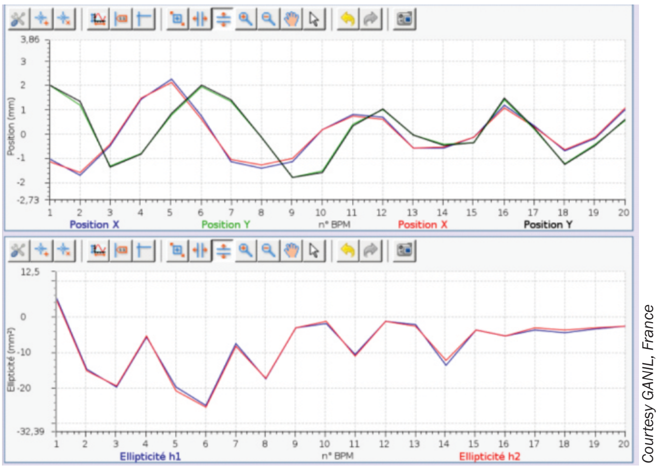

Fig.14: Beam position and ellipticity measurements by 20 BPM system.

BPM Ellipticity measurement

The linear behaviour of the BPM ellipticity was confirmed by the measurement at 88MHz and 176MHz.

Software Command Control

The command control application has been developed using the EPICS DAQ platform. The system adheres to SPIRAL2 command control architecture. The EPICS device support, record support and bpm custom record have been implemented such that one IOC supports 7 BPM systems per each VME chassis.

BPM Operation Results

The BPM systems are in regular operation in the SPIRAL2 LINAC. The performance of all the 20 BPM systems for a proton beam of 4.1mA, energy 31.9MeV and power 10kW is shown Fig.14.

Conclusion

The BPM electronic system designed at ACnD, BARC have undergone extensive testing in the lab and then at SPIRAL2 facility. Before commissioning 20 BPM systems at GANIL it has undergone 2-3 phases of prototyping. Various performance related parameters such as RMS noise, cross coupling, linearity, dynamic range, calibration constants, etc. have been measured / computed to ascertain system performance. The fabrication of multi-layer PCBs and assembly of SMD components during the prototyping and delivery phases were done using internationally accepted standards by an Indian MSME firm.

The team at GANIL has been very helpful during the prototyping and commissioning phases. They facilitated testing by collecting enormous amount of data, processing and presenting in suitably in reports. This has helped us to improve the performance of the system. The 20 BPM systems are currently operational in the LINAC of SPIRAL2 and enabling smooth operation of the accelerator.

Acknowledgment

It is a pleasure to acknowledge the constant support of all the colleagues from ACnD, the SPIRAL2 team and the IPNO team during prototyping, testing and commissioning of the BPM systems.

References

[1] “Technical Specifications of the Electronics for the BPM of the SPIRAL2 LINAC”, SPIRAL2 document 'SP2_CC_8234_lo18118V1.0, SPIRAL2, GANIL.

[2] G. Joshi et al., “An offset tone based gain stabilization technique for mixed-signal RF measurement systems”, Nucl. Instr. Meth., vol.A 795, 2015, pp. 399-408

[3] M. Ben abdillah et al., “Development of Beam Position Monitors for the SPIRAL2 LINAC”, in Proc. 1st Int. Beam Instrumentation Conf. (IBIC'12), Tsukuba, Japan, October 2012, paper TUPA18, pp. 374-377.

[4] P.Ausset et al., “Development of the Beam Position Monitors system for the LINAC of SPIRAL2”, in Proc. 2nd Int. Beam Instrumentation Conf. (IBIC'13), Oxford, UK, Sep 2013, paper WEPC15, pp. 702-705.

[5] R.E.Shafer, “Beam Position Monitor Sensitivity for Low-β Beams”, in Proc. 17th Linac Conf. (LINAC'94), Tsukuba, Japan, August 1994, paper THPA84, pp. 905-907.

[6] P.D. Motiwala et al., “Beam Position Monitoring System for LEHIPA”, in InPAC-2015, Dec-2015, TIFR, Mumbai.

[7] P. Ausset et al., “OPERATION OF THE BEAM POSITION MONITOR FOR THE SPIRAL2 LINAC ON THE TEST BENCH OF THE RFQ”, International Beam Instrumentation Conference (IBIC) 2016, Barcelona, Spain

[8] G.D. Randale et al., “Performance analysis of BPM electronics for SPIRAL2, GANIL, FRANCE”, InPAC 2019, Nov 18-21 2019, IUAC, New Delhi.

उच्च तीव्रता प्रोटॉन त्वरक

5

अतिचालकता और सामान्य चालकता गुहिका के लिए आरएफ कैविटी एम्युलेटर

*राधिका नासेरी, संदीप भराडे, आलोक आगाशे, एम.वाई. दीक्षित एवं गोपाल जोशी
त्वरक नियंत्रण प्रभाग, भाभा परमाणु अनुसंधान केंद्र (भापअ केंद्र), ट्रांबे-400085, भारत

एम्युलेटर के साथ एलएलआरएफ एकीकरण

सारांश

निम्नस्तरीय आर एफ (एलएलआरएफ) प्रणाली के साथ एकीकृत परीक्षण के लिए एक आरएफ गुहा अनुकरणकर्ता विकसित किया गया है। गुहा मॉडल को एफपीजीए पर डिजिटल में लागू किया गया है और इसमें मौलिक गुहा गतिशीलता मोड, डिट्यूनिंग मॉडल, विलंब मॉडल और इलेक्ट्रोमैकेनिकल मोड शामिल है। आरएफ गुहा के मापदंड, जैसेकि गुहा आवृत्ति, गुणवत्ताकारक, युग्मनकारक और डिट्यूनिंग , को प्रोग्राम करने योग्य रखा गया है ताकि सुपर कंडक्टिंग और सामान्य संचालन गुहिकाएँ दोनों के व्यापक मापदंडों की श्रृंखला के व्यवहार का अनुकरण किया जा सके। एलएलआरएफ के साथ एकीकृत परीक्षण सफलतापूर्वक निष्पादित किया गया और परिणाम प्रस्तुत किए गए।

High Intensity Proton Accelerator

5

RF Cavity Emulator for Superconducting and Normal Conducting Cavity

***Radhika Nasery, Sandeep Bharade, Alok Agashe, M. Y. Dixit and Gopal Joshi**
Accelerator Control Division, Bhabha Atomic Research Centre (BARC), Trombay-400085, INDIA

LLRF integration with Emulator

ABSTRACT

A RF cavity emulator is developed for integrated testing with Low Level RF (LLRF) system. Cavity model is implemented in digital on FPGA and includes cavity dynamics of fundamental mode, detuning model, delay model and electromechanical modes. RF cavity parameters such as cavity frequency, quality factor, coupling factor and detuning are kept programmable to emulate behaviour over wide range of these RF parameters covering both, superconducting and normal conducting cavities. Integrated testing with LLRF is successfully performed and the results are presented.

KEYWORDS: *RF cavity emulator, LLRF, Controls, Signal Processing, Particle Accelerator*

**Author for Correspondence: Radhika Nasery*
E-mail: radhikan@barc.gov.in

Introduction

Accelerator Control Division (ACnD) is involved in design, development and commissioning of Low Level RF(LLRF) control system for a number of accelerators, including Low Energy High Intensity Proton Accelerator (LEHIPA) at BARC [1], Horizontal Test Stand (HTS) at RRCAT [2] and BARC-TIFR Superconducting Linac [3]. LLRF systems monitor, control and regulate the amplitude, phase and frequency of cavity RF fields in particle accelerators. LLRF signal processing algorithms are designed in digital domain to monitor the change in the RF field of cavity and to provide feedback and/or feed-forward regulations depending on system configuration and operational scenarios such as type of RF cavity : superconducting or normal, pulse width of operation, beam-loading effect, amplifier characteristics etc. Testing LLRF and control algorithms directly at plant is not only difficult but also undesirable as it involves interfacing with sensitive and costly entities such as RF cavities and RF power amplifiers. With this motivation, RF cavity emulator is developed. Fig.1 shows the simplified block diagram for testing LLRF with cavity emulator.

Using the emulator, LLRF systems and the control algorithms can be thoroughly tested in the lab before commissioning in the plant. The RF cavity model implemented in digital domain provides for programmability of cavity parameters. Cavity pickup and reflected power drives are generated for normal conducting cavities which are deployed at LEHIPA, BARC and for superconducting cavity commissioned at HTS, RRCAT. The article presents the architecture, signal processing flow and implementation aspects of RF cavity emulator. Results are illustrated in the form of pickup and reflected power for normal conducting as well as superconducting cavity. Integrated testing with LLRF system is also demonstrated.

Architecture and Implementation

The cavity emulator is cPCI crate based and its signal processing chain [1] shown in Fig.2 consists of ADC, FPGA, DAC and modulator. It takes the outputs from LLRF i.e. RF forward power drive and generates pickup and reflected power. The Forward Power output of LLRF is digitized using direct sampled ADC, using a clock that is derived from the Reference clock, and processed in FPGA. RF cavity emulator is implemented using cavity equation [3] given by:

$$\ddot{V_c} + 2 * w_{\frac{1}{2}} * \dot{V_c} + w_0^2 * V_c = w_{\frac{1}{2}}\dot{U}$$

Where V_c is cavity voltage, $w_{1/2}$ is cavity half bandwidth, w_0 is resonant frequency of the RF cavity and U is the normalized input drive to the cavity. The continuous time equation is first expressed in in-phase and quadrature signals in the base-band and subsequently transformed to discrete time and implemented on the FPGA. The in-phase and quadrature components of the drive are the inputs to this model. The output of the model is the in-phase and quadrature signal of the Pickup. The in-phase and quadrature components of the reflected signal are generated by subtracting the drive signal from the pick-up. Reflected Power and Pick-up signals in the base-band are fed to DACs. The analog outputs of the DACS are up-converted to RF in a quadrature modulator. RF reference signal feeds the RF port of the modulator. This model is for fundamental mode of the RF cavity. Quality Factor, Frequency, coupling factor and detuning are the programmable parameters of the model.

Results of Normal Conducting Cavity

The RF cavity emulator for normal conducting cavity is modeled after Drift Tube Linac of LEHIPA with a frequency of 352 MHz, Quality Factor of 38000, coupling factor of 2 [4]. All the parameters are programmable to model plant conditions. Fig.3 and Fig.4 show Pickup Power and Reflected Power RF signals on oscilloscope.

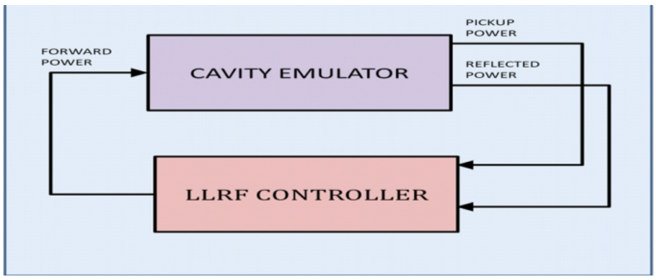

Fig.1: Testing of LLRF with Cavity Emulator.

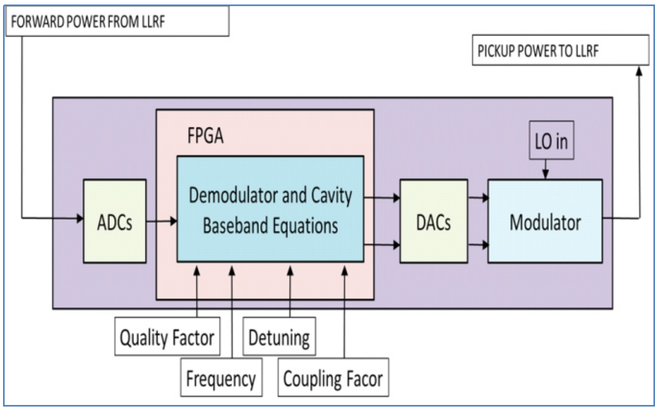

Fig.2: Signal Processing chain of RF cavity.

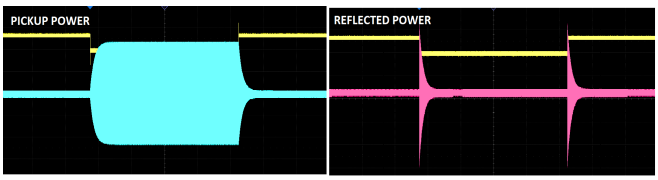

Fig.3: Normal conducting cavity with no detuning.

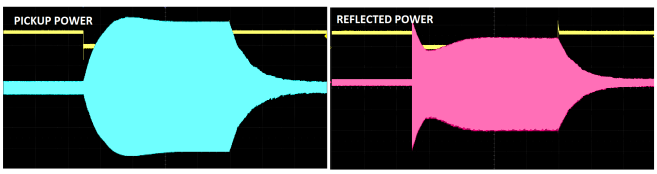

*Fig.4: Normal conducting cavity with a detuning of 2*$w_{1/2}$.*

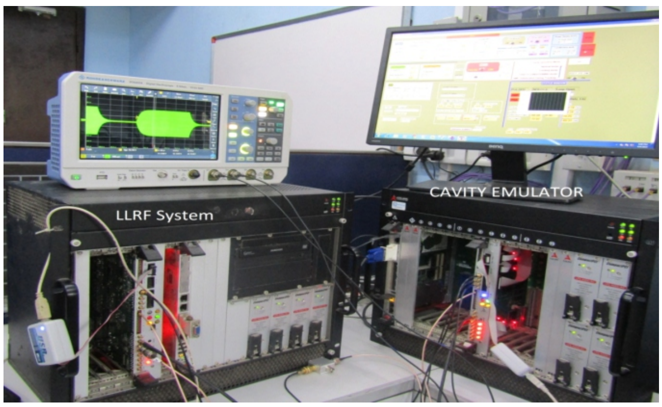

Fig.5: LLRF integration with Emulator.

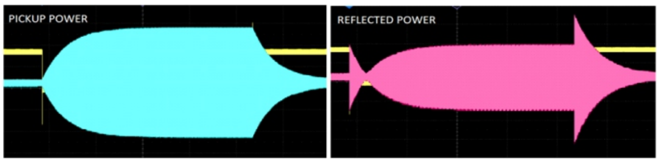

Fig.6: Superconducting cavity with no detuning.

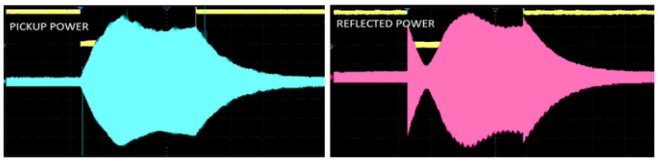

Fig.7: Superconducting cavity with Electromechanical mode at 100 Hz.

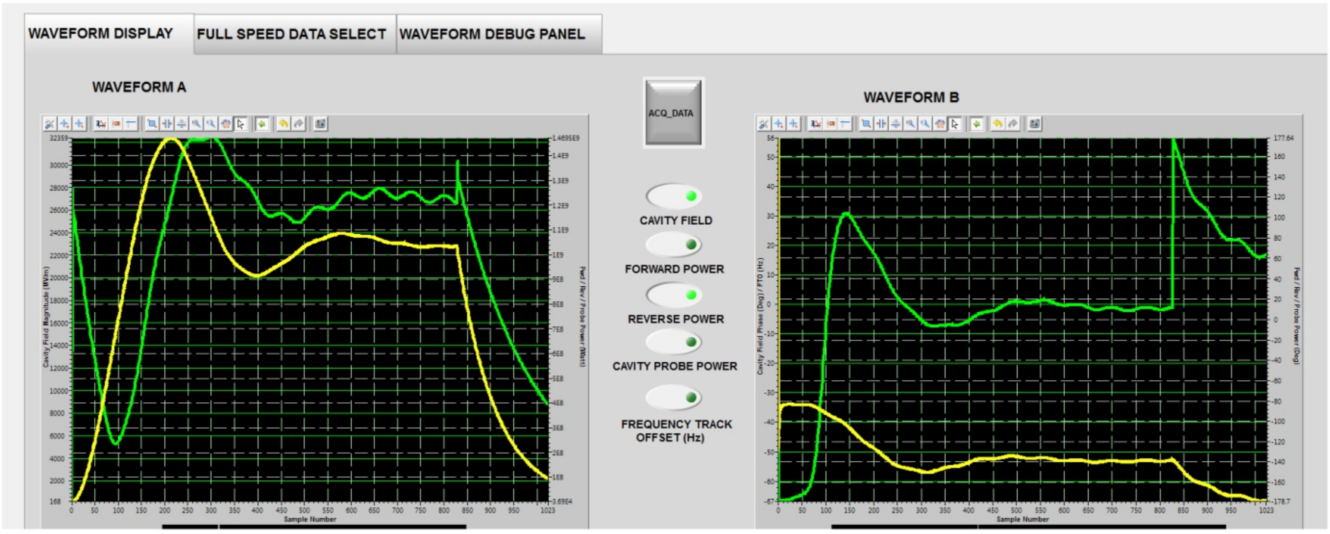

Fig.8: LLRF GUI with Reflected Power and Pickup Power.

Results of Super Conducting Cavity

The RF cavity emulator for a superconducting cavity is modeled after AES-010 [5] Superconducting RF cavity at HTS, RRCAT of 650 MHz with quality factor of $2*10^{10}$, coupling factor of 1000 and with no detuning. Fig.6 shows the successful implementation of emulator for superconducting cavity with Pickup Power and Reflected Power RF signals on oscilloscope.

Electromechanical dynamics of superconducting RF cavities cause detuning, called Lorentz force detuning (LFD), which is given by the equation given below [3].

$$\Delta\ddot{w}_1 + \frac{w_1}{Q_1}\Delta\dot{w}_1 + w_1^2\Delta w_1 = -k_1 {V_{cav}}^2 w_1^2$$

Where w_1 is the resonance frequency of mechanical mode, Q_1 is the Quality factor of mechanical mode 1, k_1 is the dynamic detuning coefficient of mode 1, V_{cav} is the cavity voltage. Detuning effects of LFD are also implemented in the cavity emulator and Fig.7 shows the results.

Conclusion

RF cavity emulator has been successfully developed and demonstrated for normal conducting cavity as well as for superconducting cavity with electromechanical modes. Integrated testing with cPCI based LLRF system developed for LEHIPA DTL normal conducting cavity 352 MHz is successfully carried out. Integrated testing with LLRF system developed for HTS, RRCAT superconducting cavity of 650 MHz is tested. Using this emulator, resonance control system's detuning correction algorithms are being tested.

References

[1] Alok Agashe, P.D. Motiwala, S.K. Bharade, Shyam Mohan and Gopal Joshi, "Digital LLRF System for RFQ" InPac2015, Mumbai, India.

[2] Nibandh Kumar Shahi, Paresh Motiwala, Radhika Nasery, Rajesh Keshwani, C.I. Sujo, Sandeep Bharade, Gopal Joshi, Dheeraj Sharma, Ekansh Mishra "Commissioning of LLRF system for control of field in AES-10 SCRF cavity in HTS at RRCAT", InPAC2022, Kolkata, India.

[3] Gopal Joshi et al., "Development of the Model of a Self Excited Loop," PAC' 09, Canada.

[4] Shweta Roy (2015), "Physics Design and Prototype Development of Drift Tube Linac Cavity for High Current Applications", Homi Bhabha National Institute.

[5] A. Sukhanov et al., "STC QUALIFICATION TESTS OF PIP-II HB 650 CAVITIES", 20th Int. Conf. on RF Superconductivity, USA.

ठोस-अवस्था प्रवर्धक

6

त्वरकों के लिए यूएचएफ में kW और MW स्तर की ठोस-अवस्था प्रवर्धक प्रणालियाँ

*जे.के. मिश्रा, बी.वी. रामाराव, संदीप श्रोत्रिय, स्निग्धा सिंह, एस.एस. जेना, निरंजन पटेल, शिजू ए., एस. मुथु, मंजिरी पांडे और गोपाल जोशी

त्वरक नियंत्रण प्रभाग, भाभा परमाणु अनुसंधान केंद्र (भापअ केंद्र), ट्रांबे-400085, भारत

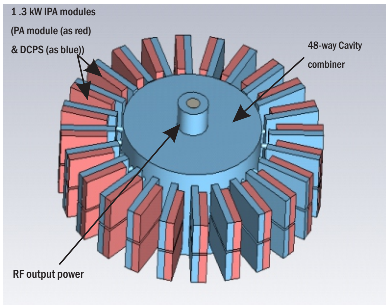

50 kW, 325 MHz SSA HPRF सेक्शन की व्यवस्था

सारांश

ठोस अवस्था प्रवर्धक (एसएसए) तकनीक अत्यन्त प्रमापीय, रेडियो आवृत्ति (आरएफ) सामर्थ्य विस्तार योग्य, कम वोल्टता पर प्रचालित, और आकर्षक निम्नीकरण जैसी सुविधा प्रदान करती है। ये विशेषताएं इसे सामान्य तथा अतिचालक गुहिकाओं पर आधारित त्वरकों के लिए उपयुक्त बनाती है। भापअ केंद्र ने स्वयं और अपने सहयोगात्मक कार्यक्रमों के लिए एसएसए तकनीक के विकास पर सफलतापूर्वक कार्य किया है। एसएसए प्रौद्योगिकी के विकास की इन गतिविधियों के परिणाम स्वरूप विभिन्न रेडियो आवृत्तियों पर कुछ वाट से लेकर 20 किलोवाट तक उच्च शक्ति प्रवर्धकों का विकास किया गया है। मासफेट और सर्कुलेटर जैसे घटकों के अतिरिक्त, इस एसएसए तकनीक का विकास पूर्णतः स्वदेशी है। अभिकल्पन और एकीकरण की मौलिक पद्धतियों की मदद से, एसएसए की कुल सामर्थ्य, सामर्थ्य घनत्व, प्रतिवाट लागत, उपलब्धता आदि जैसे मापदंडों में सुधार किया जा सकता है। भापअ केंद्र , पऊवि ने अपना महत्वाकांक्षी, स्वदेशी रेडियो आवृत्ति (आरएफ) त्वरक कार्यक्रम शुरू किया है, जो किरणपुंज त्वरण के लिए रेडियो आवृत्ति (आरएफ) सामर्थ्य की मदद से गुहिकाओं में विद्युतचुम्बकीय क्षेत्र स्थापित करता है। इसलिए, एक नई अनुसन्धान और विकास गतिविधि के रूप में, आरएफ शक्ति की घरेलू आवश्यकताओं को पूरा करने के लिए किलोवाट एवं मेगावाट स्तर के एसएसए तंत्रों की सकंल्पना की गई है। मध्यम ऊर्जा, उच्च तीव्रता वाले प्रोटॉन त्वरक (मेहिपा) के लिए 325 मेगाहर्टज पर 50 किलोवाट के और रेडियो आवृत्ति चतुर्ध्रुव (आर एफ क्यू) या बहाव नलिका लिनैक (डी टी एल) के लिए 325 मेगाहर्टज पर 280 किलोवाट के स्वदेशी एसएसए विकास की सकंल्पनात्मक अभिकल्पन योजना को अंतिम रूप दिया गया है। अनुसन्धान और विकास के प्रयासों के इसी क्रम में, सामान्य प्रचालक आधारित त्वरक के लिए 352/325 मेगाहर्टज पर 1 मेगावाट के एसएसए की भी सकंल्पना की गई है। इन सभी स्वदेशी एसएसए तंत्रों की वैचारिक अभिकल्पन योजनाओं की चर्चा को इस लेख के माध्यम से प्रस्तुत किया गया है।

Solid-state Amplifier

6

Solid-State Amplifier Systems of kW and MW level at UHF for Accelerators

***J. K. Mishra, B. V. Ramarao, Sandip Shrotriya, Snigdha Singh, S. S. Jena, Niranjan Patel, Shiju A., S. Muthu, Manjiri Pande and Gopal Joshi**

Accelerator Control Division, Bhabha Atomic Research Centre (BARC), Trombay-400085, INDIA

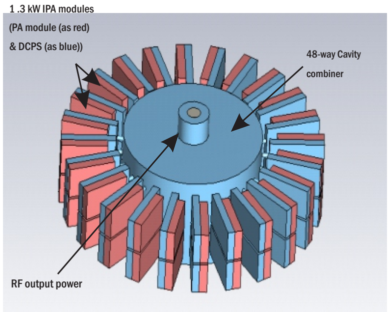

Arrangement of HPRF section of 50 kW, 325 MHZ SSA

ABSTRACT

Solid state amplifier (SSA) technology is highly modular, scalable in radio frequency (RF) power, has low voltage operation and offers graceful degradation. These features make it technology of choice for both normal and superconducting cavity based accelerators. BARC has worked successfully on SSA technology for its own program and for collaboration program. These development activities on SSA technology have led to the development of high power amplifiers starting from few watts to 20 kW at different frequencies. This SSA technology is indigenous except for basic components like MOSFET, circulator etc. With the help of innovative design and integration methodologies, the SSA parameters such as overall power rating, power density, cost/W, availability etc. can be improved. BARC, DAE has launched its ambitious domestic radio frequency (RF) accelerators program, which uses RF power at various levels to set up RF field in RF cavities for beam acceleration. So, as a new research and development activity, SSA systems in kW and MW level is conceptualized to cater to this domestic RF power need. Conceptual design scheme of indigenous 50 kW SSA at 325 MHz for medium energy high intensity proton accelerator (MEHIPA) and 280 kW SSAs for radio frequency quadrupole (RFQ) or Drift Tube LINAC (DTL), at 352/325 MHz is finalized. In continuation of same R&D efforts, a 1 MW SSA at 352/325 MHz for normal conducting accelerator has also been conceptualized. The conceptual design schemes of all these indigenous SSAs are discussed and presented in this article.

KEYWORDS: *ADS, AC to RF efficiency, MTBF, Particle Accelerator, Power divider and combiner, Solid State*

*Author for Correspondence: J. K. Mishra
E-mail: jkmishra@barc.gov.in

Introduction

Application areas of accelerators include basic sciences, energy, medical, and security systems. Accelerator development in a country is one of its defining parameter to measure technological advancement. Radio frequency (RF) linear accelerator (LINAC) for accelerator driven sub critical system (ADS) is being developed at Bhabha Atomic Research Centre (BARC) as a multi-phase program. One of the major research and development (R&D) activity involves development of high power RF (HPRF) systems for Indian accelerator program and DAE's international collaborations. Worldwide, international laboratories including ANL [1][2], BARC [3][4][5], RRCAT are pursuing HPRF systems based on SSA technology among other options. With innovative ideas and advance design techniques, BARC has designed and developed high power solid state amplifier (SSA) systems with acclaimed performance specifications for accelerator application. This article presents conceptual design scheme (CDS) of SSA inclusive of its architecture, innovative integration and layout schemes for three SSAs of RF power levels 50 kW, 280 kW and 1 MW having features like high efficiency, compactness and ruggedness.

The guiding factors of CDS of SSA

Theme of this CDS is based on four I's i.e. ideas, innovate, implement and indigenise for self-reliance in high power SSA technology. In SSA, with the help of these four I's, four C's can be achieved i.e. comprehensive design, cost effectiveness, compactness and competitive performance.

The important features of SSAs designed and developed at BARC are high efficiency performance (~54 to 55% wall plug efficiency), compact design (approximately 13.7 kW/m^3 power density), cost effective implementation, compliance to international standards (EMI/EMC and vibration standards) [5] and, reliable operation. Efforts are made to constantly improve SSA performance parameters by innovative design efforts. SSA R&D for the RF accelerators presented in this article will highlight these efforts, which incorporate innovative design methodologies, new ideas of system integration and implement them to achieve better performance.

Conceptual Design of kW/MW SSAs

Medium energy high intensity proton accelerator (MEHIPA) phase 1 is an accelerator program to develop a 40 MeV proton accelerator. It has normal conducting section up to 10 MeV incorporating RFQ and DTL and superconducting accelerator sections above 10 MeV incorporating Single Spoke Resonator (SSR)).

As per LEHIPA measurement data, RF power requirement for DTLs at 3-11 MeV and 11-20 MeV is around 800 kW (4 ports, 200 kW) each, and around 560 kW (2 ports, 280 kW) for 3 MeV RFQ. These RF power measurements are inclusive of insertion losses across the RF power system and reflected power from accelerator.

The maximum RF power requirement of superconducting SSR cavities of MEHIPA with adequate margin is about 50 kW. Hence, a SSA of 50 kW at 325 MHz is designed. Conceptual designs of 50 kW SSA for SSR cavities, 280 kW and/or 1 MW SSAs for RFQ/DTLs are presented in this article. Depending on accelerator power requirements, the output power of SSAs can be scaled up to 500 kW and 1 MW by combining multiple 280 kW SSA blocks. These SSAs can be built for both 325 MHz and 352 MHz with minor modifications in IPA module and Power combiner/dividers.

The main sub-systems of these SSAs are, a low power RF (LPRF) driver, power amplifier (PA) modules, direct current (DC) bias power supplies, power divider, power combiner, interlock protection and monitoring system (IPMS), AC power distribution arrangement and a number of directional couplers. The first basic SSA tower uses a modular topology where power output from multiple power amplifier (PA) modules are combined via power combiner to achieve overall high-power output.

The preliminary design of major sub systems of these SSAs inclusive of innovative ideas and integration methodologies to meet 4 C's is discussed below.

- *Integrated PA (IPA) module*: The number of interconnecting cables increases with the number of PA modules and DC power supplies (DCPS). This results in increase in complexity of cable routing, requirement of more space, increase in cable losses, system noise etc. A design innovation by integrating PA module, DC PS and its protection circuit, known as Integrated PA (IPA) module on a single heat sink and with direct interface between them resolves most of the issues. It reduces number of DC cables, noise, uses single heat sink and single protection circuit for both PA module and DCPS, ensuring high level of integration with power combiner. This effectively reduces size and cost, increases efficiency, increases availability due to increased mean time between failure (MTBF) and reduced mean time to repair (MTTR).

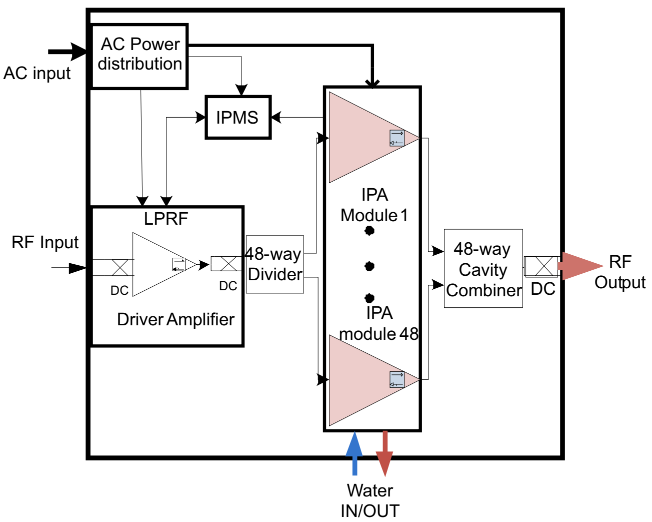

Fig.1: Architecture of 50 kW SSA at 325 MHz for MEHIPA-phase 1.

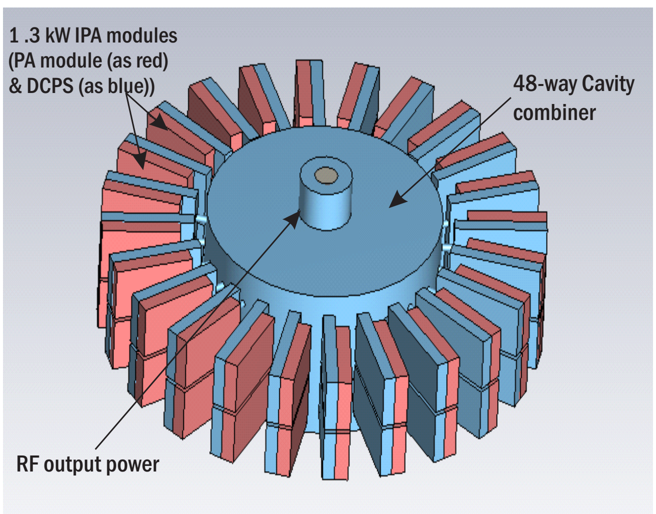

Fig.3: Arrangement of HPRF section of 50 kW, 325 MHZ SSA.

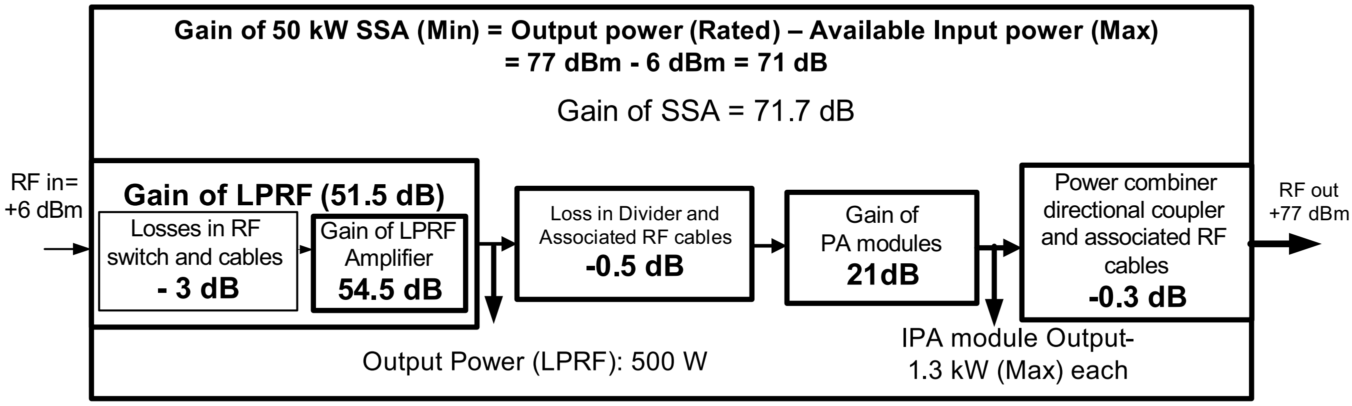

Fig.2: SSA Gain budget for 50 kW, 325 MHZ SSA.

- *Cables-less high power interfaces*: Innovative interface design of IPA modules and their direct mounting on cavity combiner enables the cable-less high power RF interface. It further improves compactness, and reduces cost, improves efficiency and eases maintenance.

- *Modular IPMS*: Modular and distributed IPMS design implementation helps simpler design, easy diagnosis, less cabling, less noise and easy maintenance with improved reliability.

- *Power combining methodology*: Overall design concept for power combining methodology for these three SSAs is same except for levels of combining. In 50 kW SSA, single stage cavity combiner based power combining is used. The 280 kW SSA design uses two stages of power combining and 1 MW SSA design uses four stages of high power combining. Architectural details and salient features of these SSAs are presented in this section.

Design of 50 kW SSA at 325 MHz for MEHIPA

Architecture of the proposed design of 50 kW, 325 MHz SSA for SSR cavities is shown in Fig.1. The 50 kW SSA integrates all 48 IPA modules, each rated for 1.3 kW RF power, by directly mounting on a single cavity combiner. This cavity combiner and IPA arrangement achieves higher level of IPA module integration with lower combining losses and linear combining. Other sub systems of SSA like LPRF, AC-PDP, IPMS will be housed in a separate cabinet, and will be located very near to SSA installation.

SSA design involves estimation of SSA gain requirements and gain budget for various sub-systems. Gain budget of the 50 kW SSA at 325 MHz (assuming +6 dBm (maximum) input from low level RF (LLRF)) and its sub-systems is shown in Fig.2. Fig.3 shows the arrangement of high power RF components. The power density of the complete 50 kW SSA is estimated at around 13.6 kW/ m^3.

Wall plug efficiency of the SSA is estimated at 53% (min.) based on conservative efficiency values for sub-systems like integrated PA module 58% (min.), and efficiency of cavity combiner around 95% (min.). Some of the critical specifications for this SSA are given in Table 1.

Conceptual design of 280 kW SSA

To meet the requirements of RFQ and DTLs, innovative design adopted for 50 kW has been extended for 280 kW SSAs at 352 MHz for LEHIPA and 325 MHz for MEHIPA. In this SSA, maximum possible input ports on the cavity combiner were estimated based on the dimensions of cavity combiner and IPA module. Redundancy of IPA module has also been considered to increase SSA reliability. Cylindrical cavity combiner operating in TM_{010} mode at 325 MHz/352 MHz has its resonance frequency related to its radius. The Radius of cylindrical combiner cavity for resonance frequency of 352 MHz/325 MHz is approximately 350 mm. Cavity dimensions and IPA module size dictates the maximum input ports feasible on the cavity combiner. For these frequencies and dimensions of IPA module, maximum 128 nos. of IPA

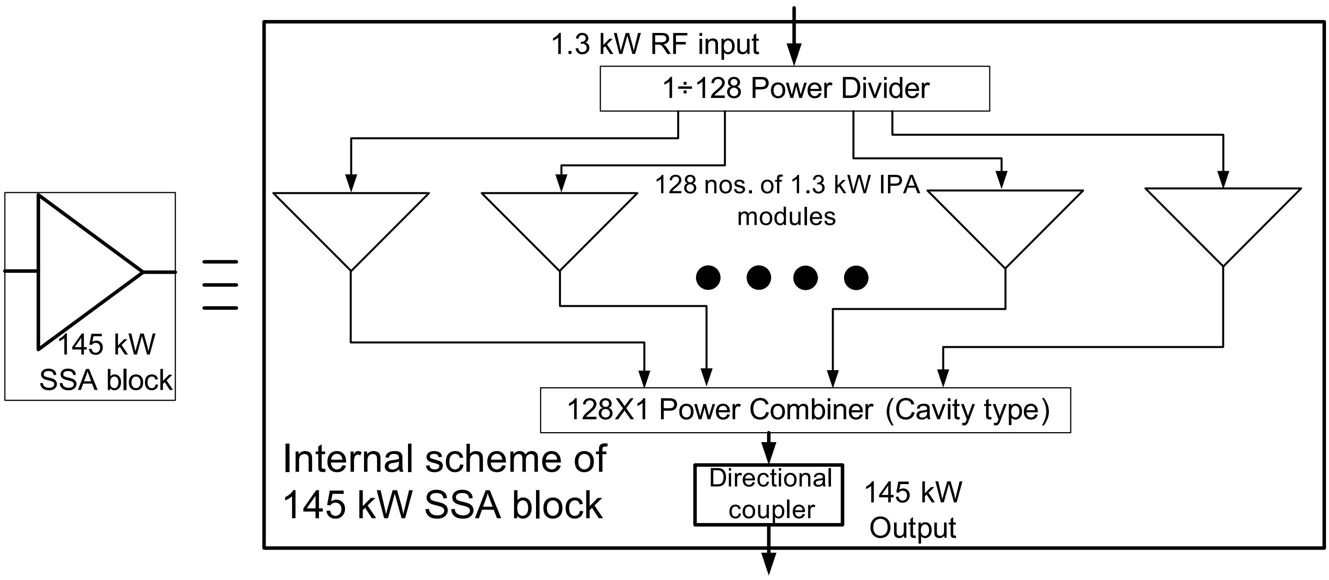

Fig.4: Internal Scheme of 145 kW SSA block.

modules can be integrated with the cavity combiner. With IPA module rating at 1.3 kW, power of each SSA block or tower is 145 kW and offers redundancy of about 15 IPA modules for nominal power of 140 kW. Internal RF Scheme of 145 kW SSA tower is shown in Fig.4.

145 kW SSA blocks comprises of a 128-way power divider, outputs of which feeds to 128 nos. of 1.3 kW IPA modules. Output from these IPA modules is combined using a 128-way cavity combiner. 128 IPA modules are assembled directly on the 128-way cavity combiner with cable-less RF interface and hose-less water interface for compact and efficient assembly. This scheme reduces footprint size and cost of the implementation by saving inventory of RF cables and water circuit.

LPRF (Driver) unit that feeds RF power to 128-way divider of this SSA block comprises of 1.3 kW IPA module. AC power distribution sub-system distributes and manages AC power flow for reliable and safe operation of the SSA block. IPMS unit is designed as distributed topology to provide functions like interlock, protection and monitoring of various parameters and keep amplifier operational under normal operating conditions and helps during diagnosis of failures.

Combining of two such SSA blocks is estimated to deliver 280 kW output which is sufficient to directly feed each ports of DTL/RFQ. Output port of 145 kW SSA block is 8 - 3/16”, 50-ohm flange. The two-way power combiner for combining these two SSA towers will be coaxial line to waveguide type combiner, whose output will be available on waveguide WR2300 HH port. Some of the critical specifications of the 280 kW SSA are listed in Table 1.

Conceptual design scheme of 1 MW SSA

The present R&D efforts for 1 MW SSA at 352 MHz are aimed to provide overall scheme and mitigate the challenges involved in its design and implementation to achieve compact, cost effective, high efficiency and high availability. The design is aimed at enabling self-reliance and ‘Make in India’ to reduce import dependence. The architecture cum concept scheme (Fig.5) of 1 MW SSA consists of three stages namely the input

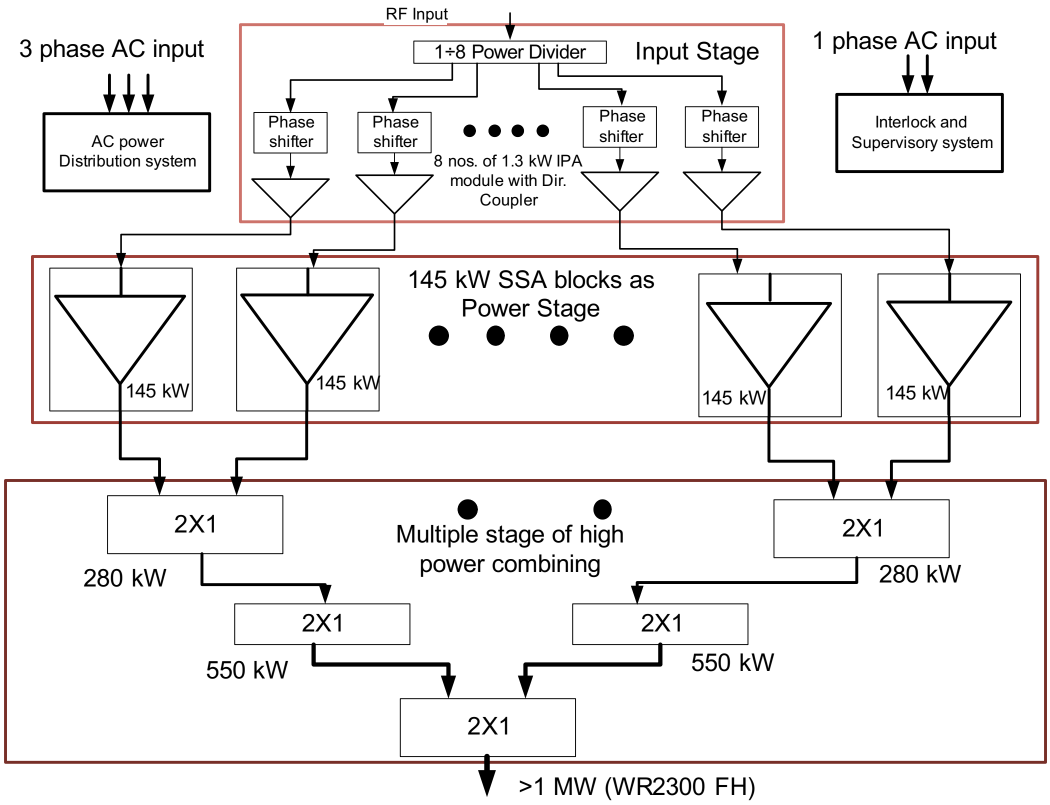

Fig.5: General Block Diagram Super Power 1 MW, 352 MHz SSA System.

Table 1: Critical specifications of SSAs 352/325 MHz SSA.

Sr. No	SSA specification	Parameter values for 1 MW	Parameter values for 280 kW	Parameter values for 50 kW
1	Guaranteed Output power at 352/325 MHz	1 MW (CW and pulse)	280 kW (CW and pulse)	50 kW (CW and pulse)
2	Bandwidth (-3 dB)	= 4 MHz	= 4 MHz	= 4 MHz
3	Power gain requirement	= 84 dB	= 78.5 dB	= 71 dB
4	Harmonics*	< -25 dBc	< -25 dBc	< -25 dBc
5	Spurious*	< -55 dBc	< -55 dBc	< -55 dBc
6	AC to RF Efficiency$	~ 40% (@1 MW)	~ 42% (@280 kW)	~ 50% (@50 kW)
7	Smallest amplification unit (Basic building block)	1.3 kW IPA module	1.3 kW IPA module	1.3 kW IPA module
8	Smallest integrated amplification sub-system	~145 kW SSA block, 8 nos.	~145 kW SSA block, 2 nos.	50 kW SSA block, 1 no.
9	Output connector and VSWR	WR2300 FH/HH, <1.4	WR2300 HH, <1.4	6 1/8” EIA, <1.4
10	Input connector and VSWR	SMA (F), <1.2	SMA (F), <1.2	SMA (F), <1.2
11	System cooling	Water cooled	Water cooled	Water cooled

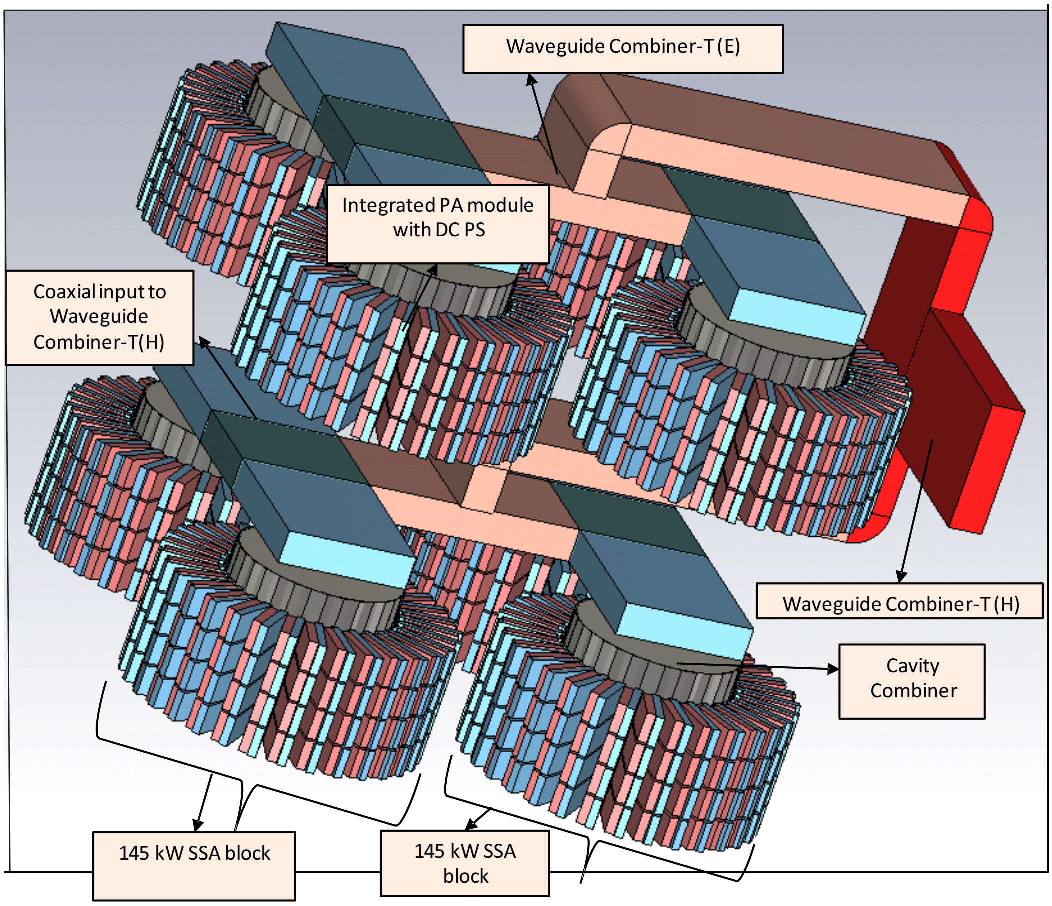

Fig.6: : Physical arrangement scheme of 1MW segment of 1 MW SSA.

stage, the power stage and high power combining stage. It uses 145 kW SSA tower as the main building block as shown in Fig.5. This scheme, has following salient features.

■ The 'Input stage' consists of an eight (8) - way power divider that feeds the input RF power via phase shifter (to provide flexibility in phase matching) to eight (8) numbers of 1.3 kW IPA modules. Output from these modules is fed to 145 kW SSA block.

■ Power stage comprises of eight nos. of 145 kW SSA blocks.

■ Multi-stage high power combining: As described in previous section, two 145 kW SSA towers are combined to deliver 280 kW maximum power per port of normal conducting accelerating cavity. However, if 500 kW or 1 MW output power is needed. If power required per port is less that 145 kW, SSA blocks will have more redundancy and availability, it can be delivered by power combining as shown in Fig.5. Availability of RF Power at 145 kW, 280 kW, 500 kW and 1 MW level provides flexibility to the accelerator facility.

■ Modular protection and monitoring at IPA module level simplifies overall interlock, protection and monitoring system (IPMS).

Some of the critical requirements cum design specifications of this scheme of 1 MW SSA that can be achieved are listed in Table 1.

Physical arrangement scheme of eight nos. of 145 kW SSA blocks of is shown in Fig. 6 as cylindrical towers. To achieve output power of 1 MW, further combining is done using waveguide-based network. The design, development and deployment experience of various waveguide components for LEHIPA reduces risk in these designs.

*Harmonics and spurious levels of 1.1 kW PA module (on which IPA modules of 1.3 kW are based) is -30 dBc and -60 dBc. These values are standard acceptable range for accelerator RF systems.

$The AC to RF efficiency is based on measured AC to DC efficiency of DCPS, measured DC to RF efficiency of PA modules, combining loss calculations based on gain magnitude and phase spread.

Conclusion

BARC has focused on the design and development of state of the art high power SSAs for Indian accelerator program. Innovative design techniques and integration topologies adopted to develop these SSA are aimed to achieve high efficiency, compact and cost effective SSAs with reliable operation. Objectives further include enabling self-reliance and indigenous manufacturing of high end SSAs technology via Indian industries. This further accomplishes 'Made in India objectives of Govt. of India and provides critical import substitute. Main features of these high power SSA design are high power density from 12 kW/m^3 for 50 kW up to 15 kW/ m^3 for 280 kW and 1 MW and low cost per watt.

Acknowledgement

The authors gratefully acknowledge constant support and guidance of Shri U.D. Malshe, Group Director, Multi-disciplinary Research Group (MRG) and Shri Vivek Bhasin, Director, BARC.

We sincerely thank Shri S. Muthu, Shri Jagdish Bowlekar and Shri Hitesh Kadam for their technical support during assembly and testing of SSAs.

References

[1] P. Marchand; M. Diop; R. Lopes; J. Polian; F. Ribeiro; T. Ruan, High Power (35 kW and 190 kW) 352 MHz Solid State Amplifiers for the Soleil Synchrotron, IEEE Conference on Particle Accelerator, 16-20 May 2005, USA, DOI: 10.1109/PAC.2005.1590572

[2] D Horan, "352-MHz Solid State RF System Development at the Advanced Photon Source", Proceedings of 12 International Particle Accelerator Conference 2021 (IPAC2021), Brazil.

[3] B.V. Ramarao, S. Muthu, J. K. Mishra, Manjiri Pande, Gopal Joshi et al "Coupling and Energising of 10 kW, 352 MHz Solid-state RF Power Amplifier for Buncher Cavity of Proton Accelerator", Indian Particle Accelerator Conference (InPAC-2019), 18-21 November 2019, New Delhi

[4] J.K. Mishra, B.V. Ramarao, Manjiri. M. Pande, P. Singh, "A Compact High Efficiency 8 kW 325 MHz power amplifier for accelerator applications", Journal of Nuclear Instruments and Methods in Physics Research A, 764 (2014)

[5] Manjiri Pande, James Steimel et al., "Development and Operation of PIP-II Injector Test, SSR1 Cryo-module, 325 MHz Amplifiers, Proceedings of Superconducting RF Conference (SRF 2021), SRF2021, East Lansing, MI, USA, JACoW Publishing, doi:10.18429/JACoW-SRF2021-MOPTEV017

[6] J.K. Mishra, et al, Status of Solid state RF Amplifier Development at BARC, Proc. Of InPAC 2022 held at VECC Kolkata, India

कृत्रिम मेधा

7

परिदृश्य पथ-निर्देशन : कण त्वरकों के संबंध में कुछ चुनौतियों के समाधान के लिए मशीन लर्निंग अनुप्रयोग और आधुनिक नियंत्रण तकनीक

***राधिका नासेरी, संदीप भराडे, आर.टी. केशवानी और एम.वाई. दीक्षित**
त्वरक नियंत्रण प्रभाग, भाभा परमाणु अनुसंधान केंद्र (भापअ केंद्र), ट्रांबे-400085, भारत

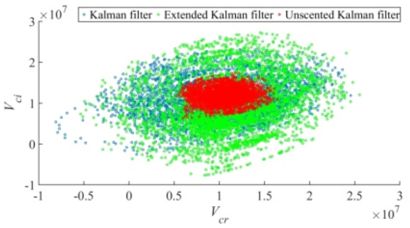

केएफ, ईकेएफ एवं यूकेएफ द्वारा आरएफ गुहिका उद्ग्रहण अनुमानित बनाम कल्पित घटकों का आरेख

सारांश

कण त्वरक विविध घटकों का अंतरसंबंध होता है। त्वरक प्रणालियों में निहित जटिल डेटापैटर्न उच्च गुणवत्तावाले डेटासेट प्रदान करते हैं , जो उन्नत मशीन लर्निंग (ML) एल्गोरिदम के प्रशिक्षण के लिए आदर्श हैं। इस लेखमें त्वरक EPICS SCADA और डेटाआर्काइविंग के साथ ML फ्रेमवर्क के एकीकरण को प्रस्तुत किया गया है। इसके अलावा , लोलेवलआरएफ (LLRF) नियंत्रक के लिए आनुविंशक एल्गोरिदम और पुनरावृत्तिशिक्षणनियंत्रण के अनुप्रयोग के परिणाम भी प्रस्तुत किए गए हैं। विभिन्न आधुनिक नियंत्रण और अनुमान तकनीकों का उन्नयन अत्याधुनिक प्रौद्योगिकी का उपयोग करके उच्च शक्तिवाले त्वरक की कई गुहा ऑपरेशन की विश्वसनीयता, दक्षता और स्थिरता को सुनिश्चित करेगा। डिट्यूनिंग अनुमान और आरएफ स्रोत रैखिकीकरण में प्रयुक्त आधुनिक नियंत्रण तकनीकों को भी पेश किया गयाहै।

Artificial Intelligence

7

Navigating the Landscape: Machine Learning Applications and Modern Control Techniques for Mitigating Some Challenges for Particle Accelerators

***Radhika Nasery, Sandeep Bharade, R. T. Keshwani and M. Y. Dixit**
Accelerator Control Division, Bhabha Atomic Research Centre (BARC), Trombay-400085, INDIA

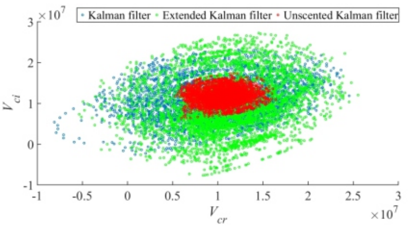

Plot of estimated real versus imaginary components of RF cavity pickup by KF, EKF and UKF

ABSTRACT

Particle accelerators constitute an interconnection of diverse components. Intricate data patterns inherent in accelerator systems provide rich datasets ideal for training sophisticated Machine Learning (ML) algorithms. This article presents integration of accelerator EPICS SCADA and Data Archiving with ML framework. Results in application of genetic algorithm and iterative learning control for Low Level RF (LLRF) controller are also presented. Augmentation of various modern control and estimation techniques using state of the art technology shall lead to reliable, efficient and stable multi-cavity operation of high power accelerator. Modern control techniques employed in detuning estimation and RF source linearization are introduced.

KEYWORDS: *EPICS, Machine Learning, Control, Particle Accelerators*

**Author for Correspondence: Radhika Nasery*
E-mail: radhikan@barc.gov.in

Introduction

Accelerator Control Division has successfully designed, developed and commissioned control and instrumentation (C&I) systems, like, Low Level RF (LLRF) [1] for RF cavity control, RF Protection and Interlock (RFPI) [2] system, Beam Position Monitor (BPM) [3] system and Programmable Timing and Control System (PTC) [4] for various accelerators facilities. As accelerators grow in complexity and scale, the demand for efficient, safe and adaptive control systems becomes increasingly crucial. Traditional control systems struggle to adapt to the inherent non-linearity and non-predictable environmental dynamics. The developed C&I systems employ RF and digital signal processing algorithms and provide digital data for logging, monitoring and post-mortem analysis. Data intensive dynamics of C&I systems make them suitable to harness the advances in the domain of ML. In this context, the integration of ML techniques into the control and instrumentation of particle accelerators has emerged as a promising avenue for enhancing performance, optimizing operation and overcoming inherent challenges.

ML integration with Accelerator Controls

Experimental Physics and Industrial Control System [5] (EPICS) is a set of open source software tools, libraries and applications developed collaboratively and used worldwide to create distributed soft real-time control systems for scientific instruments such as particle accelerators, telescopes and other large scientific experiments. Integration of ML analysis tools with accelerator control systems requires interfacing with EPICS Input Output Controller (IOC) and databases. The quality and temporal alignment of accelerator data, encompassing information from various noisy sensors and diverse subsystems, necessitate meticulous and often automated pre-processing and integration efforts. The upgraded version of EPICS - EPICS 7 is more suitable for ML integration as it provides structured Process Variables (PV) database with time stamped metadata. EPICS 7 Soft IOC for LLRF system has been developed and integrated with a Data Archiver, which supports NOSQL database. For ML integration, EPICS 7 Data Acquisition (DAQ) IOC design as shown in Fig.1 is proposed. ML algorithms require extensive datasets, and often there is a limited availability of historical data, especially for rare failure events or off beat operating scenarios. This needs continuous logging of data streams from instrumentation. In EPICS DAQ IOC, PV data stream gets the data from Device Support which is interfaced to underlying LLRF/RFPI/BPM front end equipment. Timestamp information from timing system is crucial for time alignment and is used to populate metadata of PVs. For certain

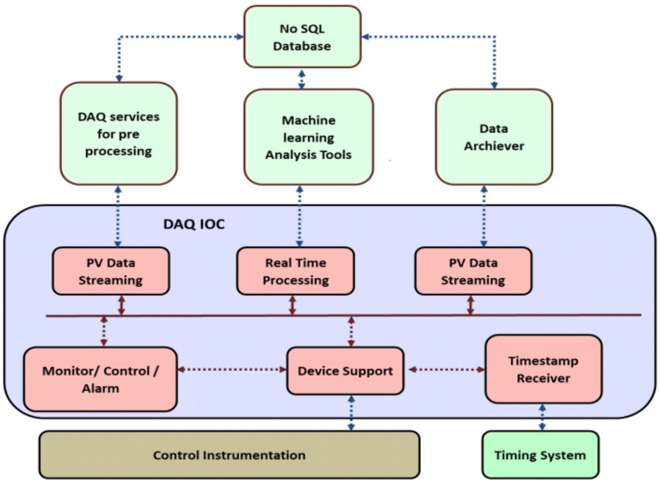

Fig.1: EPICS 7 IOC for ML integration.

PVs pre-processing services such as data merging, temporal alignment and unification is required before storage. ML analysis tools can then interface with the stored data and/or directly with real time processing in IOC.

Control Instrumentation

Performance of LLRF and Resonance Control System (RCS) defines the phase, amplitude and frequency stability of RF cavity. Generally proportional integral (PI) controller is used in LLRF system for amplitude and phase stabilization. Optimizing the performance of controller is pivotal for addressing challenges such as RF amplifier noise, cavity parameter swings, microphonics and beam loading effects. Conventional methods are limited by process modelling error and parametric uncertainties. Adaptive control system can overcome these challenges.

Many of the PI parameters optimization problems are multi-objective in nature, for example, improving both transient and steady state response, and a thorough comprehension of equilibrium between competing choices is desired. The Non-dominated Sorting Genetic Algorithm (NSGA-II) [6] emerges as a potent online optimization technique, providing an optimal set of solutions for competing system parameters, overshoot and settling time in step response. The cost function used in NSGA-II is a weighted combination of Integral Square Error (ISE) for transient response, Integral Time Absolute Error (ITAE) for steady state response and Integral Absolute Error (IAE) for overall error reduction. For evaluating the performance of NSGA-II algorithm, a RF system is modelled as a First Order Plus Dead Time (FOPDT) System and PI parameters are calculated using Zeigler Nichols (ZN), Cohen Coon (CC) and NSGA-II method. A comparative analysis of PI controller performance for a step input change is performed as shown in Fig.2. NSGA-II algorithm provides better transient and steady state response as compared to classical methods. Fig.3 shows that NSGA-II algorithm has significantly improved IAE, ITAE and

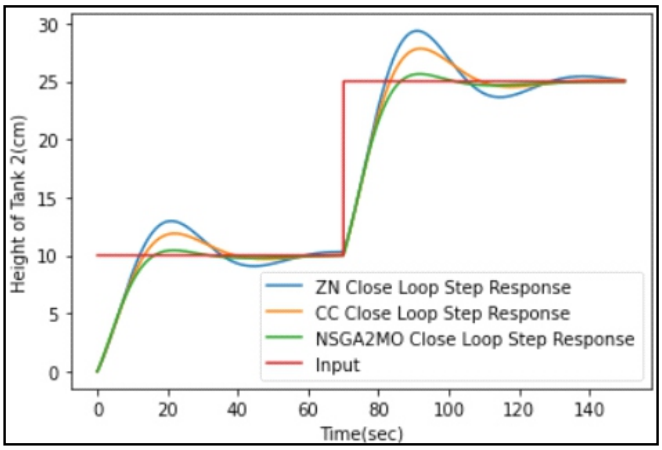

Fig.2: Response of FOPDT system for step change in input.

Table 1: Comparison of ILCs.

	PID-ILC	FNOILC
Memory requirement	Low	High
Computational complexity	Low	High
Convergence	Slow	Fast
No. of tuning parameters	Less	More

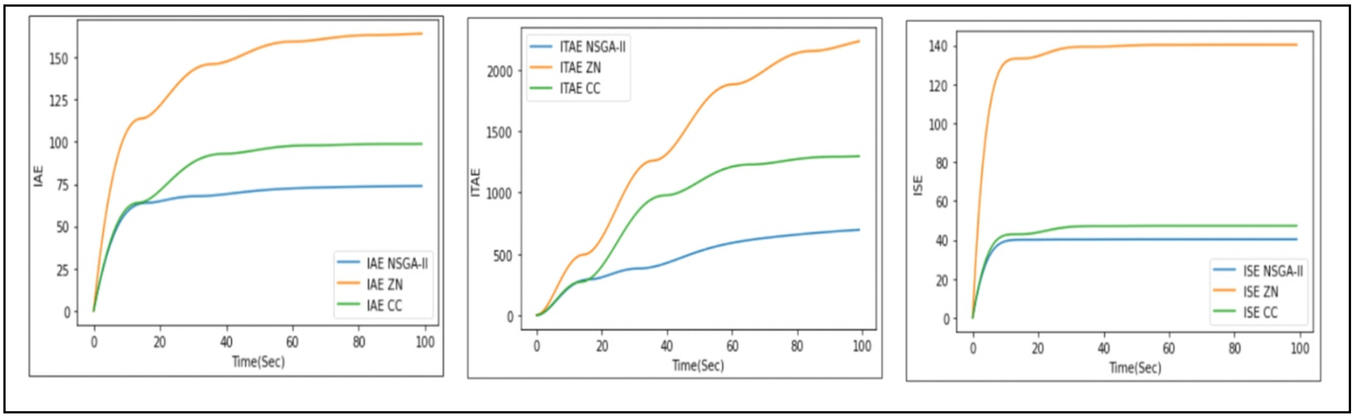

Fig.3: Plot of IAE, ITAE and ISE for ZN, CC and NSGA-II.

ISE as compared to ZN and CC. Further investigations are being carried out by experimental testing using cavity emulator.

In pulsed mode of operation of cavity, disturbances due to beam loading and Lorentz Force detuning, are repetitive in nature. Another modern control method based on Iterative Learning, finds a significant role in such applications and helps achieve high amplitude and phase stabilities, especially in instances where RF-ON times are a few micro-seconds or lower. The addition of Iterative Learning Control (ILC) enhances control loop performance over and above achievable by feedback controller. ILC learns about system dynamics by capturing input and output over previous pulses. In this technique the control output is modified as per pre-defined cost function.

This method has demonstrated huge success in many engineering applications. Though proportional-integral-derivative (PID) type of ILC has been reported as a solution, a more recent Fast Norm Optimal Iterative Learning Controller (FNOILC) [12] is better for fast error minimization with constrained control effort and faster convergence. Table 1 shows comparison of the two candidate ILCs for handling RF cavity repetitive disturbance problems.

System Identification

A number of critical systems in an accelerator are non-linear and have time dynamics evolving over multiple parameter spaces. System modelling with BPM data is another area where ML can handle the online modelling of systems by predicting the parameter space inferred from the measured data. ML can also be used to reduce dimensionality of complex systems for tuning and speedup. In an operational accelerator, ML find an application in identification of model of RF cavity along with its associated RF system. The accurately identified model is important to implement current state of art algorithms based on modern control and estimation theory, detuning estimation and RF power amplifier linearization being a two of the examples. An accurately identified model by ML enhances performance of these algorithms, thus leading to overall improvement in control system performance.

Effective resonance control of RF cavity, especially for superconducting (SC) cavity, needs precise estimation of detuning using cavity model. Conventionally, least squares estimation, linear and non-linear observer based approaches have been used, however estimation based on Kalman filter (KF) and its variants offer practical advantages of robustness in presence of sensor noise and model uncertainty.

In case of normal conducting cavity, detuning estimation based on adaptive KF [9] suffices. Due to non-linear transfer characteristics of SC cavity, a non-linear estimator like Extended Kalman Filter (EKF) or Unscented Kalman Filter (UKF) [10] perform better. A linear estimator when used for a nonlinear system like SC cavity results in more variance as seen in simulated results in Fig.4. Fig.4 also shows that for SC cavity, UKF estimates are better compared to estimates by obtained using KF and EKF. Here, state estimation problem is solved by KF, EKF and UKF for real and imaginary components of the cavity pick-up denoted by *Vcr* and *Vci*, respectively for given cavity input signals and its model parameters subsequently resulting into detuning estimation [9].

At high power operation of RF cavity, amplitude and phase non-linearity of RF power sources like Klystron or Solid State Power Amplifier (SSPA) pose control and operational difficulties. Estimators such as ordinary and recursive least squares capture RF source non-linearity and digitally pre-distort [11] LLRF output to compensate for amplitude and phase non-linearity. A predistortion needs placement of inverse transfer characteristics of SSPA at its input as shown in Fig.5, basically achieved through recursive least square estimation of Volterra model coefficients. A linearly increasing DPD input (x_{DPD}) provides its output (y_{DPD}) such that SSPA output (y_{PA}) is also linearly increasing.

Fault detection

Traditional protection systems like RFPI and Machine Protection System (MPS) are responsible for protection of equipment, personnel and facility. These systems continuously monitor signals from various sensors, compare these with predefined fault thresholds, and generate permit or stop operation of accelerator. The post-mortem data at the fault occurrence is stored and studied for root cause analysis. Unsupervised ML algorithms can be used to enhance the capability of traditional protection systems by a prior identification of detrimental conditions. This results in avoiding false fault conditions and thus, plant availability can be increased. Historic sensor data from diverse systems can be used for anomaly detection and the trained models can be deployed online. Results from the ML algorithms can be used to fine tune the threshold ranges of traditional systems.

ML for instrumentation

The deployment of ML algorithms in control and instrumentation devices for particle accelerators is challenging. Real-time control requirements demand low-latency processing, placing stringent demands on the timing precision of ML algorithms. ML algorithms are computationally intensive requiring high performance computing (HPC) platforms. HPC can be made available at edge-through

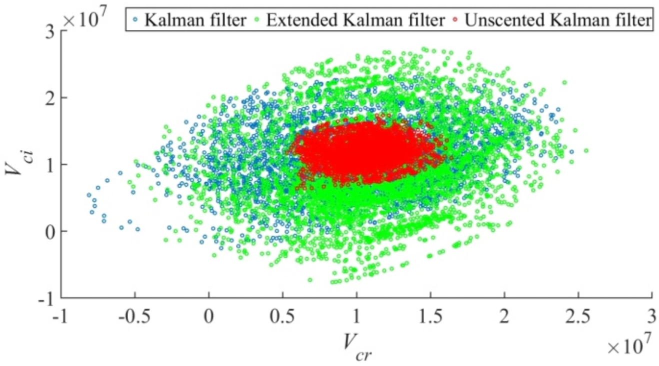

Fig.4: Plot of estimated real versus imaginary components of RF cavity pickup by KF, EKF and UKF.

physical integrated platforms or through cloud. AI at the edge is a solution for many use cases such as integration of ML solutions with embedded control systems like RFPI for protection, RCS and LLRF system for RF cavity control, which are implemented on SoC-FPGA, cPCI-FPGA and VME-FPGA based embedded systems. This needs compatibility and interoperability of ML solutions with FPGA. TinyML [7] is a type of ML that allows models to run on smaller, less powerful devices. TinyML is suitable for FPGA as it employs techniques to convert model weights from floating-point numbers to fixed-point or integer representations, removes unnecessary connections which reduce model size and computational demand. Integration of open source TinyML framework [8] for FPGA with EPICS 7 DAQ is currently under development for embedded control systems.

Conclusions

EPCIS 7 DAQ IOC architecture is proposed for ML integration with accelerator controls. Application of NSGA-II optimization algorithm, and ILC are being pursued. Opportunities and challenges for application of ML in field of machine protection, system modelling, tuning and optimization are presented. An indigenously developed elaborate control system integrated with machine learning, whose output acts as input to model based modern control approaches, seems to be a promising approach for reliable, efficient, stable and safe high power particle accelerator delivering high quality beam.

Acknowledgement

The authors acknowledge the work of Shri Karan Makwana during the Mini Project for OCES-2020 under HBNI titled “Multi-Objective Optimization for Particle Accelerator Systems”. Authors also acknowledge Dr. S. Mukhopadhyay, Director E & I group, Dr. Gopal Joshi, Head ACnD, Prof. Ravindra D. Gudi, IIT Mumbai and Ms. Sujo C. I., ACSS, ACnD for continued guidance and encouragements to carry out these investigations.

References

[1] Alok Agashe, P.D. Motiwala, S.K. Bharade, Shyam Mohan and Gopal Joshi, “Digital LLRF System for RFQ” Proceedings of InPAC2015, Mumbai, India.

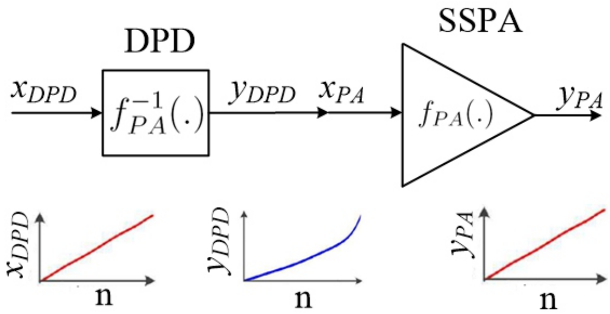

Fig.5: Pre-distortion system for SSPA.

[2] Sujo C.I., Khole S., Shukla Hitesh, Bharade S., Keshwani R., Afaash M., Joshi Gopal, Prieto Peter, “RF protection interlock system for proton linacs under Indian institutions and FERMILAB collaboration”, Proceedings of InPAC2018, RRCAT, Indore, India.

[3] Sandeep Bharade, Gurunath Randale, A. Agashe, Paresh Motiwala, Gopal Joshi, Frank Pillion, Djaid Zouaoui, Dominique Touchard, “EPICS DAQ System for beam position monitoring of SPIRAL2 LINAC at GANIL”, Proceedings of InPAC2019; IUAC

[4] Shukla Hitesh, Bharade S.K., Sujo C.I., Motiwala P.D. and Joshi Gopal, “Design, development and installation of programmable timing control system for LEHIPA”, Proceedings of InPAC2015, Mumbai, India.

[5] Argonne National Laboratory, 28 Feb 2021, “Experimental Physics and Industrial Control System”

[6] Pengzi Chu, Yi Yu, Danyang Dong,Hui Linand Jianjun Yuantiny, “NSGA-II-Based Parameter Tuning Method and GM(1,1)-Based Development of Fuzzy Immune PID Controller for Automatic Train Operation System”, 2020 Mathematical Problems in Engineering.

[7] ML Foundation, “https://www.tinyml.org/”

[8] Shvetank Prakash, Tim Callahan, Joseph Bushagour, Colby Banbury, “CFU Playground: Full-Stack Open-Source Framework for Tiny Machine Learning (TinyML) Acceleration on FPGAs”, 2023 IEEE International Symposium on Performance Analysis of Systems and Software (ISPASS).

[9] R.T. Keshwani, S. Mukhopadhyay, R.D. Gudi and G. Joshi, "Comparative Investigations on Detuning Estimator for Experimental RF Cavity," in IEEE Transactions on Instrumentation and Measurement, vol. 72, pp. 1-9, 2023, Art no. 2526309, doi: 10.1109/TIM.2023.3311075.

[10] Rajesh Keshwani, S. Mukhopadhyay, Ravindra D. Gudi and Gopal Joshi, “Unscented Kalman Filter as SC cavity detuning estimator”, Proceedings of InPAC2023, BARC, Mumbai

[11] Rajesh Keshwani, S. Mukhpadhyay , Ravindra D. Gudi , Gopal Joshi, “Digital Predistortion technique for RF power amplifier linearization: Modelling and Simulations”, Proceedings of InPAC2022 VECC, Kolkata, 22-25 March, 2022.

[12] Rajesh T. Keshwani, Siddhartha Mukhopadhyay, Ravindra D. Gudi, Gopal Joshi, “A Novel Tuning Scheme for Fast Norm Optimal Iterative Learning Controller”, IFAC-PapersOnLine, Vol. 57, 2024, Pages 179-184, ISSN 2405-8963, https://doi.org/10.1016/j.ifacol.2024.05.031.

This page intentionally left blank

ADVANCED RF SYSTEMS FOR SUPERCONDUCTING ACCELERATOR

The state-of-the-art RF systems equipped with the latest and advanced technologies are deployed for carrying out acceleration of charged particles for Superconducting RF accelerators.

This page intentionally left blank

ठोस-अवस्था प्रवर्धक

8

स्वदेशी 325 MHz ठोस अवस्था शक्ति प्रवर्धक

***मंजिरी पांडे**, जे.के. मिश्रा, स्निग्धा सिंह, संदीप श्रोत्रिया, श्याम सुंदर जेना, एन. आर. पटेल, बी.वी. रामाराव, ए. शिजू, एस. मुथू और गोपाल जोशी

त्वरक नियंत्रण प्रभाग, भाभा परमाणु अनुसंधान केंद्र (भापअ केंद्र), ट्रांबे-400085, भारत

फेर्मीलैब में पीआईपी2आईटी के एसएसआर के साथ आठ एसएसआर1 युग्मित किए गए

(photo) फोटो: फेर्मीलैब, यूएसए के सौजन्य से

सारांश

भारतीय संस्थानों और फर्मीलाब के बीच विज्ञान और प्रौद्योगिकी सहयोग के समझौते के तहत, भाभा परमाणु अनुसंधान केंद्र ने स्वदेशी रूप से 325 मेगाहर्ट्ज पर 7 किलोवाट और 20 किलोवाट ठोस अवस्था प्रवर्धक शक्ति प्रणाली डिजाइन / परिकल्पित और विकसित किया हैं। इन रेडियो आवृत्ति शक्ति प्रवर्धक में उच्च रेडियो आवृत्ति प्रदर्शन सूचकांक हैं जैसे, एसी / प्रत्यावर्ती धारा से रेडियो आवृत्ति निपुणता 50% से अधिक, शक्ति लाभ >60 डीबी, लाभ और चरण स्थिरता क्रमशः 0.02 डीबी/सी और 1 डिग्री/सी से बेहतर आदि। आठ ऐसे 7 किलोवाट प्रवर्धकको फर्मीलाब, यूए.स.ए. और एक भाभा परमाणु अनुसंधान में तैनात किया गया है। 20 किलोवाट ठोस अवस्था प्रवर्धक शक्ति प्रणाली को डिजाइन / परिकल्पित और विकसित किया गया है। दोनों ठोस अवस्था प्रवर्धक शक्ति प्रणालीयों ने त्वरक में विशेषज्ञों की अंतरराष्ट्रीय टीम द्वारा आयोजित कठोर अंतिम डिजाइन समीक्षाओं को सफलतापूर्वक पूरा कर लिया है।

Solid-state Amplifier

8

Indigenous 325 MHz Solid State Power Amplifiers

***Manjiri Pande, J. K. Mishra, Snigdha Singh, Sandip Shrotriya, Shyam Sundar Jena, N. R. Patel, B. V. Ramarao, A. Shiju, S. Muthu and Gopal Joshi**

Accelerator Control Division, Bhabha Atomic Research Centre (BARC), Trombay-400085, INDIA

Eight SSAs coupled to SSR1 of PIP2IT @Fermilab (Photo Courtesy of Fermilab, USA).

ABSTRACT

Under the agreement of science and technology co-operation between Indian Institutions and Fermilab, BARC has indigenously designed and developed 7 kW and 20 kW solid-state amplifier power systems at 325 MHz. These RF power amplifiers have high RF performance indices like AC to RF efficiencies greater than 50%, power gain >60 dB, gain and phase stabilities better than 0.02 dB/^{o}C and 1 degree/^{o}C respectively etc. Eight such 7 kW amplifiers have been deployed at Fermilab, USA and one at BARC. The 20 kW SSA has been designed and developed. Both the solid state amplifiers have successfully completed the rigorous final design reviews conducted by international team of experts in accelerator.

KEYWORDS: *Accelerator, Amplifier, Efficiency, Fermilab, FNAL, Interlock, PIPII, Proton, RF, SSA*

**Author for Correspondence: Manjiri Pande*
E-mail: manjiri@barc.gov.in

Introduction

The Department of Atomic Energy (DAE) has envisaged setting up High Intensity Superconducting Proton Accelerator (HISPA) for the Indian Accelerator Driven Sub-critical reactor System (IADS). Accelerator programs of the Department planned in the coming decades needs many critical technologies. Solid State Amplifier (SSA) i.e. radio frequency (RF) power systems are one of them and fall under custom designed high technology systems.

The Science and Technology Cooperation agreement was signed between Department of Atomic Energy (DAE), India and Department of Energy (DOE), USA. Due to the commonality of Indian interests with the Proton Improvement Plan II (PIP-II) project in the domain of accelerators technology, an Indian Institutions and Fermilab Collaboration (IIFC) was formalized. The Proton Improvement Plan II (PIP-II) of Fermi National Accelerator Laboratory (FNAL), USA involves up-gradation of its accelerator complex to support a broad physics research program as well as to power the world's most intense beam of high-energy neutrinos for the Deep Underground Neutrino Experiment (DUNE) [1].

The PIP-II design requires two levels of RF power at 325 MHz for their single spoke resonator (SSR) section with Beta = 0.22 for SSR1 & Beta = 0.47 for SSR2 of the LINAC. RF power of 7 kW at 325 MHz for the SSR1 and 20 kW at 325 MHz for SSR2 cavities is generated by solid state amplifiers (SSA). Under IIFC, Bhabha Atomic Research Centre (BARC) has the responsibility to provide 325 MHz SSAs for SSR1 and SSR2 cryomodules having superconducting cavities.

BARC has designed and developed state-of-the-art 325 MHz, 7 kW and 20 kW SSA power systems. Both these indigenous SSAs have successfully completed final design reviews (FDR) conducted by a team of experts from international accelerator laboratories like CERN, GANIL, SLAC, Fermi lab and DAE.

The SSAs use advance and new high power laterally diffused metal oxide semiconductor field effect transistor (LDMOSFET) devices. Using latest and innovative technologies, SSA's delivering 100s of kilo-watt (kW) power can be realized. The advantages of solid-state amplifiers over tube based RF power systems are multiplicity i.e. modularity, low voltage operation, graceful degradation among the others. Both 7 kW and 20 kW SSAs will also be used in Indian accelerator program like Medium Energy High Intensity Proton Accelerator (MEHIPA).

Table 1: RF performance parameters of nine 7 kW SSAs at PIP2IT.

Sr. No.	Parameters	Values
1.	Frequency (MHZ)	325
2.	RF Output Power (kW Typical)	7
3.	DC to RF Efficiency @ 7 kW (%)	61.6 to 66.35
4.	AC to RF Efficiency @ 7 kW (%)	51.4 to 54.9 %
5.	2nd Harmonics (dBc)	(-) 32.57 to (-) 43.37
6.	3rd Harmonics (dBc)	(-) 48.4 to (-) 71.37
7.	Environmental Standard	IEC 60068
8.	EMI / EMC Standard	CISPER 11 & IEC61204-3, EUT Under controlled electromagnetic category

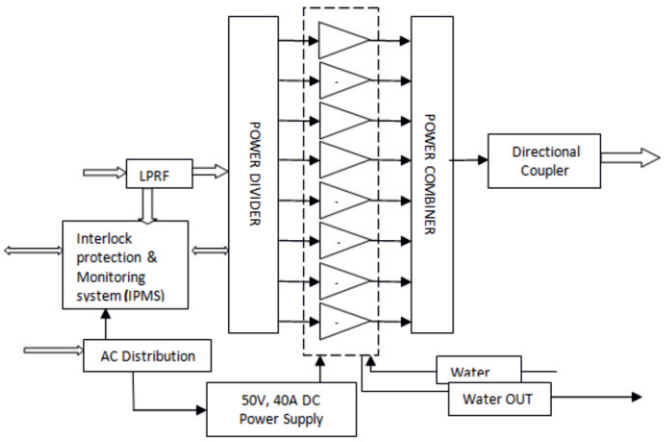

Fig.1: Modular architecture of 325 MHz, 7 kW SSA.

SSA 7 kW at 325 MHz

The SSR1 cavities, with β= 0.22, are powered by 7 kW 325 MHz RF power in the PIP II Injector Test (PIP2IT) facility - the technology demonstration part of PIP II. BARC has designed and developed state-of-the-art 325 MHz, 7 kW SSA power systems. Nine numbers of such 7 kW SSA power systems were produced by Electronic Corporation of India (ECIL) and have been deployed at PIP2IT facility Fermilab, USA. Eight SSAs have coupled the RF power to superconducting cavities (SC) of SSR1 cryomodule. The PIP2IT has successfully accelerated ionized hydrogen up to 17 MeV through one SSR1 cryomodule. One number of 325 MHz, 7 kW SSA is deployed at IADD of BARC.

These high power SSAs are designed using a modular topology wherein power output from multiple power amplifier (PA) modules are combined to achieve overall high-power output. The modular architecture of the 325 MHz, 7 kW level SSA with its sub-systems has been shown in Fig.1. It comprises of major sub-systems viz., a low power RF (LPRF) driver section, input power divider (1:8), eight power amplifier (PA) modules of 1 kW power rating each, a power combiner (8:1), eight direct current (DC) bias power supplies to power eight PA modules, an interlock protection and monitoring system (IPMS), an AC power distribution panel (PDP) and an output directional coupler. RF power from LPRF driver is split into eight in-phase power signals of equal amplitude by an input divider (1:8) and coupled to eight PA modules of 1 kW power each. An 8:1 power combiner, combines the amplified output power from eight PA

Fig.2: Power waveform in CW mode.

Fig.3: EIGHT SSAs coupled to SSR1 of PIP2IT @Fermilab (Photo Courtesy of Fermilab, USA).

modules to achieve 7 kW RF power at SSA output.

Table 1 lists some of the tested performance parameters of the nine SSAs. Fig.2 shows the RF power waveform in continuous wave (CW) mode of operation. The sub-systems of the SSAs have been subjected to stringent qualification tests as per international standards for improved and reliable performance during accelerator operation. The 7 kW SSA is capable of producing 5.37 kW power in the event of 1 PA module fail condition, thereby assuring availability of rated RF power for SSR1 cryomodule operation without interruption in beam acceleration for PIP-II operation. The 7 kW SSA can operate in both continuous wave (CW) and pulse mode. The salient features of the SSA include high AC to RF efficiency, high power gain, compactness, low harmonics, graceful degradation of power & easy maintenance. Fig.3 shows eight 7 kW SSAs [4] coupled to SSR1 cryomodule at PIP2IT facility of Fermilab, USA.

SSA 20 kW at 325 MHz

An efficient and compact 325 MHz, 20 kW SSA has been designed and developed by BARC, which will be useful to power SC SSR2 cavities.

Architecture of 20 kW SSA at 325 MHz capable of CW operation is shown in the block diagram in Fig.4. The major sub-systems of 20 kW SSA include a low power RF (LPRF) driver section, 1:24 input power divider, twenty-four power amplifier

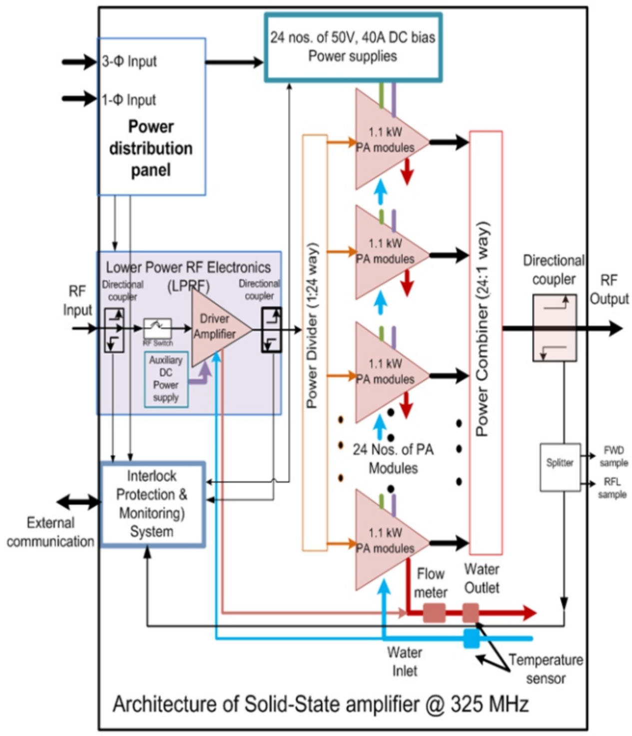

Fig.4: Modular architecture of 325 MHz, 20 kW SSA.

Fig.5: SSA 325 MHz, 20 kW.

Table 2: Important tested performance parameters or specifications of 20 kW SSA.

Important tested Specifications 20 kW SSA	
Description	**Specification**
Frequency	325 MHz
RF Output Power	20 kW Typical
1dB Bandwidth (Mhz)	7 MHz (Min.)
Power Gain	>85 dB (Min.)
Group Delay	<200 ns
Gain magnitude over 30% to 90% dynamic range	≤ 2 dB
Phase of the amplifier gain from 30% to 90% dynamic range	≤ 15^{o}
AC to RF Efficiency (at 17.1KW) (min)	>45%
AC to RF Efficiency (at 10.75KW) (min)	>40%
All Harmonics	<-25dBc
Spurious	<-60 dBc
VSWR handling (half power to full)	≤ 1.4
Power factor and THD	>0.9 and < 28%

(PA) modules of 1 kW power each, a 24:1 power combiner, twenty-four DC bias power supplies to bias the PA modules, an interlock protection and monitoring system (IPMS), AC power distribution panel (PDP) and an output directional coupler. RF power from LPRF driver is split into in-phase power signals of equal amplitude by the 24:1 input divider and fed to the twenty-four PA modules. The amplified output power from twenty-four PA modules is combined via 24:1 power combiner to achieve 20 kW RF power at SSA output.

In addition to complying with other stringent performance requirements, the amplifier has capability to deliver 17.1 kW under two failed PA modules condition. This fulfils the RF power availability of 17.1 kW using 24 modules with two PA module redundancy for PIP-II operation.

The important performance parameters of 20 kW SSA, which are experimentally verified, are listed in Table 2. The 325 MHz, 20 kW SSA designed, developed and successfully tested and is shown in Fig.5. The mean time between failure (MTBF) and mean time to replace (MTTR) calculations for these SSAs have been carried out. Based on these calculations, availability [5] of RF power from SSA has been estimated. Both these SSA have availability of of 99.995%. All the efforts of indigenous design, development, engineering, qualification and testing of the amplifiers have demonstrated excellent performance for critical parameters. These parameters include wall plug efficiency i.e. AC power to RF efficiency, overall gain, gain magnitude and phase variation, group delay, harmonic content and spurious outputs. These amplifiers will be used for Indian Accelerator Programs.

Conclusions

The technology of solid-state RF power amplifiers at 325 MHz for superconducting accelerators have been developed successfully. Eight RF power stations have been installed and commissioned at Fermilab's PIP2IT facility in the USA and proton beam has been accelerated to 17 MeV energy. The technology development of 20 kW SSA at 325 MHz is ready for deployment. Both these 7 and 20 kW SSAs have displayed excellent performance parameters including 'Availability', which are paramount for successful accelerator operation. This technology augmented with power combiner of higher ratings can be scaled up to 100's of kW of power regime.

Acknowledgements

The authors place on record that the interlock, protection and measurement system (IPMS) of earlier set of eleven 7 kW SSAs, nine of which have been delivered to Fermilab for PIP2IT, had been designed by Sujo C. I., Sandeep Bharade and R. T. Keshwani. The authors are very much thankful for their efforts, cooperation and support. Subsequently, the IPMS technology was migrated to a different technology platform.

The authors gratefully acknowledge the constant support and guidance of Shri U.D. Malshe, Group Director, Multidisciplinary Research Group (MRG) and Shri Vivek Bhasin, Director, BARC.

The authors are very much thankful to Mr. James Steimel & his team and Fermilab management for their continued efforts and corporation under IIFC.

The authors acknowledge technical help and efforts provided by Hitesh K. and Jagdish Bowlekar.

References

[1] https://pip2.fnal.gov/about/research-program/

[2] K.N. Vyas, DoE Independent Review of PIP-II CD-1 Fermilab, Chicago,12-14 December'17

[3]https://indico.fnal.gov/event/9939/attachments/75550/90629/PIP-II_RDR_v1.0.pdf

[4] Manjiri Pande, James M Steimel Jr. et al., 'Development and operation of PIP-II injector test, SSR1 cryomodule, 325 MHz amplifiers', SRF2021, East Lansing, MI, USA, JACoW Publishing, doi:10.18429/JACoW-SRF2021-MOPTEV017

[5] Shyam Sundar Jena, Sandip Shrotriya, J.K. Mishra, Snigdha Singh, Manjiri Pande, B.V. Rama Rao, N.R. Patel and Gopal Joshi, T.V. Santhosh, Gopika Vinod, J. Chattopadhyay, 'Availability estimation of 325 MHz, 20 kW solid state amplifier power system for accelerator', 5th 'International conference on Reliability, Safety and Hazard-2024' (ICRESH 2024), Feb 21-24, 2024. Published special topic conference proceeding ins in the international journal 'Springer'.

उच्च तीव्रता प्रोटॉन त्वरक

9

संदर्भ चरण उत्पादन प्रणालियाँ

*सुजो सी. आई., सत्यम रावत और गोपाल जोशी
त्वरक नियंत्रण प्रभाग, भाभा परमाणु अनुसंधान केंद्र (भापअ केंद्र), ट्रांबे-400085, भारत

325 MHz रेफरेंस फेज जनरेशन सिस्टम

सारांश

त्वरक नियंत्रण प्रभाग, भाभा परमाणु अनुसंधान केंद्र, ने भारतीय संस्थानों और फर्मीलाब के बीच विज्ञान और प्रौद्योगिकी सहयोग (आईआईएफसी) के तहत लो-लेवल रेडियो आवृत्ति नियंत्रण प्रणालियाँ विकसित की हैं, जिनमें एक अप-कन्वर्टर, एक डाउन-कन्वर्टर, एक रेफरेंस फेज जनरेशन प्रणाली, और एक डिजिटल सिग्नल प्रोसेसिंग (डीएसपी) मॉड्यूल शामिल हैं। रेफरेंस फेज जनरेशन प्रणाली एक स्थिर रेडियो आवृत्ति रेफरेंस उत्पन्न करता है, जो त्वरक कैविटी में रेडियो आवृत्ति तरंगों के फेज-नियंत्रण के लिए आवश्यक होता है, साथ ही एक लोकल-ऑस्सीलेटर (एलओ) सिग्नल प्रदान करता है जो आवृत्ति के रूपांतरण के लिए उपयोग होता है, और डीएसपी मॉड्यूल में उपयोग किए गए एफपीजीए के लिए एक क्लॉक सिग्नल भी प्रदान करता है। कैविटी के भीतर रेडियो आवृत्ति तरंगों के एंप्लिटूड और फेज की स्थिरता सुनिश्चित करने के लिए, रेफरेंस फेज सिग्नल, एलओ, और क्लॉक सिग्नल में अत्यंत कम फेज नॉइज़ बनाए रखना आवश्यक है। इसके लिए प्रणाली का तापीय स्थिरीकरण आवश्यक है ताकि अवयवों में तापमान परिवर्तनों के कारण फेज ड्रिफ्ट को कम किया जा सके। इस लेख में आईआईएफसी के तहत विकसित 325 मेगाहर्ट्ज और 650 मेगाहर्ट्ज रेफरेंस फेज जनरेशन प्रणाली की डिज़ाइन, कार्य सिद्धांत, परीक्षण परिणाम, और वर्तमान स्थिति का संक्षिप्त अवलोकन प्रस्तुत किया गया है।

High Intensity Proton Accelerator

9

Reference Phase Generation Systems

***Sujo C. I., Satyam Rawat and Gopal Joshi**
Accelerator Control Division, Bhabha Atomic Research Centre (BARC), Trombay-400085, INDIA

325 MHz Reference phase generation system.

ABSTRACT

Accelerator Control Division, Bhabha Atomic Research Centre has developed Low-Level RF control systems, each comprising of an up-converter, a down-converter, a reference phase generation system, and a digital signal processing (DSP) module under the Indian Institutions and Fermilab Collaboration (IIFC). The reference phase generation system generates a stable RF reference for phase-control of RF fields in an accelerator cavity, a local-oscillator (LO) signal for frequency translation, and a clock signal for FPGA on-board the DSP module. To ensure the stability of both the amplitude and phase of RF fields within the cavity, it is essential to maintain an ultra-low phase noise in the reference phase signal, LO, and clock signals. This requires thermal stabilization of the system to reduce phase drifts caused by temperature changes in the components. This article gives a brief overview of design, working principles, test results, and present status of the 325 MHz and the 650 MHz reference phase generation system developed under IIFC.

KEYWORDS: *Reference phase generation, Phase noise, Phase averaging.*

**Author for Correspondence: Sujo C. I.*
E-mail: sujo@barc.gov.in

Introduction

Proton Improvement Plan (PIP-II), Fermilab, USA is a high intensity proton accelerator which includes five different types of superconducting cavities with resonant frequencies at 162.5 MHz, 325 MHz, and 650 MHz. ACnD, BARC has developed LLRF systems for 325 MHz and 650 MHz cavities with technical support and guidance from Fermilab under IIFC. A 650 MHz LLRF control system has been commissioned at the Horizontal test facility (HTS), RRCAT. Additionally, two LLRF systems have been delivered to Fermilab to be tested with 325 MHz and 650 MHz RF cavities. A 325 MHz reference phase generation system has been developed as part of LLRF system. This system generates a phase-synchronized 325 MHz RF reference signal, a 345 MHz LO signal for up/down converters, and a 1320 MHz clock signal for the FPGA on-board the DSP module. Similarly, a 650 MHz reference phase system has also been developed, producing a 650 MHz reference signal, a 670 MHz LO signal, and a 1320 MHz FPGA clock signal.

Design of Reference Phase Generation Systems

The 325 MHz reference phase generation system utilizes a 325 MHz crystal oscillator as its RF source, which has an excellent phase noise characteristic. The phase noise of the crystal oscillator is -164.7 dBc/Hz at an offset of 10 kHz. Additional RF signals at various frequencies are derived from this crystal oscillator. To achieve this, RF frequency multipliers, frequency dividers, low-noise amplifiers, and single-sideband mixers with minimal additive phase noise have been carefully selected and integrated to generate the derived RF signals. The 650 MHz reference phase module utilizes the reference output from the 325 MHz reference phase system as its RF source. The reference phase generation systems also produce a 1300 MHz RF signal for utilization by beam instrumentation systems. When selecting RF amplifiers, it is essential to consider the length of the reference phase signal distribution line and the cable loss incurred over its entire length. The 325 MHz and 650 MHz reference phase generation systems are depicted in Fig.1 and 2, respectively.

Table 1 and 2 present the phase noise measurement results for various signals in the 325 MHz and the 650 MHz reference phase generation systems, respectively.

Fig.3 displays the phase noise spectral density of 1320 MHz FPGA clock signal derived from the 325 MHz master oscillator signal using frequency multipliers and single-sideband mixers. The single-sideband mixer utilizes RG 405 phase-matched coaxial cables to mitigate the quadrature phase errors resulting from temperature variations.

Fig.1: 325 MHz reference phase generation system.

Fig.2: 650 MHz reference phase generation system.

Table 1: Test results of 325 MHz reference phase generation system.

RF signal	Signal Level	Phase noise at 100 kHz offset
325 MHz reference output signal	7.9 dBm	-166 dBc/Hz
345 MHz LO signal	16.0 dBm	-148 dBc/Hz
325 MHz reference output signal to 650 MHz system	13.1 dBm	-163 dBc/Hz
1320 MHz clock signal	12.2 dBm	-149 dBc/Hz

Table 2: Test results of 650 MHz reference phase generation system.

RF signal	Signal Level	Phase noise at 100 kHz offset
650 MHz reference output	10.2 dBm	-157 dBc/Hz
670 MHz LO signal	16.7 dBm	-142 dBc/Hz
1300 MHz reference signal	7.9 dBm	-151 dBc/Hz
1320 MHz clock signal	16.8 dBm	-152 dBc/Hz

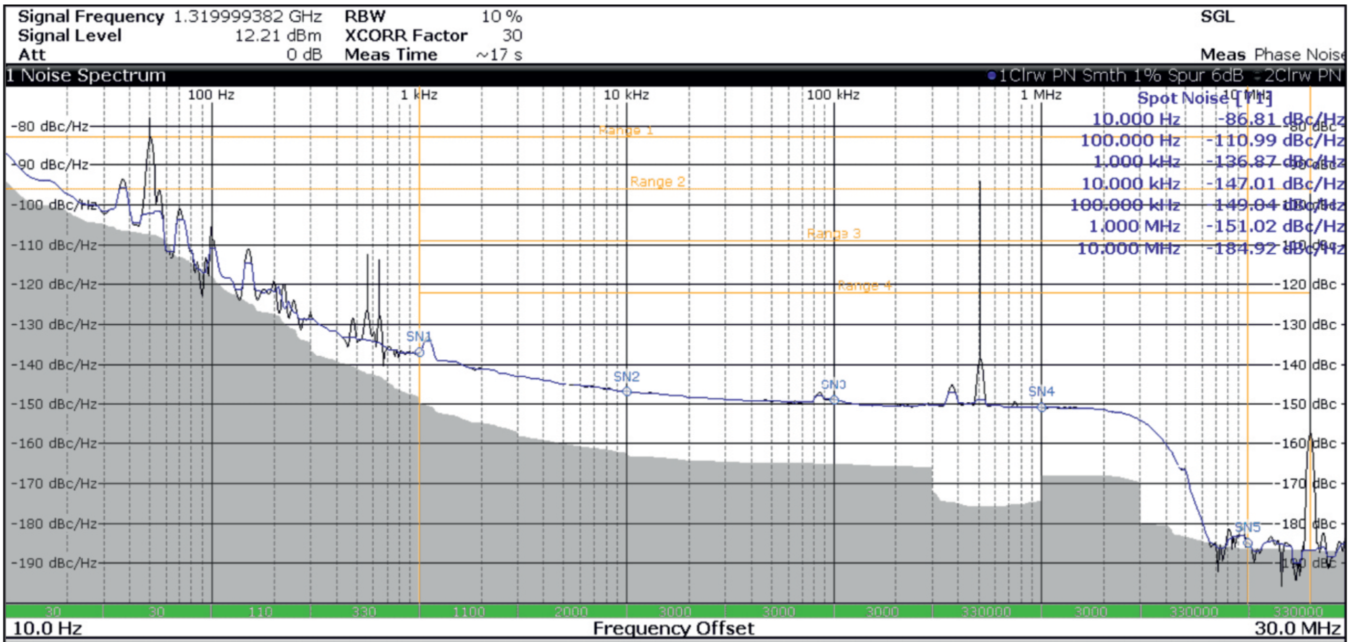

2 Integrated Measurements

Range	Trace	Start Offset	Stop Offset	Weighting	Int Noise	PM	FM / AM	Jitter
1	1	10.000 Hz	10.000 MHz		-78.76 dBc	9.35 m°/163.13 µrad	134.488 Hz	19.669 fs
2	1	10.000 Hz	20.000 MHz		-78.76 dBc	9.35 m°/163.15 µrad	138.239 Hz	19.671 fs
3	1	1.000 kHz	10.000 MHz		-85.82 dBc	4.15 m°/72.37 µrad	134.488 Hz	8.726 fs
4	1	1.000 kHz	20.000 MHz		-85.81 dBc	4.15 m°/72.41 µrad	138.239 Hz	8.730 fs

Fig.3: Phase noise spectral density of 1320 MHz FPGA clock signal.

Phase Averaging: Mitigating Phase Drifts Caused by Temperature Variation

At Fermilab, the length of the phase reference signal distribution cable, within each frequency section, spans nearly 100 meters. Variations in ambient temperature cause changes in the length of the distribution cable, thereby altering the phase of the RF reference signal. To mitigate this phase change resulting from temperature variation, the phase averaging method [1] is employed. In this method, a standing wave is induced in the reference line by introducing a short at the end of the transmission line. At any point along the reference line, both forward and reflected waves are extracted using a bi-directional coupler. The amplitudes and phases of these waves are carefully adjusted to maintain near-identical values. These adjustments are achieved through the use of variable attenuators and phase shifters. Subsequently, the two waves are combined. As long as the phase of the shorted end remains constant, the phase of the combined signal remains unaffected by changes in length, and thus, temperature. To ensure stability at the shorted end of the cable, a phase-locked loop is employed. This entire mechanism helps to maintain the phase stability of the reference signal which is an essential requirement in a LLRF system.

Temperature Stabilisation of the Reference Phase Generation System

To mitigate phase drift in the components resulting from ambient temperature variations (expected to range from 19°C to 35°C at Fermilab), the temperature of the reference phase generation system is regulated at 40°C. This is achieved through the development of heater PCBs, featuring long traces of copper uniformly distributed on an FR-4 substrate. All RF components are mounted on an aluminum plate, with the heater PCBs positioned beneath it. Thermally conductive acrylic interface pads, known as heat pads, are placed between the heater PCBs and the aluminum plate to enhance heat transmission. Temperature measurement is facilitated by a resistance temperature detector (RTD), Pt100, which is interfaced with a temperature controller. A 32V, 30A DC power supply is used to provide current to the heater PCBs. Fig.4 illustrates the heater PCBs with heat pads. It requires nearly 100 W of DC power to maintain the temperature of the reference phase generation system at 40°C (with a room temperature of 27°C).

Fig.4: Heater PCBs with heat pads.

Present Status

Based on the experimental results showing compliance with the given system specifications, the shipment of the reference phase generation systems to Fermilab was approved. Both 325 MHz and 650 MHz systems have already been sent to Fermilab for testing with 650 MHz and 325 MHz cavities. Commissioning of these systems is awaited.

Acknowledgement

The authors sincerely acknowledge and appreciate the technical support received from Fermilab during the design, fabrication, and testing phases. Additionally, the authors would like to thank all colleagues at ACnD for their invaluable support throughout the project.

References

[1] B. Chase, E. Cullerton, "1.3 GHz Phase Averaging Reference Line for Fermilab's NML ASTA Program", Beams-doc-3806-v2.

[2] M. Afaash, et al., "Reference Phase Distribution Scheme and Test Results for SSR1 under IIFC," Proceedings of the 2019 International Particle Accelerator Conference (InPAC), IUAC, New Delhi, 2019.

उच्च तीव्रता प्रोटॉन त्वरक

10

आईआईएफसी के तहत त्वरकों के लिए एकीकृत आरएफ नियंत्रण प्रणाली का विकास

निबंध कुमार, राधिका नासेरी, आलोक आगाशे, सुजो सी.आई., संदीप भराडे, आर. टी. केशवानी, सुरेंद्र सिंह सैनी, जी. रंदाले, पी. ज्योथि, परेश मोतीवाला और *गोपाल जोशी
त्वरक नियंत्रण प्रभाग, भाभा परमाणु अनुसंधान केंद्र (भापअ केंद्र), ट्रांबे-400085, भारत

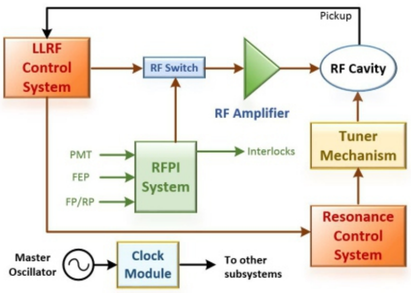

एकीकृत आरएफ नियंत्रण प्रणाली

सारांश

भारतीय संस्थानों और फर्मीलैब सहयोग के अंतर्गत त्वरक के लिए विकसित एकीकृत रेडियो आवृत्ति नियंत्रण प्रणाली गुहाओं के अंदर रेडियो आवृत्ति क्षेत्र के आयाम और चरण को नियंत्रित करने, रेडियो आवृत्ति गुहाओं की अनुनाद आवृत्ति की निगरानी करने, स्टेपर मोटर्स और पीजो एक्चुएटर का उपयोग करके गुहा अनुनाद आवृत्ति को बनाए रखने, त्वरक में महत्वपूर्ण आर. एफ. घटकों की सुरक्षा, और सभी उप प्रणालियों के समन्वय के लिए सटीक समय प्रदान करने के महत्वपूर्ण कार्य करती है। त्वरित गुहिका में रेडियो आवृत्ति क्षेत्र की स्थिरता आवेशित कणों की प्रभावी त्वरितता और कणपुंज के ऊर्जा प्रसार को कम बनाए रखने के लिए अत्यंत महत्वपूर्ण है। उच्च शक्ति वाले रेडियो आवृत्ति घटकों जैसे रेडियो आवृत्ति खिड़कियाँ, युग्मक, रेडियो आवृत्ति शक्ति स्रोत, तरंग मार्गदर्शिका, रेडियो आवृत्ति गुहा आदि की सुरक्षा के लिए रेडियो आवृत्ति सुरक्षा और इंटरलॉक (आर. एफ. पी. आई.) प्रणाली का उपयोग किया जाता है। एक एकीकृत रेडियो आवृत्ति नियंत्रण प्रणाली, जिसमें निम्न स्तरीय रेडियो आवृत्ति नियंत्रण प्रणाली, अनुनाद नियंत्रण प्रणाली , और रेडियो आवृत्ति संरक्षण और अंतरबंध प्रणाली शामिल हैं, को RRCAT, इंदौर में 650 मेगाहर्ट्ज अति चालक गुहा के परीक्षण के लिए स्थापित किया गया है।

High Intensity Proton Accelerator

10

Integrated RF Control System Developed for Accelerators Under IIFC

Nibandh Kumar, Radhika Nasery, Alok Agashe, Sujo C.I., Sandeep Bharade, R. T. Keshwani, Surendra Singh Saini, G. Randale, P. Jyothi, Paresh Motiwala and *Gopal Joshi
Accelerator Control Division, Bhabha Atomic Research Centre (BARC), Trombay-400085, INDIA

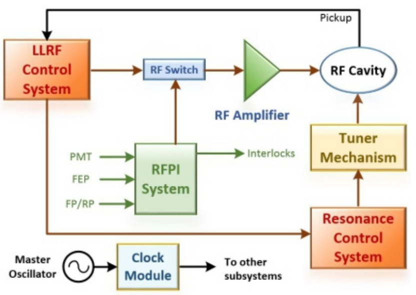

Integrated RF Control System

ABSTRACT

Integrated RF control system developed under Indian Institutions and Fermilab Collaboration (IIFC) performs important functions of controlling the amplitude & phase of the RF field inside the cavities, track the resonance frequency of RF cavities, maintain the cavity resonance frequency using stepper motors and piezo actuators, protection of critical RF components in the accelerator, and providing precision timing for synchronization to all the sub systems. Stabilization of RF field in an accelerating cavity is critical for efficient acceleration of the charged particles and maintaining low energy spread of the beam [1]. For the protection of high power RF components, such as, RF windows, Couplers, RF power sources, waveguide, RF cavity etc. RF Protection and Interlock (RFPI) system is employed. An integrated RF control system, which includes Low Level RF (LLRF) control system, Resonance Control System (RCS) and RF Protection & Interlock (RFPI) system, has been commissioned for testing of 650 MHz superconducting RF cavities in HTS at RRCAT, Indore.

KEYWORDS: *Low level RF control, RF protection, Integrated RF control, Resonance control.*

*Author for Correspondence: Gopal Joshi
E-mail: gjos@barc.gov.in

Introduction

Under IIFC, an integrated RF control system has been developed for 650 MHz superconducting RF cavity and the same is depicted in Fig.1. Sub-systems within the dashed rectangle constitute an integrated RF control system. The LLRF system employs frequency conversion to/from an intermediate frequency (IF) of 20 MHz, using down/up converters. The remaining signal processing is carried out in digital domain in a Digital Module.

Superconducting RF cavities, for which this system is designed, have a loaded quality factor of the order of 10^7 and therefore, the cavity is liable to get detuned due to Lorentz force, microphonics, helium pressure variations, slow drifts etc. RCS keeps the superconducting RF cavity at resonance and compensates for the cavity detuning to minimize RF power requirement. This is accomplished through electro-mechanical tuners coupled to the cavity. Coarse and fine adjustments in the cavity frequency can be made through the use of stepper motors coupled to the mechanical tuner assembly and piezoelectric actuators attached to the cavity. The electronics system of RCS is part of RF control system. The demodulated RF pick-up, forward & reflected power signals are transported from the LLRF system to the RCS via a multi Gb serial link for calculating the cavity detuning.

RFPI system, described in detail in the newsletter article 'RF Protection Interlock and Monitoring System developed for accelerators', continuously monitors sensor outputs installed with high power RF components and status signals from various sub-systems. This system, upon detecting a fault condition, removes the RF input from the input of the high power RF amplifier, thereby protecting the high power RF components.

LLRF System Description

RF pickup signal at 650 MHz is down converted to an IF of 20 MHz and digitized using non-IQ sampling scheme [6]. Subsequent processing is carried out in digital domain. The processed IF signals in digital domain, after passing through DACs, are up-converted to generate suitable drive for the cavity. This scheme requires additional hardware in the form of down and up converters and offers high precision. Implementation using FPGAs and communications grade ADCs and DACs enables sub-microsecond delay in the LLRF feedback loop thereby enabling wider control bandwidth.

The 8 channel down-converter translates RF pick up signal from the cavity to IF signal using low phase noise LO signal of 670MHz, RF mixer and suitable filters. Whereas using the same LO signal the 4 channel up-converter module up converts the processed baseband signal back to RF for feeding

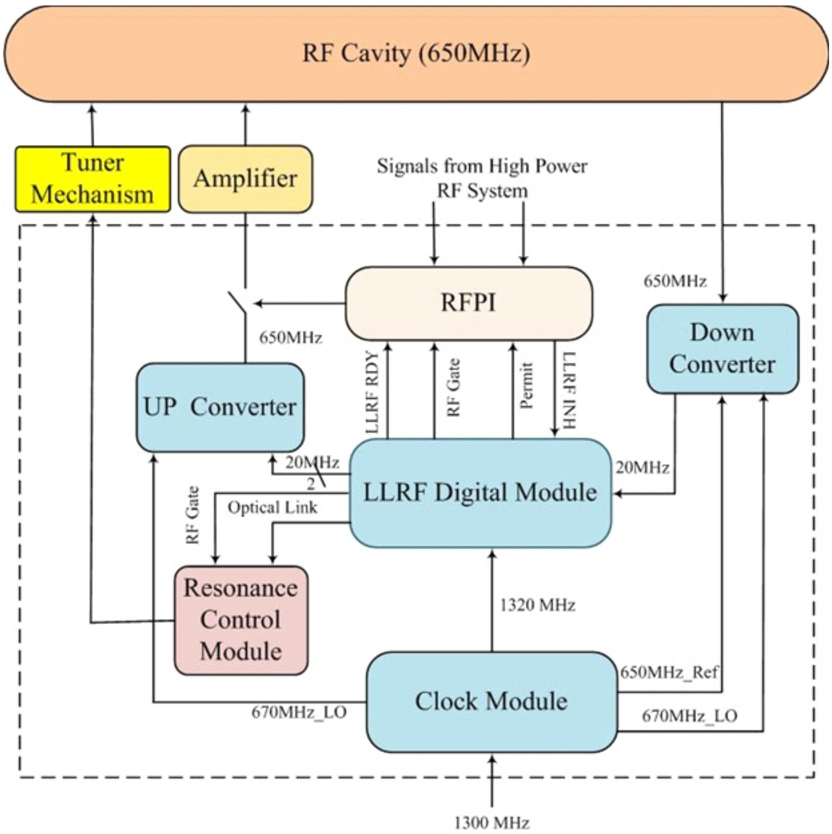

Fig.1: Integrated RF Control System developed under IIFC.

Fig.2a: 8 channel down-converter and 4 Channel up-converter modules.

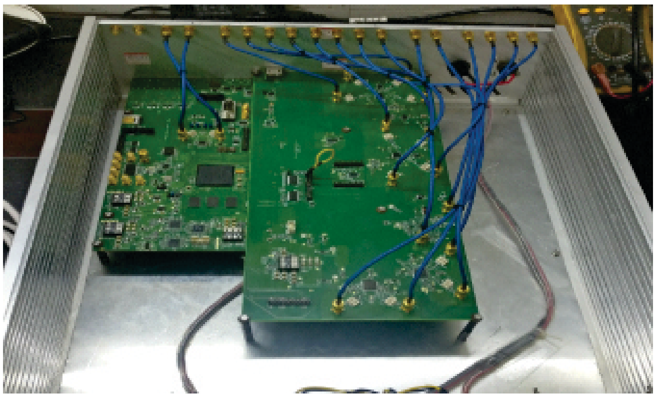

Fig.2b:LLRF digital module.

to the cavity after suitable amplification. Both the up and down converters (shown in Fig. 2a) designed to have high channel to channel to isolation (around 80dB) and linearity of better than 1% within the operating range. A high isolation (better than 60dB) RF switch has been provided at the output of each channel in the up-converter, which may be operated remotely to switch OFF the RF power to the cavity.

The Digital module, shown in Fig.2b, plays a key role in determining the overall targets of achieving high RF field stability of 0.01% in amplitude and 0.01 degrees in phase. The ADC in the Digital module is a high performance device with a 16-bit resolution and very low clock aperture jitter. The ADC sampling clock provides processing gain which helps improve the overall SNR of the system. High speed System on Chip (SoC) based FPGA situated in the digital module implements the entire digital signal processing chain. The FPGA provides interfaces such as Ethernet, USB, UART etc. to communicate with the host.

For achieving high precision, all the modules of the LLRF control system require stable and low phase noise RF sources. Generally, a Reference Phase Distribution System is provided in accelerator to meet this requirement. A separate article titled "Reference Phase Generation Systems Developed under IIFC" is included in this newsletter describing such a system in detail. For HTS this requirement is met by developing a Clock Module. The Clock Module accepts 1300MHz RF signal from a signal generator and generates all the necessary clocks for the LLRF system. Clock dividers with low additive phase noise, single side-band mixer circuits and cavity filters have been used for this purpose. The phase noise of LO signal at an offset frequency of 100 KHz is measured as -130 dBc/Hz.

LLRF Digital Signal Chain Description

The digital signal processing chain is shown in Fig. 3. For each cavity, four signals viz; Cavity pick-up, RF Reference, Forward and Reflected are processed inside the FPGA for control and monitoring purposes. All the four incoming signals to FPGA are centred at an IF of 20MHz which is digitized with a 16 bit, quad channel Analog to digital converter. The demodulated pick-up signal is compared with the desired value. The resulting error signal is passed through a P-I controller to correct the errors. The output signals are digitally up converted to 20MHz and sent to DAC.

The firmware and software of LLRF system enables operation in Generator Driven Resonator (GDR), Self Excited Loop (SEL) and Open Loop modes of operation. In GDR mode the cavity is driven with RF signal, phase synchronized with the RF reference using CORDIC and NCO. In SEL mode, the system can track the resonant frequency of the cavity within a certain bandwidth and in Open Loop mode, the system can synthesize drive signal of required amplitude and phase into the cavity using feed-forward tables. The open loop mode helps in system calibration and diagnostics.

An extensive data acquisition scheme has been developed and incorporated for monitoring and analysis. Implementation of data acquisition scheme is shown in Fig. 4. It can be divided into low speed and full speed data transfer. In low speed data transfer 1024 data points of 40 different waveforms can be displayed whereas in full speed data

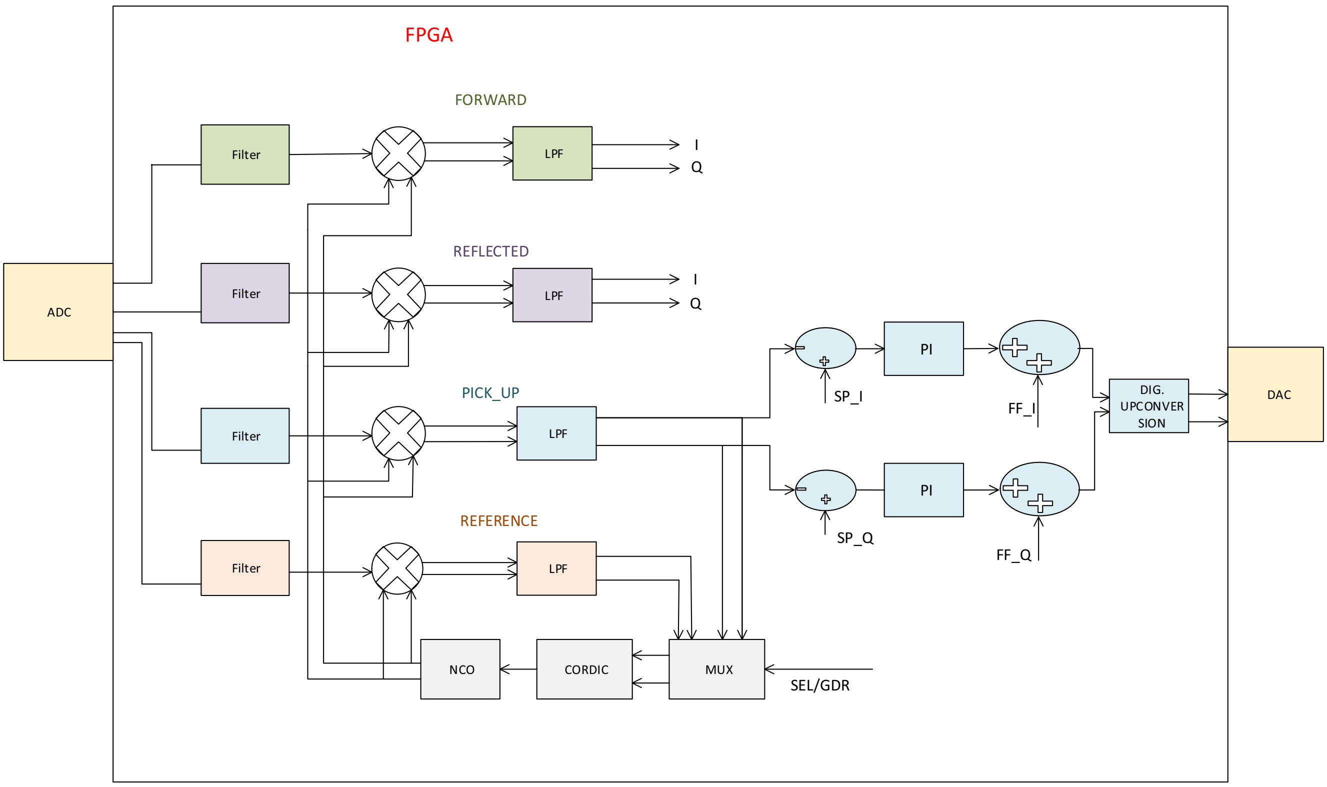

Fig.3: Digital signal chain architecture.

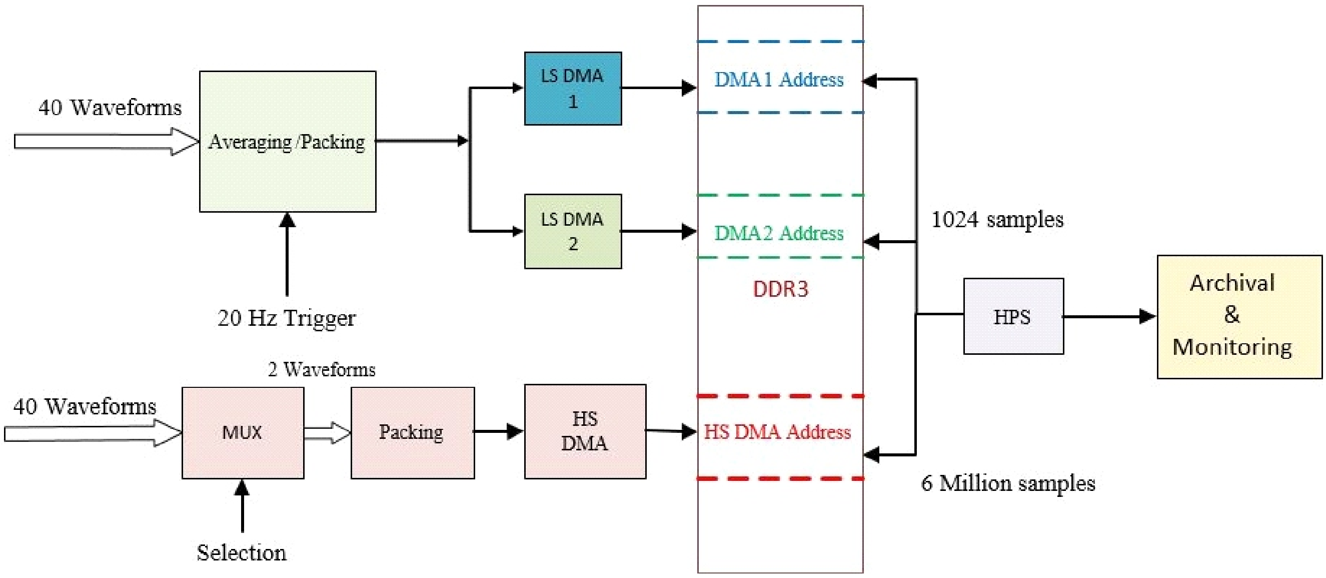

Fig.4: Data acquisition and display implementation in FPGA.

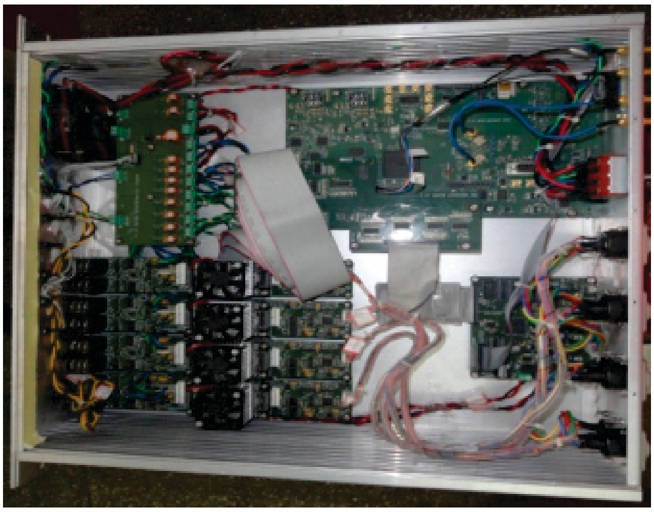

Fig.5: RCS chassis.

transfer any two of the 40 waveforms are acquired for duration of 64 ms. The high speed data transfer functionality helps in diagnostics and characterization.

Resonance Control System

The Resonance Control System is a 19" rack mountable 3U size, standalone system, which is an independent operable sub-component of the integrated RF control system. Fig.5 shows the chassis of RCS with stepper motor driver, piezo drivers and digital board. Each RCS chassis supports tuning of four SCRF cavities. The system is interfaced to a host via Ethernet link and supports operation in manual as well as remote modes.

The system computes detuning of the cavity by using cavity base band equation. Excitation of Piezo actuator by half sine wave has also been implemented. Programmable half sine wave parameters, namely, width, amplitude, bias and delay with respect to RF pulse have been implemented in firmware and software.

Control Software Description

The software platform consists of open source Preloader, U-boot, and Linux OS image and the Experimental Physics and Industrial Control System (EPIC)S SCADA [7]. Open source Preloader and U-boot have been configured in-house and cross-compiled using GNU bare-metal compiler for the SoC-FPGA platform. A custom configuration of the open-source embedded Linux is cross-compiled using GNU GCC compiler to prepare a bootable SD-card with the binaries of Preloader, U-boot, and OS image. EPICS IOC, responsible for LLRF system functionalities, is cross-compiled for ARM-based Linux OS and interacts with the FPGA using indigenously developed device drivers, loaded into the embedded Linux using customised device tree. EPICS IOC is then deployed on the HPC of the SoC-FPGA platform and interfaced with the FPGA.

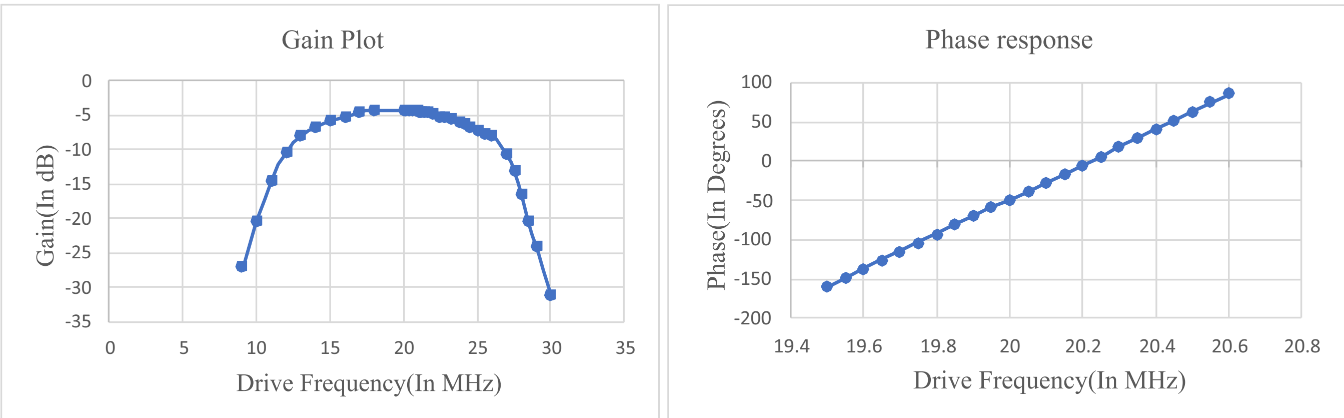

Fig.6: Gain and Phase plot corresponding to different drive frequencies.

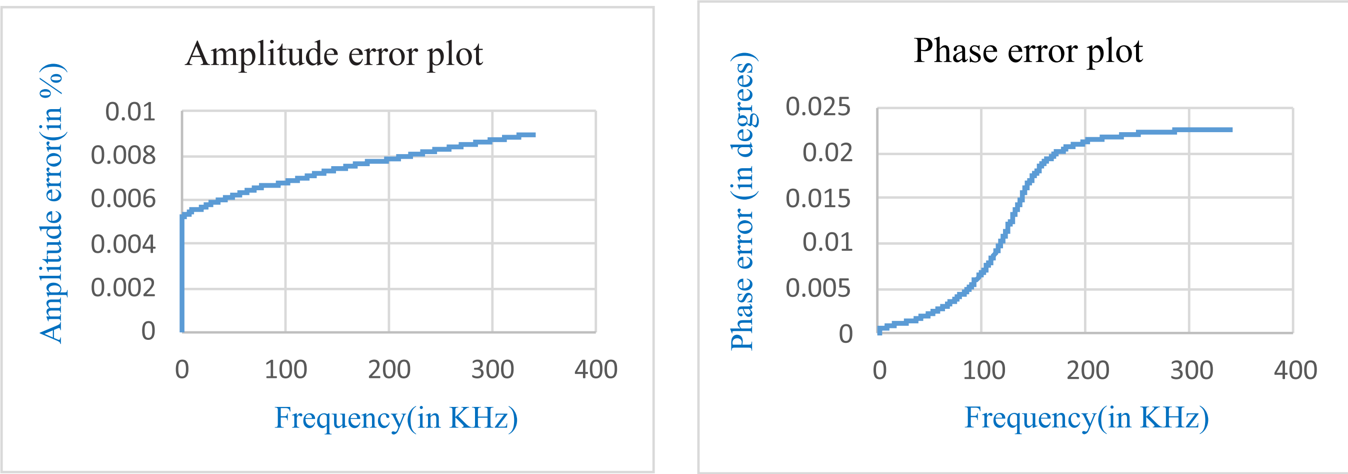

Fig.7: Integrated Amplitude and Phase error w.r.t Frequency.

Table 1: Amplitude and phase measurement error w.r.t different ADC levels.

Sr. No.	Input level (percentage of ADC full range)	Amp error	Phase error (in degrees)
1.	25 %	0.0106 %	0.0237
2.	32 %	0.0094 %	0.0233
3.	62 %	0.0082 %	0.0228
4.	78 %	0.0077 %	0.0230

Testing in the Lab

The hardware and firmware have been thoroughly characterised through different tests in lab. In one of the tests, the digital module, up-converter and down-converter were connected to form a closed loop and drive signal was generated from feed forward tables in GDR mode. Phase and amplitude of the received signal in firmware were computed corresponding to different drive frequencies and results were used to estimate group delay and 3dB bandwidth of the system.

The gain and phase plot corresponding to different drive frequencies are shown in Fig. 6. The 3 dB bandwidth of the system is around 10 MHz and group delay was found to be 631.8 ns. The experiment was repeated after removing the up-converter filter and group delay in that case was found to be 541.9 ns with filter contributing around 90 ns of group delay.

In another experiment, capture and lock range of NCO phase loop was measured by driving the loop with different frequencies. Lock and capture range is a function of loop gain and for a typical loop attenuation value of 16, the Lock and capture range was found to be 340 kHz and 310 kHz respectively.

In order to achieve amplitude and phase stability of 0.01% and 0.01 degrees respectively, it is imperative that the noise in measurement of amplitude and phase should be much less than these values. In the test set up to estimate the intrinsic noise of the measurement chain, the required signals are generated through high quality signal generators locked to each other. The analog down-converter is fed with 650 MHz pick up and reference signals. The resulting IF signals are given to quad channel ADC and the phase and amplitude stability of the demodulated signal is calculated with firmware operating in GDR mode with feedback loop open.

The noise present in demodulated signal corresponding to pick-up has contributions from both amplitude dependent as well as independent sources, therefore, amplitude and phase stability has been calculated at various ADC input levels. The results are listed in Table 1. Integrated amplitude and phase fluctuations with frequency corresponding to an ADC input level of 32 % is shown in Fig. 7. As can be seen from Fig.7, measurement noise in closed loop bandwidth, which is of the order of few tens of kHz, is much less than the desired stability specifications.

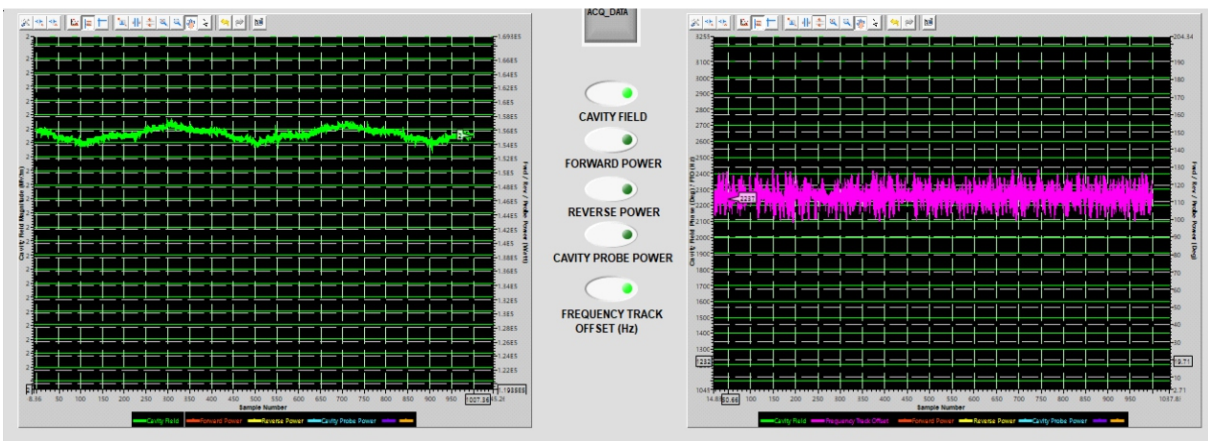

Fig.9: SEL Mode of operation.

Fig.8: Integrated RF control system commissioned at HTS, RRCAT.

Commissioning at RRCAT

Subsequent to thorough testing in the lab at BARC, the integrated RF Control system, shown in Fig.8, was installed and commissioned at RRCAT for testing of 650MHz SCRF cavity in HTS. The cavity was tuned to the required resonance frequency with the use of tuning mechanism under stepper motor control. In SEL mode the cavity was tested up to 4.6 kW power. Fig.9 below shows field and detuned frequency of the cavity at 536 W power. The waveform in green represents RF field in the cavity. Even in the absence of amplitude feedback, the amplitude modulation is very small, highlighting the usefulness of SEL mode of operation. Adjoining plot in magenta represents offset of the cavity resonance frequency, which is observed to be 2200Hz from 650MHz.

The system was operated in pulsed mode at different power levels and duty cycles. Phase of the loop was adjusted to find the peak of pick-up signal. GUI screenshot corresponding to 3KW of output power and 30 percent duty cycle is shown in Fig.10. A zoomed view is displayed in Fig.11. As can be seen from Fig.10, cavity field (Green trace) gradually builds and then decays during pulse off time. Initially when the field is not present, the resonant frequency is higher and as the field builds up, resonant frequency decreases because of Lorentz force detuning. The cavity was also tested in generator driven resonator (GDR) mode. The cavity could be successfully driven in CW mode at 1 kW of power.

The RCS was integrated with the cavity tuner assembly already existing at RRCAT and the stepper motor was moved beginning with the cavity at resonance frequency of 650MHz. The new resonance frequency was measured with the help of LLRF control system in SEL mode. A linear response of stepper motor control was observed over the entire tuning range of up to 50 kHz. The piezo actuators were evaluated by measuring the resonance frequency of the cavity over a range of 0V and 100V, and the corresponding detuned frequency was observed to be 1 kHz.

Fig.12a shows the graph of stepper motor steps versus cavity detuning frequency and Fig. 12b shows the piezo voltage versus cavity detuning frequency.

At HTS the operation of the RFPI system along with LLRF system was observed. The RFPI system operated the RF switch at the output of the LLRF system as required and successfully protected various RF components whenever the reflected power exceeded the set limit. The response time of the system

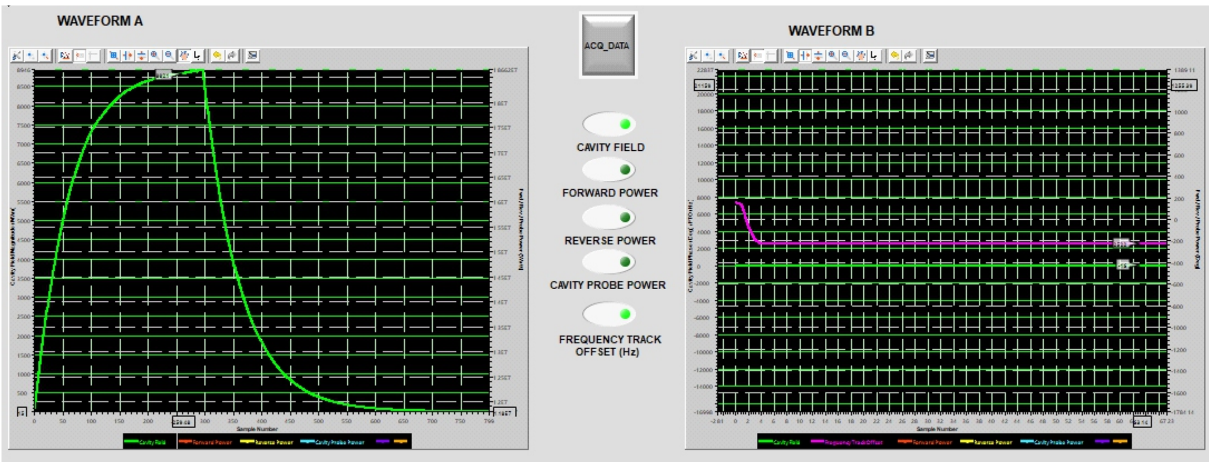

Fig.10: SEL mode operation in pulsed mode.

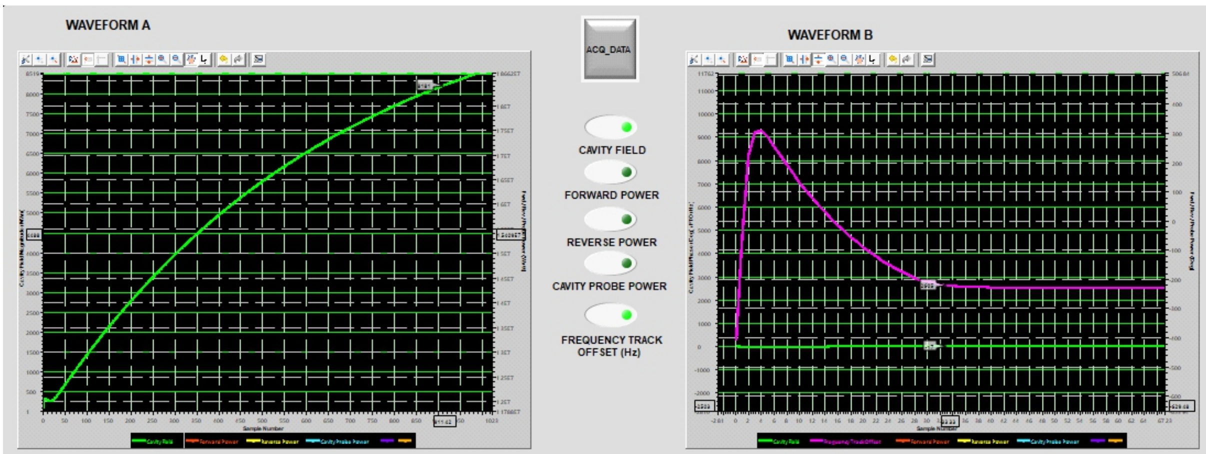

Fig.11: Lorentz force detuning illustration in Pulsed mode.

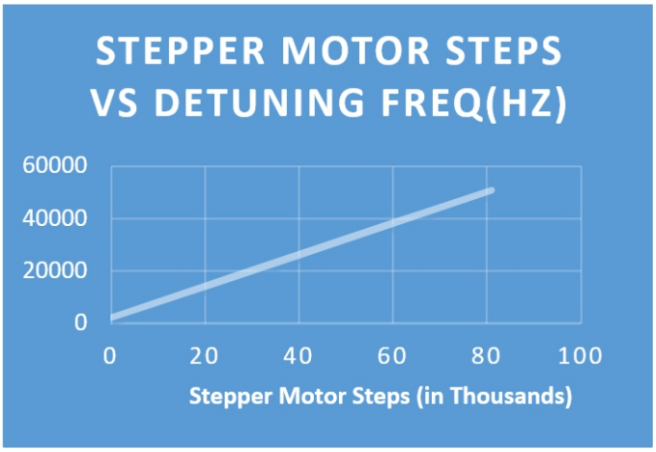

Fig.12a: Performance of Stepper Motor at 2°K.

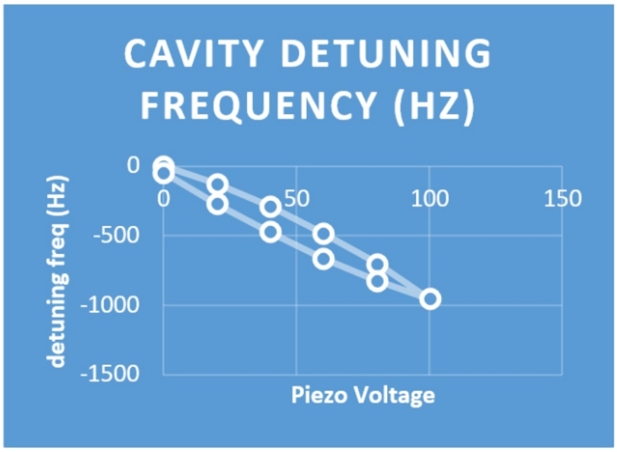

Fig.12b: Performance of Piezo Tuner at 2°K.

was within 1-2μs. Functionalities of RFPI system has been tested for long hours while characterising 650MHz, elliptical superconducting cavity. Different sub systems and signals interfaced to RFPI has been shown in Fig.13.

Conclusion

Integrated RF control system consisting of LLRF system, RCS, and RFPI system. has been developed at ACnD, BARC under IIFC and commissioned at HTS, RRCAT for testing of 650 MHz superconducting RF cavities.

The LLRF system successfully established the RF fields in the cavity in SEL and GDR modes. It was observed that a few times, during conditioning phase of the cavity, RFPI switched OFF RF power to the cavity due to high reflected power and also due to fault status signal from MPS. The cavity was powered to 4.6 kW in the SEL mode and 1 kW in GDR mode without the need of automatic frequency tuning mechanism. The operation of HTS at RRCAT for the testing of 650 MHz RFSC gave an opportunity to validate the functioning of the RCS. The performance of the RCS with stepper motor controller was observed to be linear over the entire range. The plot above shows slight difference in the traces while raising and lowering the piezo voltage between 0 to 100V. The data acquisition system has aided in the operation and collection of data for analysis.

Based on the performance of the LLRF, RCS and RFPI systems in the HTS, an approval was received to deliver these systems to Fermilab for further testing. The systems have been shipped to Fermilab and await testing with the SCRF cavity.

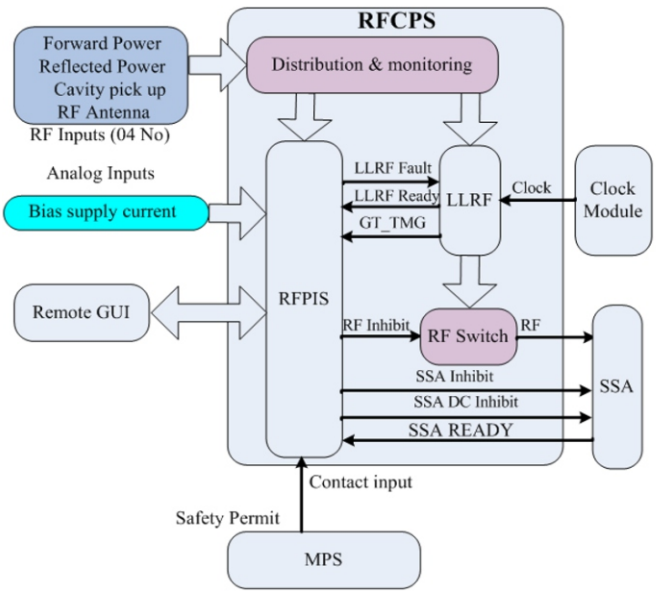

Fig.13: Signals interfaced to RFPI at HTS, RRCAT.

Acknowledgment

We acknowledge the help and support of all the colleagues of ACnD during the entire development phase. The systems have been developed under IIFC and we sincerely acknowledge and appreciate technical support from the Fermilab during the design, fabrication and testing phases. The support of RRCAT team during the installation and commissioning of the systems was extremely valuable in all respects and is highly appreciated.

References

[1] Thomas Schilcher, “Vector Sum Control of Pulse Accelerating Fields in Lorentz Force Detuned Superconducting Cavities,” Ph.D. Thesis, University of Hamburg, (1998).

[2] Nibandh kumar, et. al., “Development of Digital Feedback control for 650 MHz superconducting RF cavity in HTS”, InPAC 2019, IUAC Delhi.

[3] Lawrence Doolittle “Low-Level RF control system Design and Architecture”,

[4] Paresh D. Motiwala, Gopal Joshi, “Digital Technology based RF Control and Instrumentation for Accelerators”, InPAC2022, VECC, Kolkata.

[5] Rajesh Keshwani, et al (2019), "Design Architecture of RF Interlock, Protection & Monitoring system for HTS control electronics", Proceedings of Inpac 2019 at IUAC Delhi.

[6] T. Schilcher, “RF applications in digital signal processing”

[7] Radhika Nasery, et al, "Design and Development of Embedded EPICS IOC based software for Low Level RF at Horizontal Test Facility (HTS-2), RRCAT", InPAC 2022.

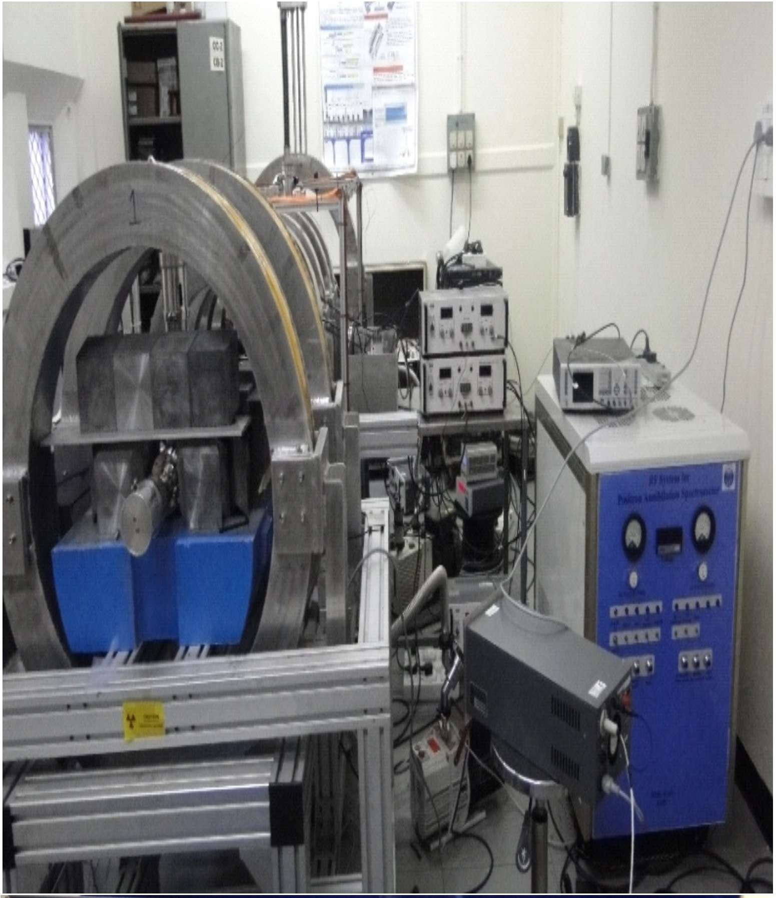

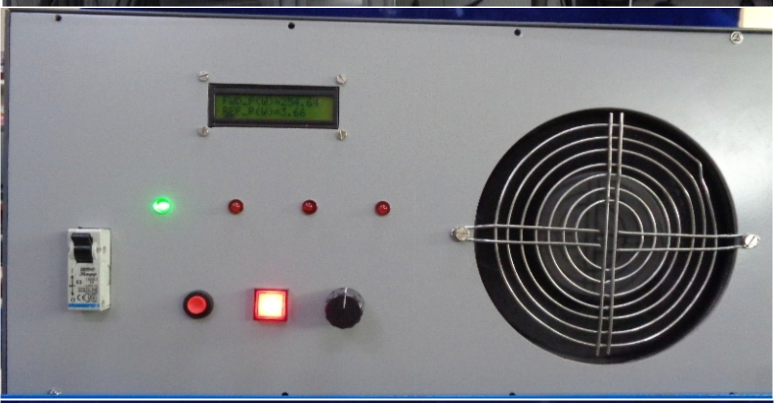

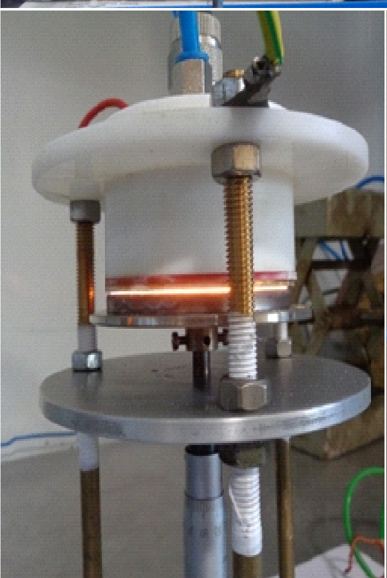

RF TECHNOLOGY SPIN-OFFS FOR SCIENTIFIC AND SOCIETAL APPLICATIONS

Several new spin-off technologies were developed as part of intense R&D in core and advanced RF technologies, integrated multi frequency and single frequency systems.

This page intentionally left blank

बहु-विषयक अनुसंधान

11

पॉज़िट्रॉन विलोपन लाइफटाइम स्पेक्ट्रोमीटर के लिए एकीकृत आरएफ प्रणाली

***संदीप श्रोत्रिया, एस.एस. जेना, ए. शिजू, एन. पटेल और मंजिरी पांडे**

त्वरक नियंत्रण प्रभाग, भाभा परमाणु अनुसंधान केंद्र (भापअ केंद्र), ट्रांबे-400085, भारत

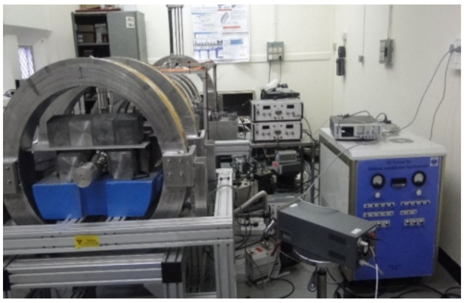

आरसीडी में पीएएलएस कणपुंज रेखा

सारांश

पॉज़िट्रॉन निम्न सांद्रता और उच्च संवेदनशीलता के साथ सामग्री दोषों की जांच कर सकते हैं। पॉज़िट्रॉन एनीहिलेशन जीवनकाल स्पेक्ट्रोस्कोपी (PALS/पी.ए.एल.एस.) बहुलक, सरंध्र सामग्री, धातुओं, अर्धचालकों आदि में परमाणु स्तर के दोषों की जांच के लिए एक सुस्थापित शोध पद्धति है। पारंपरिक PALS/पी.ए.एल.एस. में गहराई चयनात्मकता का अभाव है, और इसलिए गहराई चयनात्मक जानकारी प्राप्त करने के लिए ट्यूनेबल / मिलाने योग्य ऊर्जा धीमी पॉज़िट्रॉन किरण का उपयोग किया जाता है। एक स्पंदित धीमी पॉज़िट्रॉन किरण आधारित गहराई चयनात्मक PALS PALS/पी.ए.एल.एस. को भाभा परमाणु अनुसंधान केंद्र में परिकल्पित और विकसित किया गया है, जो अपने किरण लाइन संरचनाओं को शक्ति देने के लिए एक एकीकृत रेडियो आवृत्ति प्रणाली का उपयोग करता है। बहु आवृत्ति एकीकृत स्वदेशी रेडियो आवृत्ति प्रणाली अपने सिग्नल इनपुट को एक सामान्य स्रोत से प्राप्त करती है और उसके बाद उसे तीन शाखाओं में विभाजित करती है। इनमें से प्रत्येक शाखा में एक रेडियो आवृत्ति शक्ति प्रवर्धक, विभाजक, क्षीणक, चरण परिवर्तक, अलगक /आइसोलेटर, डीसी बाधक, मिलान परिपथ और रेडियो आवृत्ति फांसा युग्मक शामिल हैं जो रेडियो आवृत्ति शक्ति को प्रत्येक स्पंदित पॉज़िट्रॉन किरण लाइन संरचनाओं से जोड़ते है। यह आलेख RCD / आर.सी.डी., भाभा परमाणु अनुसंधान केंद्र के पॉज़िट्रॉन किरण आधारित PALS /पी.ए.एल.एस के साथ डिज़ाइन, विकसित और युग्मित एकीकृत रेडियो आवृत्ति प्रणाली का विवरण देता है।

Multi-disciplinary Research

11

Integrated RF System for Positron Annihilation Lifetime Spectrometer

***Sandip Shrotriya, S. S. Jena, A. Shiju, N. Patel and Manjiri Pande**

Accelerator Control Division, Bhabha Atomic Research Centre (BARC), Trombay-400085, INDIA

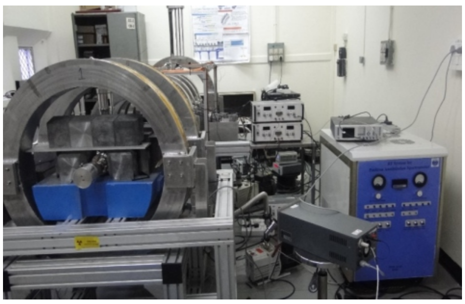

PALS Beam line at RCD

ABSTRACT

Positrons can probe material defects with low concentrations and high sensitivity. The positron annihilation lifetime spectroscopy (PALS) is an established research methodology for investigation of atomic level defects in polymers, porous materials, metals, semiconductors etc. Conventional PALS lacks depth selectivity, and so tunable energy slow positron beams are used to get depth selective information. A pulsed slow positron beam based depth selective PALS is designed and developed in BARC, which employs an integrated RF system to power its beam line structures. The multi frequency integrated indigenous RF system derives its signal input from one common source and thereafter splits the same in three branches. Each of these branches include one RF amplifier, splitter, attenuator, phase shifters, isolators, DC blocks, matching circuits and RF loop couplers that couple the RF power to each of pulsed positron beam line structures. This article gives details of integrated RF system designed, developed and coupled with positron beam based PALS of RCD, BARC.

KEYWORDS: *Amplifier, Annihilation, Attenuator, Atomic-defect, PALS, Positron, Radio Frequency, Splitter.*

**Author for Correspondence: Sandip Shrotriya*
E-mail: sds@barc.gov.in

Introduction

A variety of phenomena and material properties on an atomic scale can be studied by positron annihilation spectroscopy. A Positron Annihilation Lifetime Spectrometer (PALS) has been operational in Radio Chemistry Division (RCD), BARC. It is used as a non-destructive probing system for nanometre size voids and defects in solid materials. It uses radio frequency (RF) electronics to power its resonant structures.

In PALS, an implanted positron thermalizes in the sample and gets trapped in a low electron density area (e.g. defects) in a material. It annihilates with an electron in the sample resulting in emission of two gamma rays. In conventional PALS, the time difference between birth of positron (i.e. emission time from a radioactive source, signalled by almost simultaneous emission of gamma ray) and the detection of annihilation gamma rays emitted from the sample is measured to give the life time of the positrons. The positron lifetimes in alloys, metals, semiconductor can be of the order of hundreds of picoseconds (ps). In porous materials, the measured lifetimes can be in the range of nanoseconds.

The conventional PALS using beta-spectrum of positron emitters lacks depth selective information due to continuous energy distribution of emitted positrons from radio isotope sources. In case of DC positron beams, the timing information about the birth of positron is usually lost. Hence, to carry out lifetime spectroscopy, a positron beam is usually pulsed using RF electric fields.

Advancements in this field include, moderating the positrons from beta emitters, pulsing them and accelerating to desired energies to implant positrons as desired and extract depth selective information of defects. These are possible with the use of radio frequency (RF) for pulsing of positrons. Such RF pulsing of positrons gives time resolutions of a few hundred picoseconds, which is ideal for measurement of the lifetimes in metals and alloys.

Description

A modified version of Suzuki's [1] pulsed positron beam is developed at Bhabha Atomic Research Centre (BARC), Mumbai. The PALS beamline comprises of structures viz., chopper, pre-buncher and buncher, and can deliver positron pulses in the range of ≤ 350 ps at the sample position. The radio frequency (RF) power energizes or excites these beam line structures meant for pre bunching and then bunching of the incoming chopped particles. The required integrated RF electronic system for bunching the positron beam up to a few 100s of pico-sec has been designed and developed indigenously except 40 Watt amplifier. Its RF system comprises of RF amplifiers at 37.5 MHz and 150 MHz, RF coupling lines developed using RF components for amplitude and phase matching and respective impedance matching unit and RF couplers.

Indigenous Integrated RF System

The indigenous multi frequency integrated RF system (Fig.1 and 2) [2] consists of three RF amplifiers, splitters, attenuators, phase shifters, isolators, power measurement units, DC blocks, matching circuits and RF loop couplers. The three RF amplifiers, a 37.5 MHz, 40 W amplifier for chopper, another 40 W amplifier for pre-buncher and a 150 MHz, 200 W RF amplifier for buncher cavity have been designed and developed indigenously. For effective RF power transfer from amplifiers to beamline structures, dedicated matching circuits along with loop couplers have been designed, developed and integrated with these RF cavities or structures. Phase and amplitude of the three RF systems has been optimized for effective bunching using the combination of phase shifters, attenuators etc.

To reduce the interference among the RF signals and the detector electronics, various RF interference suppression techniques like filtering, shielding, isolation, proper grounding topology, EM suppression etc. were implemented.

The RF power amplifier 200 Watt at 150 MHz for buncher cavity has been designed around the N channel

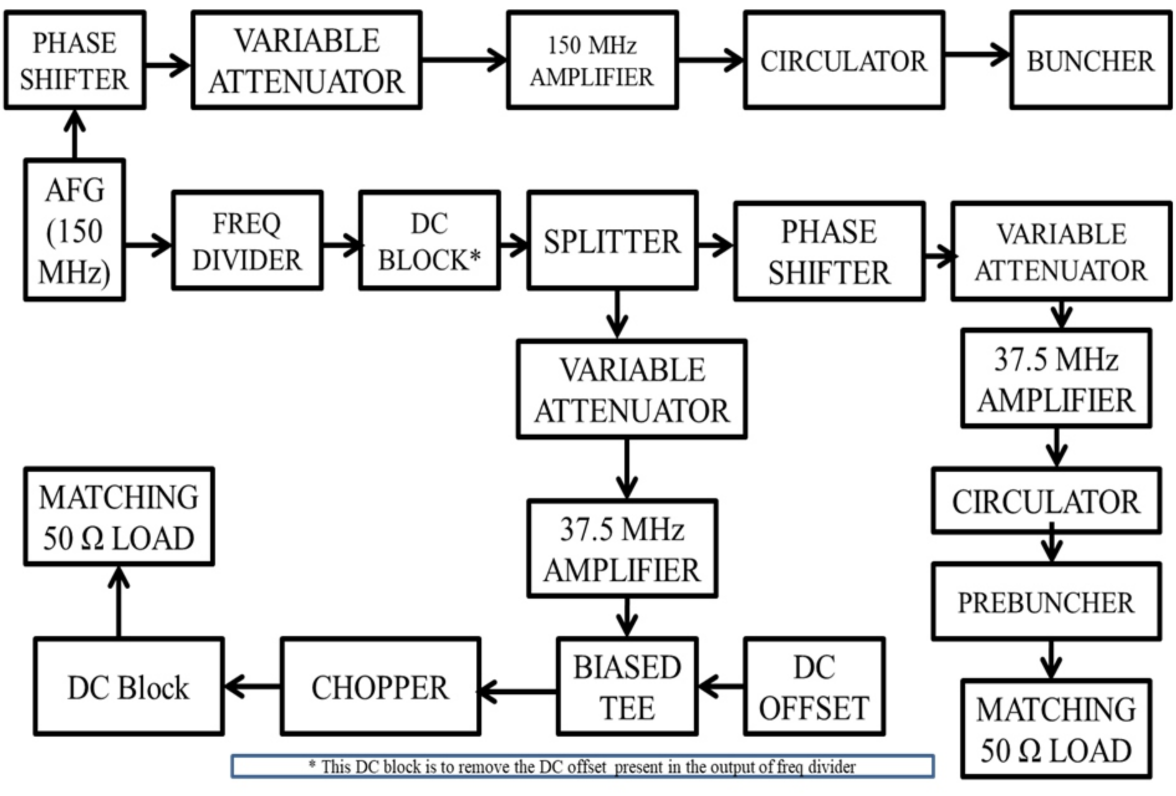

Fig.1: An overall integrated RF system.

Fig.2: Integrated RF system.

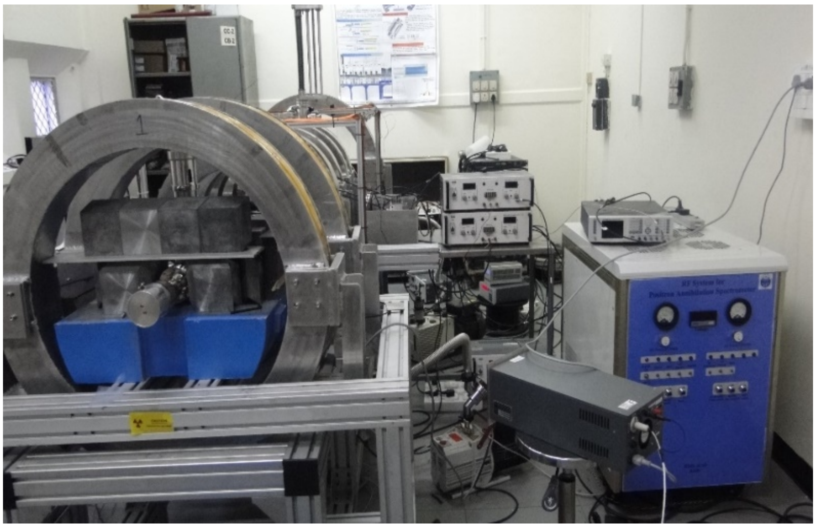

Fig.3: PALS Beam line at RCD.

MOSFET- MRF151G (Gemini package). It is biased in class AB push pull configuration with LC tuned circuits at its input and output to maintain linearity. It has achieved 58% efficiency, and 2nd and 3rd harmonics better than -30 dBc. The RF amplifier was integrated with buncher cavity via a circulator and a loop coupler.

The RF amplifiers for pre-buncher and chopper operate at 37.5 MHz, can deliver a maximum power of 40 Watts with efficiency 50 %, gain 43 dB and 2nd harmonic of -30 dBc. An external matching circuit i.e. a parallel resonant circuit [2] comprising of an inductance in parallel with resistance and distributed capacitance of RF structure was designed, developed and coupled to pre-buncher cavity to match [2] the impedance of pre-buncher cavity with 50 ohm output impedance of RF amplifier. In a similar way, the second RF amplifier at 37.5 MHz was coupled to chopper via another matching circuit [2] of an inductance in parallel with resistance and distributed capacitance of RF structure. Both these parallel resonant circuits maintain the sinusoidal signal wave shape across grids of respective cavities.

Results

The tested parameters of 150 MHz RF amplifier are given in table 1. Initially Table 1: Performance parameters of 150 MHz RF amplifier, chopper, pre buncher and buncher were

Table 1: Performance parameters of 150 MHz RF amplifier.

Sr. No.	Operating parameters	Values
1.	Frequency	150 MHz
2.	Output power	200 Watt CW
3.	Input power	6 Watt
4.	Drain Voltage	50 V
5.	Efficiency	58 %
6.	Gain	15.2 dB
7.	1 dB Bandwidth	1 MHz
8.	-1 dB saturation power (W)	210 Watt
9.	2nd and 3rd Harmonic	-30 dBc

characterized for their design parameters at low power. Individually, these structures were tested with their respective RF system for characterization and validation of the RF system with respect to beam line structures. The integrated RF system (Fig.1 and 2) was then coupled with beam line structures i.e. chopper, pre buncher and buncher and tested. This ensured desired power transfer from integrated RF systems to beam line components. After integrating and aligning all the structures of PALS (Fig.3), initial testing of the pulsed beamline, inclusive of RF system, was carried out with the electron beam [2].

After further optimisation of the parameters of the chopper, pre buncher and the buncher, pulsed beamline (Fig.3) was tested with positron beam and a final pulse width of 325 ps of positron beam was achieved. A few experiments including the defect analysis of the polymer sample have been carried out using PALS. Pulsed positron beam has been used to probe the porosity of the surface and the bulk layer of Reverse Osmosis membrane of water purifier. The photograph of the PALS at RCD is given in Fig.3.

Conclusion

Various RF and other components/structures of PALS were aligned and characterized with RF. The indigenous multi frequency integrated RF system was coupled with the beam line. The final pulsed positron beam line was initially tested with a low energy DC electron beam. Upon energizing, tuning and synchronization of the chopper-pre buncher-buncher assembly, the electron beam was bunched up to 280 ps, thereby establishing the overall functionality of the pulsed beamline with its associated electronics. Subsequently, electron source was replaced with a positron source and further optimization and tuning of the beamline with a slow positron beam was completed to achieve and a final pulse width of 325 ps of positron beam [4] was achieved.

Acknowledgement

The authors would like to sincerely thank the PALS team from RCD comprising of Dr. Saurabh Mukherjee, Dr. Priya Maheshwari, Dr. S. K. Sharma, Dr. D. Dutta, Dr. Kathi Sudarshan, Dr. P.K. Mohapatra and Dr. P.K. Pujari for their excellent support and collaboration.

The authors acknowledge for the immense technical help and efforts provided by Shri Hitesh Kadam and Shri Jagdish Bowlekar. The authors thank Dr Gopal Joshi, Head

ACnD from his excellent support and guidance.

The authors sincerely thank Shri Vivek Bhasin, Director, BARC and Shri U. D Malshe, Group Director, MRG for their constant encouragement and continued support.

References

[1] R Suzuki, Y Kobayashi*, T Mikado, H Ohgaki, M Chiwaki, T. Yamazaki and T Tomimasu, Pulsing of slow positrons for variable energy positron lifetime spectroscopy. Electro technical Laboratory, 1-1-4 Umezono, Tsukuba, Ibaraki 305 Japan.

[2] Sandip Shrotriya, Saurabh Mukharjee, S.S Jena, A. Shiju, N. Patel, Priya Maheshwari, S. K. Sharma, D. Dutta, Kathi Sudarshan, Manjiri Pande Gopal Joshi and P.K. Pujari, Design and development of Radio Frequency system for Pulse Positron Low Energy Beam and its electron beam Journal of Instrumentation, Volume 16, September 2021, JINST 16 (09): T09002 DOI 10.1088/1748-0221/16/09/T09002

[3] Saurabh Mukherjee et al., Theme Meeting on Nuclear Probes for Materials, Medicine and Industry-2022 (NPMMI-2022) March 04-05, 2022, BARC, Mumbai.

[4] S Mukherjee, Sandip Shrotriya, Priya Maheshwari, S. K. Sharma, D. Dutta, K.Sudarshan, Manjiri Pande, P. K. Pujari, Design of picosecond pulsed positron beam for defect characterization, 15th International Workshop on Slow Positron Beam Techniques and Applications (SLOPOS-15), Prague September 2-6, 2019.

रेडियो आवृत्ति प्रणाली

12

रिक्त कैथोड आधारित शीत वायुमंडलीय प्लाज्मा (HC-CAP) उपकरणों के लिए स्वदेशी आरएफ प्रणालियां

*श्याम सुंदर जेना[1], एन. पटेल[1], ए. शिजु[1], श्याम मोहन[1], संदीप श्रोत्रियां[1], सुरेंद्र सिंह सैनी[1], सी.आई. सुजो[1], मंजिरी पांडे[1], गोपाल जोशी[1], आर.टी. केशवानी[1], राजीव कर[2,3], नमिता मैती[2], वनिता शेखर[2], आर.एल.भारद्वाज[2] और मार्टिन मास्करेंहस[2]

[1] *त्वरक नियंत्रण प्रभाग, भाभा परमाणु अनुसंधान केंद्र (भापअ केंद्र), ट्राम्बे-400085, भारत*
[2] *लेजर और प्लाज्मा प्रौद्योगिकी प्रभाग, भाभा परमाणु अनुसंधान केंद्र (भापअ केंद्र), ट्रॉम्बे-400085, भारत*
[3] *होमी भाभा राष्ट्रीय संस्थान, ट्रॉम्बे-400085, भारत*

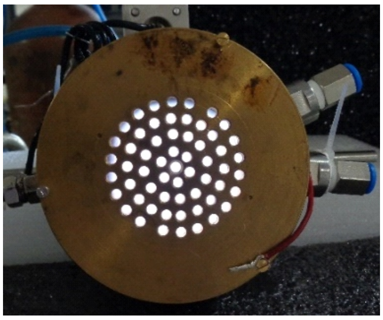

~60 W RF पावर पर 16cm2 प्रभावी प्लाज्मा क्षेत्र वाला युक्त एचसी सीएपी उपकरण

ABSTRACT

खोखले कैथोड आधारित शीत वायुमंडलीय प्लाज्मा (एचसी-सीएपी) उपकरणों को एल एंड पीटीडी द्वारा स्वच्छता अनुप्रयोग के लिए एक आशाजनक तकनीक के रूप में प्रदर्शित किया गया है। रेडियो आवृत्ति शक्ति को एचसी-सीएपी उपकरणों से युग्मित करके शीत प्लाज्मा को उत्पन्न किया जाता है। एसीएनडी ने इस उपकरणों के लिए स्वदेशी रेडियो आवृत्ति प्रणालियोंको विकसित किया है। दो प्रकार की प्रणालियाँ विकसित की गई हैं, अर्थात् / नामतः, एक मैनुअल प्रतिबाधा मिलान नेटवर्क (आईएमएन) के साथ 13.56 मेगाहट्र्ज 250 W रेडियो आवृत्ति प्रणाली, और दूसरी स्वचालित प्रतिबाधा मिलान नेटवर्क (ऑटो-आईएमएन) के साथ 2 से 30 मेगाहट्र्ज तक ट्यून करने योग्य 200 W रेडियो आवृत्ति स्रोत (प्रणाली)। शीत प्लाज्मा, रेडियो आवृत्ति प्रणाली के लिए एक गतिशील भार प्रतिबाधा प्रस्तुत करता है, जो सर्कुलेटर की अनुपस्थिति में इसके डिजाइन को और अधिक चुनौतीपूर्ण बनाता है। यह पेपर वायुमंडलीय दबाव वाले शीत प्लाज्मा उत्पादन के लिए लागत प्रभावी और अनुकूलित रेडियो आवृत्ति प्रणालियों के विकास के विवरण पर चर्चा करता है।

Radio Frequency System

12

Indigenous RF Systems for Hollow Cathode Based Cold Atmospheric Plasma (HC-CAP) Devices

***Shyam Sundar Jena[1], N. Patel[1], A. Shiju[1], Shyam Mohan[1], Sandip Shrotriya[1], Surendra Singh Saini[1], C. I. Sujo[1], Manjiri Pande[1], Gopal Joshi[1], R. T. Keshwani[1], Rajib Kar[2,3], Namita Maiti[2], Vanita Sekar[2], R. L. Bhardwaj[2] and Martin Mascarenhas[2]**

[1]*Accelerator Control Division, Bhabha Atomic Research Centre (BARC), Trombay-400085, INDIA*
[2]*Laser and Plasma Technology Division, Bhabha Atomic Research Centre (BARC), Trombay-400085, INDIA*
[3]*Homi Bhabha National Institute, Trombay-400085, INDIA*

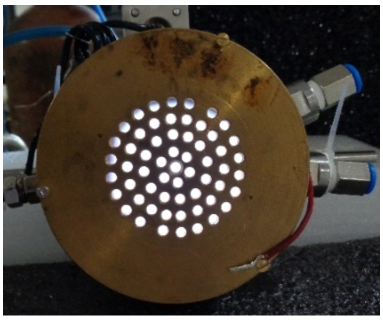

HC CAP device with effective plasma area 16 cm^2 at ~ 60 W RF power.

ABSTRACT

Hollow Cathode based Cold Atmospheric Plasma (HC-CAP) devices have been demonstrated as a promising technology by L&PTD for sanitization application. Cold plasma is generated by coupling RF power to the CAP devices. ACnD has developed indigenous RF systems for these devices. Two types of systems have been developed, viz. a 13.56 MHz 250W RF system with manual impedance matching network (IMN), and a 200W RF source tunable from 2 to 30 MHz with Automatic Impedance Matching Network (Auto-IMN). The cold plasma presents a dynamic load impedance to the RF system, which makes its design more challenging in absence of circulator. This paper discusses the details of development of cost effective and customized RF systems for atmospheric pressure cold plasma generation.

KEYWORDS: *Amplifier, Hollow Cathode Cold Atmospheric Plasma (HC-CAP), Impedance matching, Radio frequency, Power measurement*

**Author for Correspondence: Shyam Sunder Jena*
E-mail: ssjena@barc.gov.in

Introduction

RF power sources are used for driving plasma devices for various applications e.g. cleaning, coating, surface activation, disinfection or decontamination of pathogens, sputtering etc. The commercially available RF systems are expensive and are locally non-repairable and non-maintainable. For hollow cathode based cold atmospheric plasma (HC–CAP) [1,2] devices developed by L&PTD, the RF power requirement is generally in the range of 100 to 200 W. To mitigate above challenges, ACnD has designed and developed indigenous RF power systems, as import substitutes for cold plasma generation. The development of two types of RF systems viz. a 13.56 MHz RF system with manual matching network, and a 2 to 30 MHz tunable RF system with auto matching network are described in the following sections.

The 13.56 MHz 250W RF systems with manual impedance matching network

This indigenous, standalone 13.56 MHz RF power system is designed, developed and optimized for high efficiency and cost effectiveness for use with different cold atmospheric plasma devices (CAP) designed and developed by L&PTD [1,2]. The indigenously developed subsystems include, a crystal oscillator with low power driver, high gain & high efficiency power amplifier [3,4], high directivity-directional coupler based digital power measurement [5,6], DC bias supplies, interlock and protection circuit and a customized L-type impedance matching network. Fig.1 shows the architecture of 13.56 MHz RF system for HC-CAP. The MOSFET based main power amplifier is biased in class C configuration with tuned resonant circuit at its input and output stages to reduce the harmonic contents in RF power. A novel protection scheme based on reflected power and MOSFET junction temperature is used to protect RF amplifier against continuous high reflected power. All these subsystems are housed in a single standard 5 U rack as a standalone and portable RF power system.

The important & critical performance parameters achieved, and salient features of RF system are:

- Efficiency (DC to RF): > 70%.
- Efficiency (AC to RF): > 64%.
- Load variations: No damage with Short and Open load termination.
- High directivity directional coupler based RF power measurement.
- EMI/EMC compatible.
- Modular, Portable & Field deployable.

The high AC to RF and DC to RF efficiencies have led to reduced electrical power consumption further leading to low operational cost and low thermal load, respectively. The RF power source incorporates an independent RF signal source thereby no external signal generator is needed for its operation. Being tolerant to load variations/VSWR changes assures ruggedness. An in-house designed and developed high directivity bi-directional coupler based RF power measurement [5,6] assures accurate power measurement. EMI/EMC compatibility ensures non-interference with other electronic systems. Its modularity ensures easy replicability & maintainability.

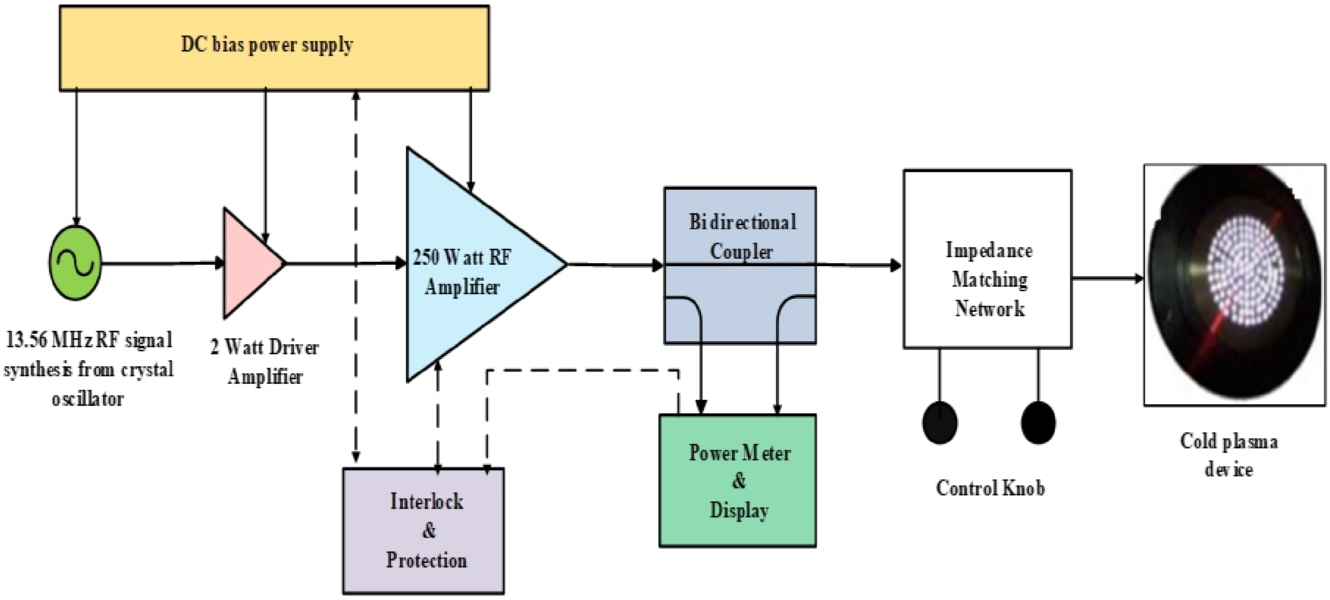

Fig.1: Architecture 13.56 MHz RF system for HC-CAP.

Fig.2: 13.56 MHZ, 250 W RF source.

Fig.3: Impedance matching network.

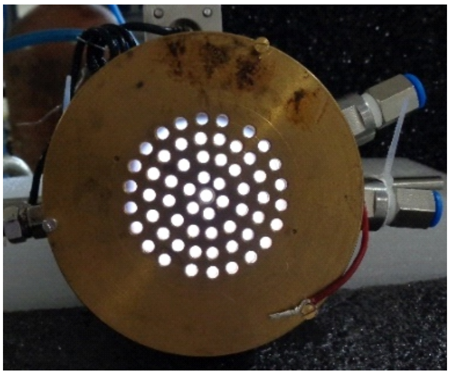

HC CAP device with effective plasma area 16 cm^2 at ~ 60 W RF power.

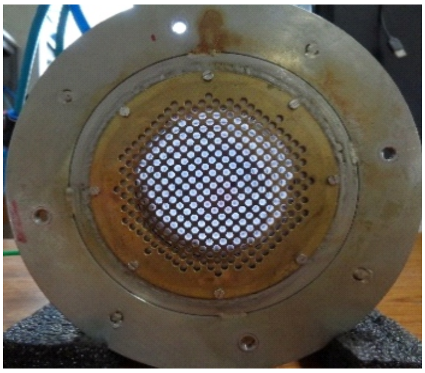

HC CAP device with effective plasma area 50 cm^2 at ~ 90 W RF Power.

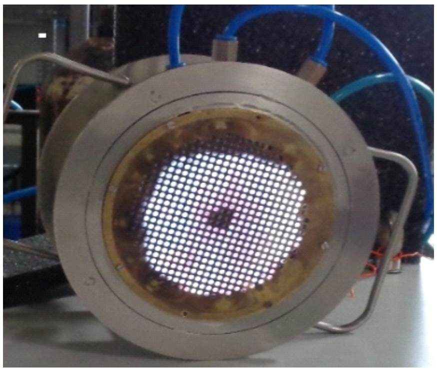

HC CAP device with effective plasma area 80 cm^2 at ~ 140 W RF Power.

Fig.4: Three different HC-CAP devices driven by indigenous RF power system and its IMN.

An L-type impedance matching network (IMN) has been designed and developed to match the impedance of HC-CAP device to 50 Ohm output impedance of 13.56 MHz RF system. The impedance of HC-CAP device changes dynamically while transiting from Argon gas stage into its plasma stage. These changes are accommodated by IMN to have stabilized cold plasma. The architecture of 13.56 MHz RF system customized and coupled to HC-CAP device via impedance matching network is shown in Fig.1.

Fig.2 shows the RF system developed and its impedance matching network is shown in Fig.3. During field trials, the 13.56 MHz, 250 W system with L-type impedance matching network has been successfully coupled with three different HC CAP devices available at L&PTD having different diameters. Argon plasma was successfully generated in each of these devices (Fig.4) and was found to be stable against load variations and argon gas flow rate changes.

Variation in forward and reflected RF power coupled with the CAP device of 185 mm diameter over a period of time (11.15 Hrs to 16 Hrs) is shown in Fig.5. RF power and gas flow requirement for three different HC-CAP devices are listed in Table 1.

RF system with He, Ar & O_2 based HC-CAP

The same 13.56 MHz, 250 W RF system was also coupled with another plasma device having a different configuration, shown in Fig.6, and full intensity plasma was observed with forward RF power of 94 W. The plasma was generated with combination of Helium, Argon & Oxygen gases.

13.56 MHz 50 W RF system

A number of other CAP devices catering to different applications require less than 50 W of RF power at 13.56 MHz. Therefore, a standalone 50 W RF system, shown in Fig.7, has also been designed and developed. It is a low-cost, portable, compact (19", 3U) light weight unit.

200W RF source tuneable from 2 to 30 MHz with Automatic Impedance Matching Network (Auto-IMN)

ACnD, with support of L&PTD, has also developed a 200W, 2 to 30 MHz RF source incorporating an automatic impedance matching unit [7]. The auto-matching system which had to be imported at a premium cost has been developed in house including the high power components. Fig.8 shows the source coupled to HC-CAP device at L&PTD.

Wideband RF power amplifier has been developed so that plasma can be generated at both 13.56 MHz and 27.12 MHz. The system incorporates a Direct Digital Synthesis IC, which has been programmed to generate required RF input signal over the frequency range. The high power RF source has a dynamic range of 31.5 dB. Adequate protection has been provided for the RF source against over-drive, over-temperature and high reflected power. The input DC supply voltage and current are controllable from local panel for the RF source. The important parameters of RF source are displayed on the local panel, including forward power, reflected power, temperature, drain voltage and current. These parameters are accessible remotely using Ethernet controller.

The automatic impedance matching network is realized by an in-house developed tunable LC network, which incorporates, high power RF air core variable capacitors and inductor. The value of the capacitors is varied by driving geared stepper motors. An algorithm has been developed for the

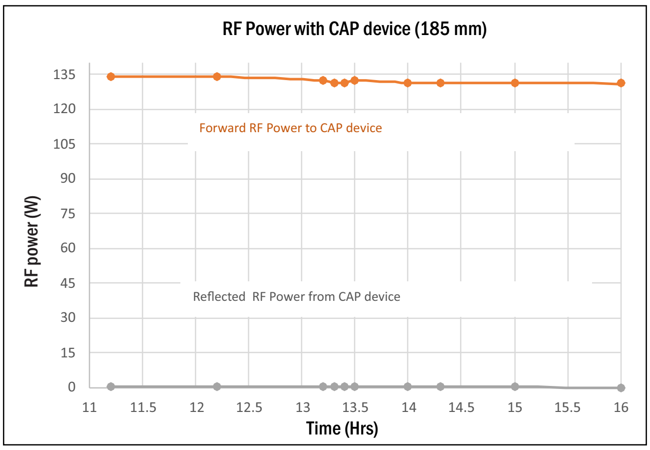

Fig.5: Variation of RF power with CAP device with time.

Table 1: RF Power with CAP devices of different diameters.

Parameters	CAP (85 mm)	CAP (130 mm)	CAP (185 mm)
Frequency (MHZ)	13.56	13.56	13.56
Forward Power (W)	60	80	140
Reflected Power (W)	3	5	10
Gas	Argon	Argon	Argon
Gas flow rate (LPM)	8	12	20
CAP Assembly (Dia. in mm)	85	130	185

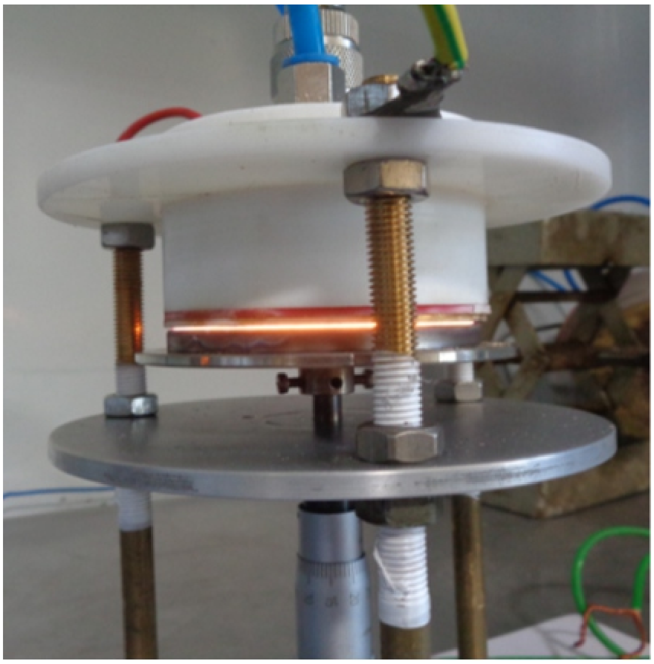

Fig.6: Cold plasma with combination of Helium, Argon & Oxygen gases.

measurement of load impedance and control of matching network which ensures matching to 50 ohm. The firmware has been written using C++ programming language for microcontroller. The control algorithm for auto-impedance matching may be tuned for other applications like antenna tuning and communication applications.

This system was also integrated with three different HC-CAP devices having effective plasma generation area of ~16 cm^2, ~ 50 cm^2 and ~ 80 cm^2 at L&PTD, BARC. Argon gas was used to generate plasma in all these cases whereas, Ar gas flow rate was changed from 15 to 30 LPM and power was also varied. The generated plasma remained stable under the operating window and no significant fluctuation was observed during the

Fig.7: 13.56 MHz, 50 W RF power source (3U).

course of experiments. Generated Ar plasma also remained stable against load variations.

An auto-igniting system has been developed and integrated with the plasma device. With the auto-ignition system, discharge from the plasma torch could be started without any manual intervention. This auto-ignition system is a very useful feature as often striking the initial discharge requires some form of manual intervention. This is especially the case when HC-CAP devices age, and when physical access to the device is difficult, e.g. when the device is put into fume hoods/containments etc. It is planned to carry out more field trials to further optimize the robustness of the matching algorithm and also the form factor.

Conclusions

A standalone and plug and play type 13.56 MHz RF system with manual matching network, and a 2 to 30 MHz tunable RF system with auto matching network and have been totally indigenously developed. These systems have been successfully integrated with HC-CAP devices for plasma generation. The generated plasma may be used for sanitization or disinfection of pathogens. These RF systems are versatile and may also be used for generation of other types of plasma. RF amplifier technology with manual-IMN has also been customized for 50 W for other plasma applications.

Fig.8: 2-30 MHz, 200W RF source with Automatic Impedance Matching & Auto-Igniting system integrated with the plasma device. The blue-pink glow state of Ar plasma can be seen.

Acknowledgements

The authors would like to sincerely thank the team of L&PTD and Dr. Archana Sharma, Director, BTDG. The authors acknowledge ttechnical support and efforts provided by Shri Hitesh Kadam, Shri Jagadish Bowlekar, Smt. Charulata Shinde, Shri Mayur M Sutar and other colleagues who have helped on various occasions.

The authors are very much thankful to Shri U.D. Malshe, Director, MRG and Shri Vivek Bhasin, Director, BARC for his constant encouragement and continued support for this valuable BARC program.

References

[1] Kar, Rajib, Naresh Chand, Arundhati Bute, Namita Maiti, A. V. S. S. Rao, V. Nagar, R. Shashidhar, D. S. Patil, S. K. Ghosh, and A. Sharma. "Cold plasma: Clean technology to destroy pathogenic micro-organisms." Transactions of the Indian National Academy of Engineering 5, no. 2 (2020): 327-331.

[2] "Evaluation of virucidal efficacy of cold plasma on bacteriophage inside a three-layered sterilization chamber", V. Nagar, R. Kar, L. Pansare-Godambe, N. Chand, A. Bute, D. Bhale, A.V.S.S.N. Rao, R. Shashidhar, Namita Maiti, Accepted in Plasma Chemistry & Plasma Processing, published online https://doi.org/10.1007/s11090-022-10269-9

[3] Patel N.R et.al. "An indigenous 13.56 MHz solid state RF power system for cold atmospheric plasma" Proceedings of the DAE-BRNS International Symposium on Vacuum Science and Technology and its Applications in Accelerators-2022.

[4] Jena, S.S et.al. "Indigenous development of 13.56 MHz RF amplifiers" Proceedings of the Indian particle conference (InPAC) - 2023.

[5] Jena, S.S et.al. "Indigenous RF Power meter development for HF band RF amplifier" Proceedings of the Indian particle conference (InPAC) -2022.

[6] Jena, S.S et.al. "An indigenous development of bi-directional coupler for high frequency solid state RF power system" Proceedings of the DAE-BRNS International Symposium on Vacuum Science and Technology and its Applications in Accelerators-2022.

[7] Shyam Mohan, Surendra Singh Saini, Sujo C.I, R.T. Keshwani, Rajib Kar, Naresh Chand, Vanita Sekar, Namita Maity and Gopal Joshi, "Indigenous Development of RF Source For Plasma Generation", BU-Plasma 2022

This page intentionally left blank

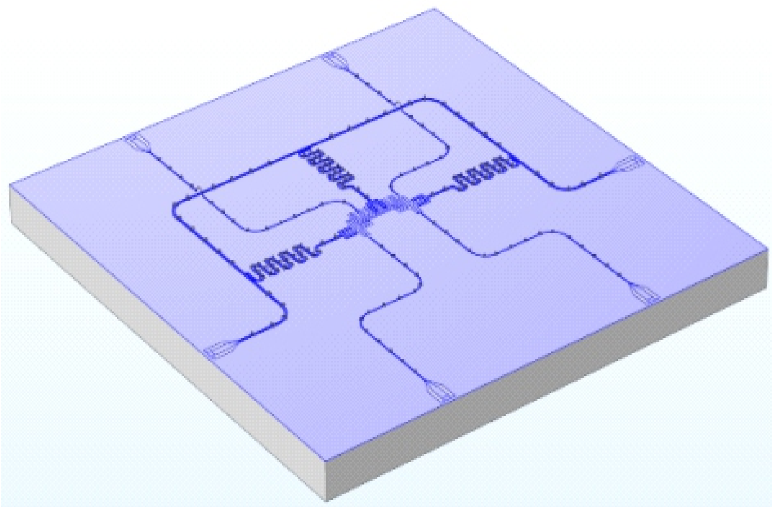

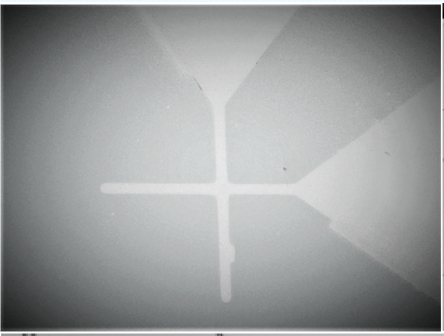

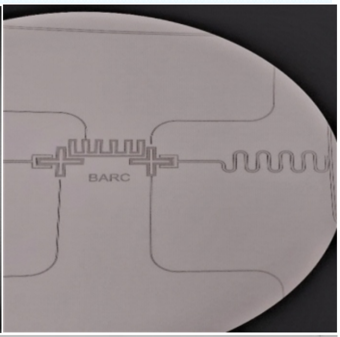

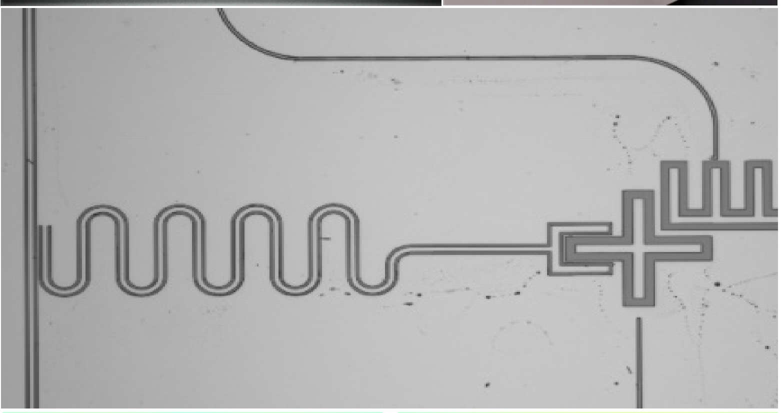

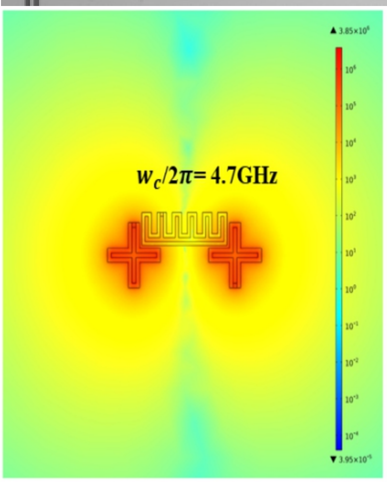

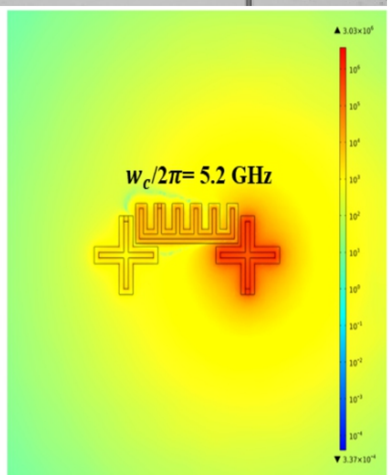

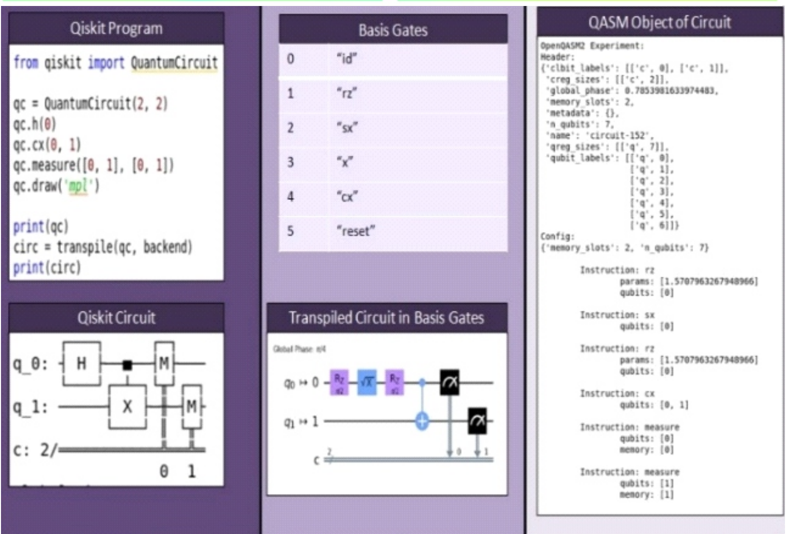

QUANTUM TECHNOLOGIES

Quantum technology harnesses principles of quantum mechanics to develop advanced technologies. It includes quantum computing, which performs computations using quantum bits (qubits) that can exist in superposition and entangled states, leading to faster problem-solving capabilities.

This page intentionally left blank

अतिचालक क्यूबिट

13

समायोजनीय युग्मक का अभिकल्पन : दो क्यूबिट के साथ किए गए अनुकरण

*सुमिता सुरा[1], दिपक पास्टे[1], प्रवीण कुमार सुग्गिसेट्टी[1], एम.वाई. दीक्षित[1], गोपाल जोशी[1], विजय राघवन[2]

[1]त्वरक नियंत्रण प्रभाग, भाभा परमाणु अनुसंधान केंद्र (भापअ केंद्र), ट्रांबे-400085, भारत
[2]क्वांटम मापन और नियंत्रण (क्यूएमएसी) संघनित पदार्थ भौतिकी और सामग्री विज्ञान विभाग
टाटा मूलभूत अनुसंधान संस्थान (टीआईएफआर), मुंबई

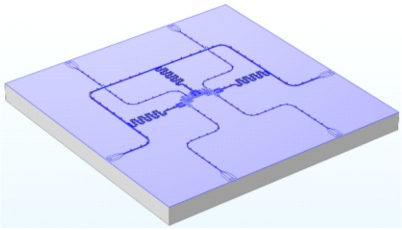

दो-क्यूबिट समायोजनीय युग्मक हेतु चिप संरचना

सारांश

एक समायोजनीय युग्मक (ट्यूनबल क्पलर) के मध्यस्थता के अधीन दो-क्यूबिट वाले क्वांटम प्रोसेसर के विभिन्न घटकों को डिजाइन करने के लिए विद्युत चुंबकीय और क्वांटम अनुकरण किया गया है। इन अनुकरणों के माध्यम से, प्रणाली के वांछित हैमिल्टनियन को प्राप्त करने के लिए विभिन्न डिजाइन पैरामीटरों की गणना की गई है। क्यूबिट्स के बीच स्थिर अवांछित ZZ युग्मन के दमन के लिए समायोजनीय युग्मक की आवृत्ति सीमा की पहचान की गई है, और समायोजनीय युग्मक का उपयोग करके क्यूबिट्स के बीच स्थितियों की अदला-बदली का प्रदर्शन किया गया है।

Superconducting Qubits

13

Designing a Tunable Coupler: Simulations with Two Qubits

Sumita Sura[1], Deepak Paste[1], Praveen Kumar Suggisetti[1], M. Y. Dixit[1], Gopal Joshi[1] and R. Vijayaraghavan[2]

[1]*Accelerator Control Division, Bhabha Atomic Research Centre (BARC), Trombay-400085, INDIA*
[2]*Quantum Measurement and Control (QuMaC) Laboratory, Department of Condensed Matter Physics and Materials Science, Tata Institute of Fundamental Research (TIFR), Mumbai*

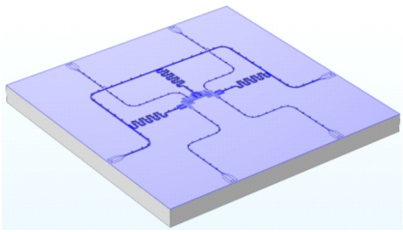

Chip architecture for two-qubit tunable coupler

ABSTRACT

Electromagnetic and Quantum simulations have been performed to design different components of a quantum processor having two qubits mediated via a tunable coupler. Through these simulations, various design parameters have been extracted to achieve the desired Hamiltonian of the system. Frequency range of tunable coupler has been identified to suppress the static parasitic ZZ coupling between qubits, and swapping of states between the qubits, using the tunable coupler, has been demonstrated.

KEYWORDS: *Superconducting qubits, Tunable coupler architecture, Microwave simulation*

*Author for Correspondence: Sumita Sura
E-mail: sumitasura@barc.gov.in

Introduction

Superconducting quantum circuits have demonstrated promising potential in various applications [1-5]. These circuits are solid state devices with macroscopic dimensions. The Josephson junction element [6] introduces non-linear inductance, thus making quantum energy levels to be unequally spaced. By employing lowest two energy levels as quantum bit (qubit), superconducting qubits have shown immense potential for information processing [7]. Manipulation and readout of qubit states is achieved through the concepts derived from circuit quantum electrodynamics (cQED) [8], where microwave pulses are employed to control and read qubit states. Advancement in the field of microwaves and microfabrication has enabled integration of these qubits into chips [9].

Despite advancements, performance of these devices is limited due to unwanted parasitic couplings and noise [10]. To overcome the challenge posed by parasitic coupling, an additional circuit element is inserted between two qubits to control the interactions. This element, known as tunable coupler, removes the parasitic coupling by destructively interfering direct interaction between qubits with the virtual interaction mediated by the states of the coupler [11]. Furthermore, by tuning the frequency of the tunable coupler, desired coupling strength between qubits can be generated, enabling implementation of fast gates [11-12].

This article presents results of the electromagnetic simulations performed on a two-qubit tunable coupler system including readout and control channels. Through numerical simulations, effect of change in the coupler frequency on the coupling between qubits is obtained. Also, the always on static ZZ parasitic [12-13] interaction has been estimated. Two qubit iSwap gate operation using tunable coupler has been demonstrated.

System architecture

Layout of the quantum chip is shown in Fig.1. It consists of two xmons coupled via a transmon acting as Coupler [12]. Ease of connections and minimization of cross talk have been important considerations in deciding the orientation of remaining parts of the chip. Specifically, the quantum chip consists of following components:

- Two xmon qubits Q_1 and Q_2 on silicon substrate, Q_1 is fixed frequency and Q_2 incorporates flux tunablity,

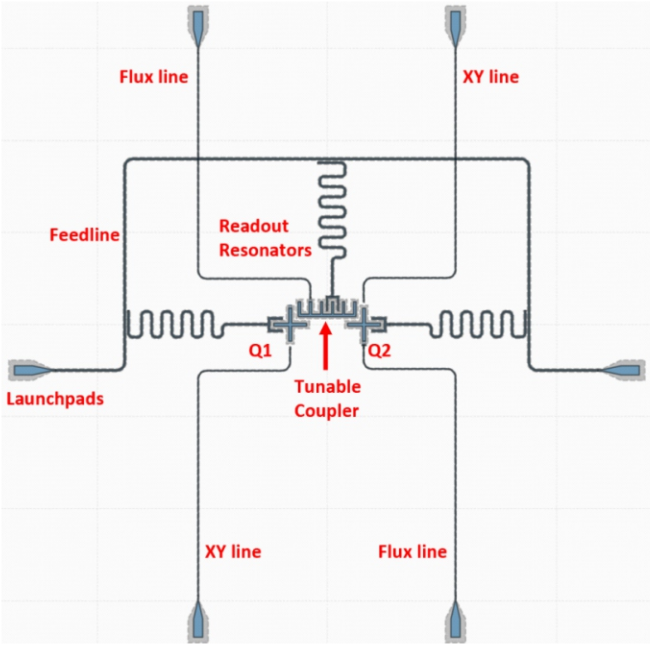

Fig.1: Layout of Quantum Chip.

- Two XY control lines, capacitively coupled to Q_1 and Q_2, and a flux line inductively coupled to Q_2,
- A flux tunable transmon as Coupler, and
- Three readout resonators capacitively coupled to Q_1, Q_2 and Coupler, respectively, and inductively coupled to a 50 Ω transmission line.

The frequency of the xmon qubits, Q_1 and Q_2, is kept close to 4 GHz. Geometrical parameters of all the three qubits have been finalized based on simulations. Open-source package, Qiskit Metal [14], has been used extensively for design and simulation.

Electromagnetic Simulations

Qubit parameters

An E_j over E_c ratio more than 50, anharmonicity close to 200 MHz and frequencies of Q_1 and Q_2 xmons about 4 GHz, have guided the design pertaining to Q_1 and Q_2. Capacitance analysis has been performed to get the required shunt capacitances. By optimizing the geometries, Q_1 and Q_2 qubit

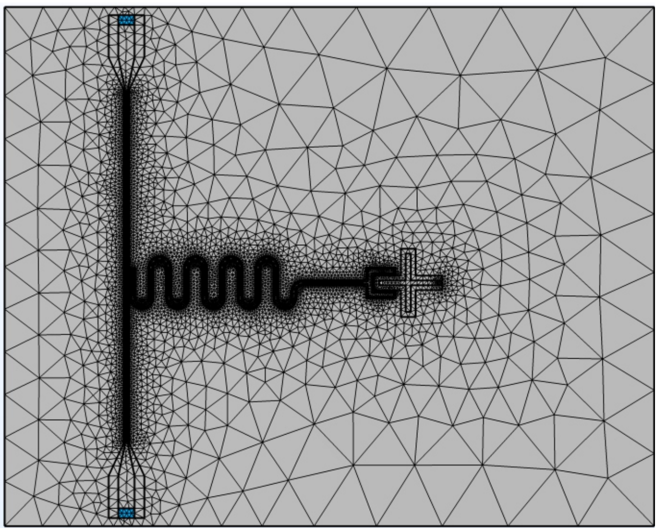

(a)

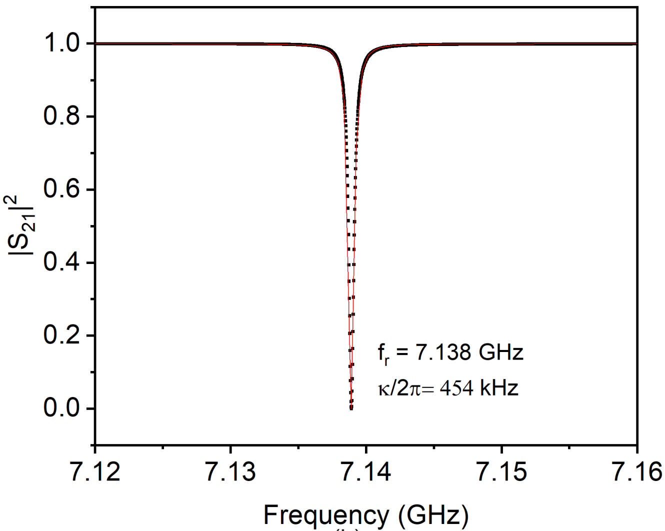

(b)

Fig.2: (a) Mesh distribution for a resonator-qubit structure (b) $|S_{21}|^2$ vs frequency.

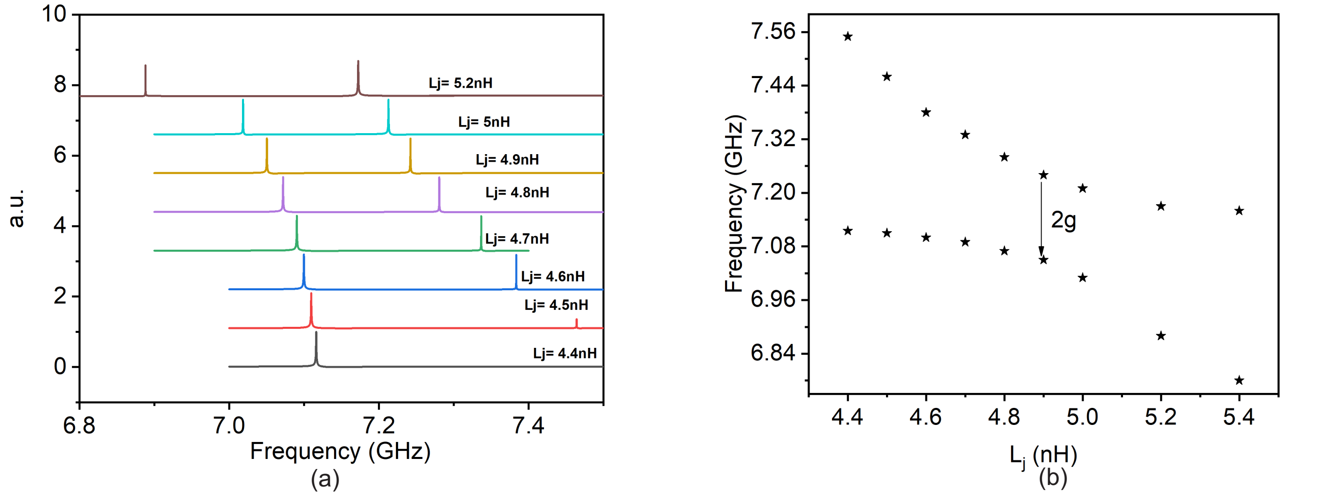

Fig.3: (a) $|S_{21}|^2$ as a function of the frequency for different inductance value L_j, which determines the qubit frequency, (b) avoided crossing plot.

frequencies (f_1, f_2) equal to 4.1 and 4.2 GHz, and qubit anharmonicity (α) equal to 217 MHz, are obtained.

Readout resonator

A quarter-wavelength (λ/4) resonator has been designed for dispersive readout of qubit state. This resonator is capacitively coupled to qubit and inductively coupled to a transmission feedline. The resonator frequency, which determines its length, is aimed to be close to 7 GHz. The coupling of resonator to feedline is so selected that the line-width of resonator is close to 500kHz. Through simulations, transmission coefficient S_{21} of feedline coupled to the resonator-xmon system, shown in Fig.2 (a), has been studied. By fitting Lorentzian function to $|S_{21}|^2$, as shown in Fig.2 (b), the resonator frequency is obtained as 7.138 GHz. Full-width-half-maximum of the peak, k/2π Hz, which determines how fast the photons in the resonator decay, is estimated as 454 kHz.

The coupling strength, g/2π, of resonator to qubit has been estimated from the gap between qubit and resonator frequency at avoided crossing. The qubit frequency is changed by changing the inductance parameter of the qubit, L_j, as shown in Fig.3 (a). By fitting a second order polynomial to the avoided crossing, the coupling strength g/2π has been estimated to be about 99 MHz. The simulated avoided crossing plot has been shown in Fig.3 (b).

The readout scheme, where coupling strength g/2π is very less than frequency detuning between resonator and qubit, is known as dispersive readout. In this regime, the state of qubit induces a frequency shift in coupled resonator. This state dependent frequency shift, $\chi/2\pi$, known as dispersive strength of resonator, has been calculated to be about 156 kHz [15]. This coupling of resonator to qubit also induces Purcell decay in qubit states. This decay rate of the qubit, $\gamma/2\pi$, has

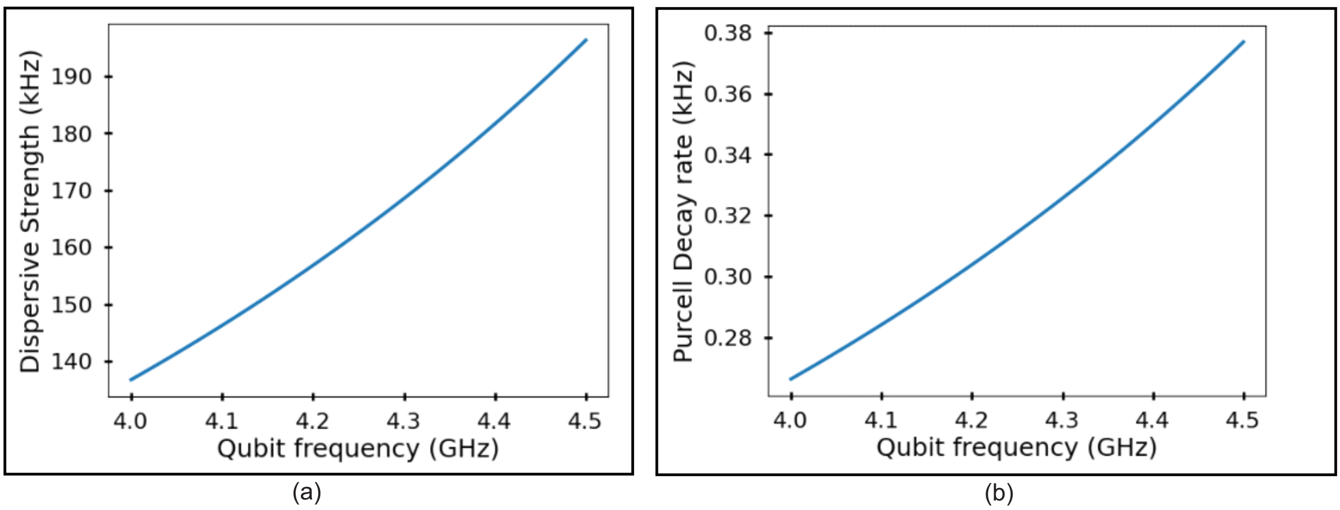

Fig.4: (a) Dispersive strength, (b) Purcell decay rate with qubit frequency.

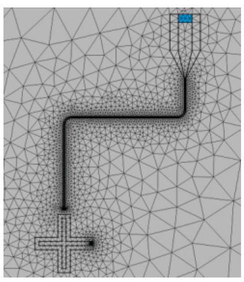

Fig.5: Mesh distribution for a XY Line-qubit structure at 40 um gap.

Table 1: Coupling capacitances and decay time T_1 at different gaps.

Gap between qubit and XY control line (um)	Coupling capacitance (aF)	Decay time T_1 (us)
15	72.8	169
30	43.8	374
40	33.6	546

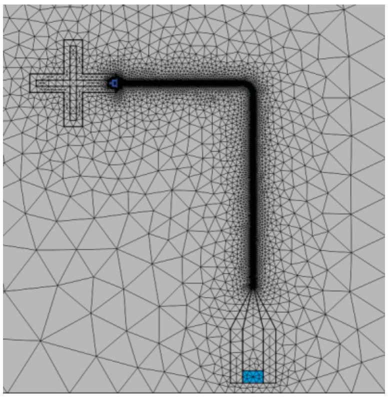

Fig.6: Mesh distribution for the Flux line inductively coupled to squid of qubit.

been calculated using formula given in reference [15] to be 0.30 kHz. This formula used for the decay rate is based on single mode approximation of the readout resonator. Detailed EM simulations are planned to get more accurate results at large detuning. The variations in $\chi/2\pi$ and $\gamma/2\pi$ have been plotted with respect to qubit frequency in Fig.4 (a) and (b), respectively. For qubit frequency range 4 to 4.5 GHz, the dispersive strength ranges from 135 to 195 kHz and the Purcell decay rate ranges from 0.26 kHz to 0.37 kHz, as shown in Fig.4.

Control lines

These are 50 Ω transmission lines which carry microwave pulses to manipulate state of qubit. For the present design, these include XY control lines to change states of qubit, and Flux control line to change frequency of the qubit. Choosing optimum coupling parameter to the qubit is a crucial step as too strong coupling will induce decoherence/noise channel and a too weak coupling will degrade the performance of qubit.

(a) XY control line: The XY control line is capacitively coupled to

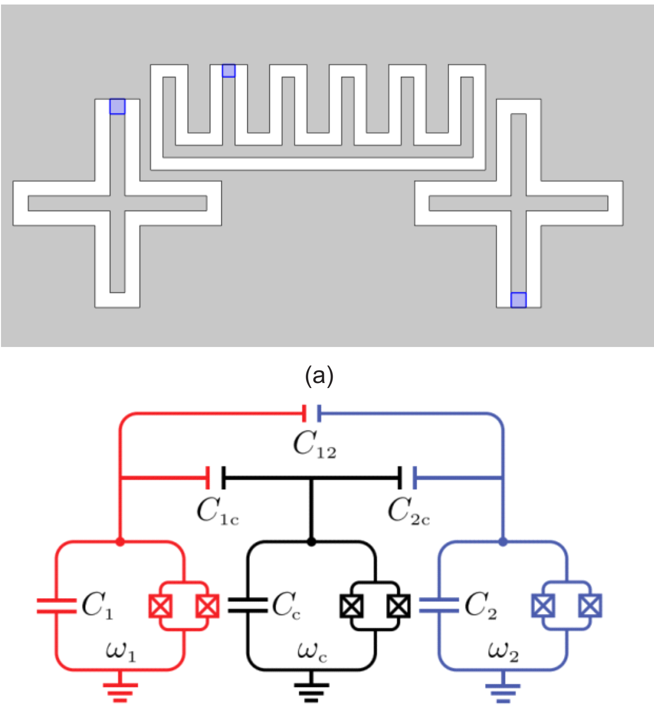

(a)

(b)

Fig.7: (a) Physical arrangement of Tunable coupler capacitively coupled to qubits, (b) Equivalent circuit diagram.

Table 2: Capacitance values obtained from Quasi-electrostatic simulations.

Symbol	Capacitance (fF)
C_1	96.60
C_2	96.60
C_c	191.29
C_{1c}	3.84
C_{2c}	3.85
C_{12}	0.1125

the qubit. The coupling capacitance is optimized parameter to minimize the decay while ensuring reasonable drive strength for gate implementation. The simulations have been carried out to get this optimal capacitance by varying gap between qubit and control line. By using black box quantization method [16] we have simulated the decay time at each gap position. Estimated capacitances and decay time of qubit due to energy loss through XY control line is listed in Table 1. We have obtained a decay time of 546 μs at 40um gap where the coupling capacitance is 33 aF. This gives an excitation π-pulse magnitude as −67.5 dBm [17].

(b) Flux control line: The flux line is inductively coupled to the SQUID of qubit. Sufficient mutual inductance between the flux line and the qubit SQUID loop needs to be ensured. The coupling of flux line is optimized to achieve a mutual inductance of 1.08 pH.

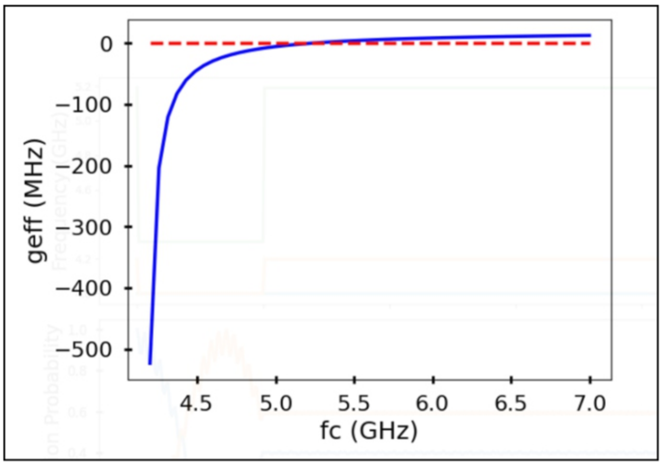

Fig.8: Effective coupling strength between qubits at different coupler frequency.

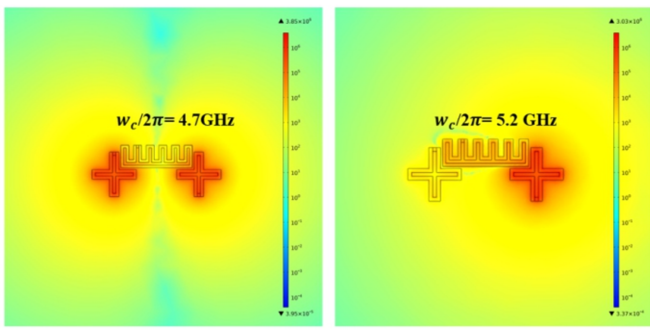

Fig.9: Electric field distribution at coupler frequency 4.7 GHz and 5.2 GHz for Q_2 resonant mode

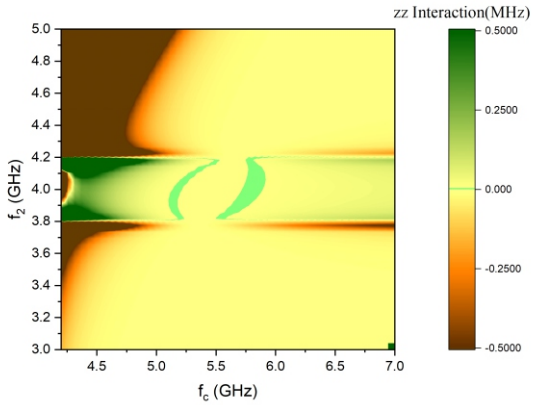

Fig.10: Parasitic ZZ interaction with Coupler and Q_2 frequency.

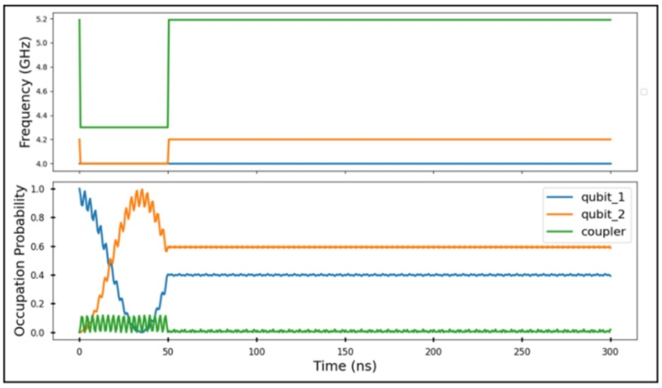

Fig.11: State evolution of Q_1, Q_2 and Coupler with time.

Tunable coupler

In the present case a transmon qubit has been taken as tunable coupler. The physical arrangement and the equivalent circuit of the qubits with the tunable coupler [12] is shown in Fig.7 (a) and 7 (b), respectively. In this scheme the two qubits are directly coupled with each other via capacitance networks, and indirectly via the states of tunable coupler. The coupler is capacitively coupled to the qubits with capacitance C_{1c} and C_{2c} giving rise to coupling strength of g_1 and g_2, respectively. The direct capacitance between the qubits is given by C_{12} and contributes to the direct coupling given by g_{12}. With coupler frequency higher than the frequencies of qubits, the coupling through the coupler states is negative. The coupler has been designed to have weak anharmonicity of about 90 MHz and frequency tunability from 4 to 5.5 GHz. The coupling capacitances between the qubit and the coupler have been selected to achieve zero coupling around 5.2 GHz of the coupler frequency. The values of the required capacitances are obtained from quasi-static simulations and are listed in Table 2.

The effective coupling strength between the qubits Q_1 and Q_2 is estimated using the formula given in reference [11] and plotted against coupler frequency in Fig.8. It is observed that at coupler frequency, $\omega_c/2\pi$, of about 5.19GHz, effective coupling between the qubits become zero. Fig.9 shows the electric field distribution with coupler frequency at 4.7 GHz and 5.2 GHz, respectively.

Quantum simulations

By employing open-source python library Quantum Toolbox in Python (QuTiP) [18], evolution of quantum states with time has been simulated. The system Hamiltonian consists of sum of Hamiltonians of individual qubits and coupler, and interaction terms between them. Hamiltonian has been modelled as duffing oscillator [11]. For present simulations readout resonators and control lines have been removed. The Hamiltonian is given by,

$$H = \sum_{i=1,2,c} (\omega_i \hat{c}_i^\dagger \hat{c}_i + \alpha_i \hat{c}_i^\dagger \hat{c}_i^\dagger \hat{c}_i \hat{c}_i) + \sum_{i=1,2} g_i (\hat{c}_i^\dagger \hat{c}_c + \hat{c}_c^\dagger \hat{c}_i - \hat{c}_i^\dagger \hat{c}_c^\dagger - \hat{c}_i \hat{c}_c) + g_{12}(\hat{c}_1^\dagger \hat{c}_2 + \hat{c}_2^\dagger \hat{c}_1 - \hat{c}_i^\dagger \hat{c}_c^\dagger - \hat{c}_i \hat{c}_c)$$

where, $\hat{c}_i^\dagger$ and $\hat{c}_i$ are creation and annihilation operators, respectively, defined in the eigen-basis of the corresponding mode.

Estimation of static ZZ parasitic interaction between the qubits

For two qubits, ZZ interaction originates from interactions between higher levels. It creates error in two qubit gates and is a major problem for scalability. It can be quantified as,

$$ZZ = E_{101} - E_{001} - E_{100} - E_{000},$$

where, E_m denotes the eigen-energy of state $|m\rangle$. Using numerical simulations, ZZ interaction strength has been obtained and plotted with coupler frequency and Q_2 frequency in Fig.10.

With respect to Q_2 frequency, the region with detuning $|\omega_1 - \omega_2| <$ anharmonicity $|\alpha|$, is known as straddling region.

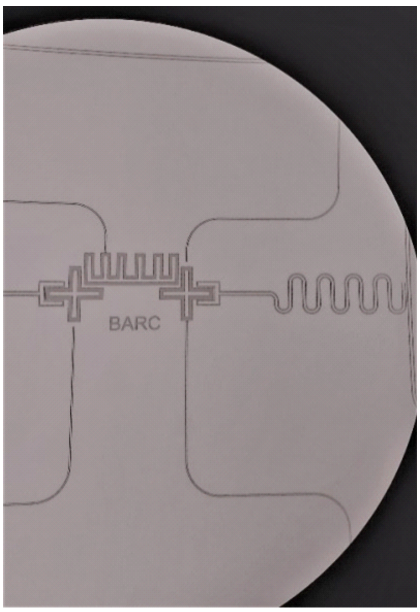

Fig.12: (a) Optical image of fabricated device.

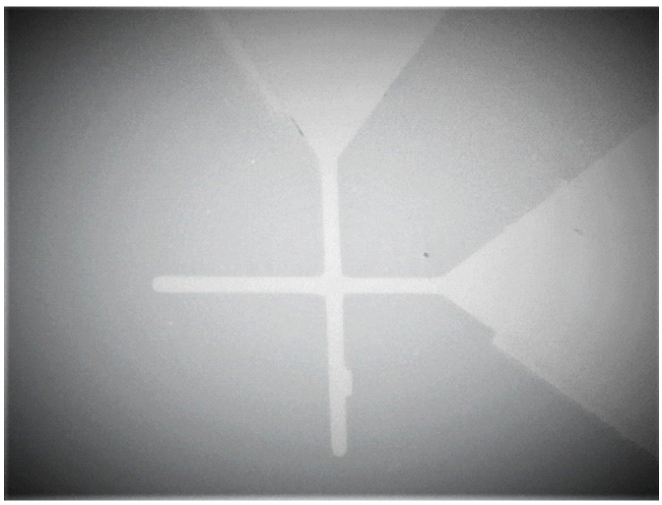

Fig.12: (b) SEM image of fabricated Josephson junction.

Otherwise, it is known as non-straddling region. The light green coloured regions in the straddling regime indicate cancellation of ZZ interaction. This condition is observed when coupler is biased at much higher frequency than qubits, and detuning is less than anharmonicity.

iSwap gate

To implement iswap gate, interaction between the qubits has to be created. If g is coupling strength between the qubits then the swapping time is given by π/2g. At coupler frequency 4.3 GHz, the effective coupling strength between the qubits at 4 GHz is approximately 45 MHz giving a swapping time of nearly 35ns.

In the simulations, the coupler frequency is first set to 5.19 GHz, where both qubits are isolated from each other. Under this idling state, with interaction between qubits nearly zero, Q_1 is excited to create state |100>. Subsequently, frequency of second qubit is changed such that states |100> and |001> become degenerate. The interaction between qubits is increased by changing the coupler frequency to 4.3 GHz. As shown in Fig.11, we need to wait about 34.7 ns for complete exchange from |100> to |001>.

Fabrication of the Quantum Chip

Presently, fabrication trials of the designed device are in progress and the process is being optimized. The Fig.12 (a) and Fig.12 (b) show the Optical and SEM image of the fabricated design and Josephson Junction, respectively.

Conclusions

Results of the simulations, performed to design components on the superconducting chip, have been presented. Effect of the change in the coupler frequency on the coupling between qubits is obtained. Also, the always on static ZZ parasitic interaction has been estimated. Two qubit iSwap gate operation using tunable coupler has been demonstrated. On-going work includes obtaining optimal control drive for the gate implementation, package simulations and fabrication of the chip.

Acknowledgments

The authors would like to thank, Prof. Shiv Govind Singh, IIT Hyderabad, and Prof. Ammanabrolu Rajini kanth, University of Hyderabad for all the technical discussions and facilitating the fabrication trails. Additionally, the authors deeply appreciate the QuMaC team for providing technical guidance and support.

References

[1] M. Hatridge, et al., Physical Review B 83, 134501 (2011).

[2] S. Barzanjeh, et al., Science 363, 6373 (2019).

[3] D. Vion, et al.,Science 296, 886 (2002).

[4] J. M. Chow, et al.,Phys. Rev. A 82, 040305(2010).

[5] J. M. Chow,et al.,Phys. Rev. Lett. 109, 060501 (2012).

[6] Y. Makhlin, et al.,Rev. Mod. Phys. 73, 357 (2001).

[7] M.A. Nielsen and I.L. Chuang, Quantum Computation and Quantum Information (Cambridge University Press, 2000)

[8] A. Blais, et al., Phys. Rev. A, 69,6 (2004).

[9] A. Frank et al., Nature, 574,7779(2019).

[10] M. H. Devoret, et al., Science, 339(2003).

[11] F. Yan, et al., Appl. Phys. Rev. 10, 054062 (2018)

[12] Y. Sung, et al., Phys. Rev. X,11 (2021)

[13] P. Krantz, et al., Appl. Phys. Rev. 6, 021318 (2019).

[14] Z.K. Minev, et al., Qiskit metal: An open-source framework for quantum device design& analysis, Generic, (2021)

[15] J.M. Chow, Quantum Information Processing with Superconducting Qubits, Ph.D Thesis, Yale University, May 2010

[16] S.E. Nigg, et al., Phys. Rev. Lett. 108, 240502 (2012)

[17] D.T. Sank, Fast, Accurate State Measurement in Superconducting Qubits, Ph.D. Thesis, University of California Santa Barbara, September 2014.

[18] J.Johansson, et al., Computer Physics Communications, 184 (2013).

अतिचालक क्यूबिट्स

14

अतिचालक क्यूबिट्स के लिए नियंत्रण एवं मापन प्रणाली

*सत्यम रावत[1], राधिका नासेरी[1], संदीप भराडे[1], दिपक पास्टे[1], प्रवीणकुमार सुग्गिसेट्टी[1], आर.टी. केशवानी[1], सुजो सी.आई[1], एम.वाई. दीक्षित[1], गोपाल जोशी[1] और आर. विजयराघवन[2]
[1]त्वरक नियंत्रण प्रभाग, भाभा परमाणु अनुसंधान केंद्र (भापअ केंद्र), ट्रांबे-400085, भारत
[2]क्वांटम मापन और नियंत्रण (क्यूएमएसी) प्रयोगशाला, संघनित पदार्थ भौतिकी और सामग्री विज्ञान विभाग, टाटा मूलभूत अनुसंधान संस्थान (टामूअसं), मुंबई

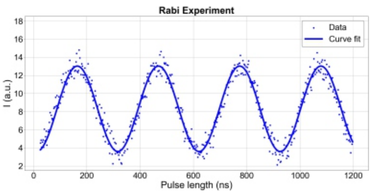

राबी प्रयोग

सारांश

अति-चालक क्यूबिट्स के नियंत्रण और माप की प्रक्रिया क्वांटम कंप्यूटिंग अनुसंधान के महत्वपूर्ण पहलू हैं, जो क्वांटम प्रणाली से जानकारी को संचालित और प्राप्त करने के लिए आवश्यक हैं। त्वरक नियंत्रण प्रभाग, भाभा परमाणु अनुसंधान केंद्र, क्यू. एम. सी., टाटा मूलभूत अनुसंधान संस्थान के सहयोग से सामान्य तापमान पर संचालित इलेक्ट्रॉनिक प्रणाली के विकास की दिशा में काम कर रहे हैं, जो अति-चालक क्यूबिट्स के नियंत्रण और माप के लिए है। इस लेख में प्रोटोटाइप क्यूबिट कंट्रोलर के साथ किए गए क्यूबिट अभिलक्षण प्रयोगों के परिणाम प्रस्तुत किए गए हैं।

Superconducting Qubits

14

Control and Measurement System for Superconducting Qubits

***Satyam Rawat[1], Radhika Nasery[1], Sandeep Bharade[1], Deepak Paste[1], Praveenkumar Suggisetti[1], R. T. Keshwani[1], Sujo C. I.[1], M. Y. Dixit[1], Gopal Joshi[1] and R. Vijayaraghavan[2]**
[1]*Accelerator Control Division, Bhabha Atomic Research Centre (BARC), Trombay-400085, INDIA*
[2]*Quantum Measurement and Control (QuMaC) Laboratory, Department of Condensed Matter Physics and Materials Science, Tata Institute of Fundamental Research (TIFR), Mumbai*

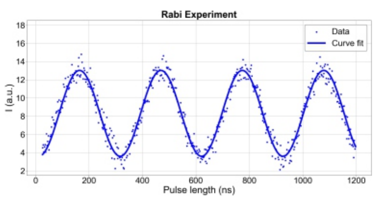

Rabi experimnet

ABSTRACT

The control and measurement of superconducting qubits are critical aspects of quantum computing research, essential for manipulating and extracting information from quantum systems. Accelerator Control Division, Bhabha Atomic Research Centre, in collaboration with QuMaC, Tata Institute of Fundamental Research is pursuing development of room-temperature electronic system for control and measurement of superconducting qubits. This article presents the test results from qubit characterization experiments conducted with the prototype qubit controller.

KEYWORDS: *Quantum system, Qubits, Superconducting qubits.*

**Author for Correspondence: Satyam Rawat*
E-mail: satyamr@barc.gov.in

Introduction

Quantum computing is a revolutionary approach to computation that harnesses the principles of quantum mechanics to process information. In quantum computing, a control and measurement system plays an important role in manipulating the state of qubits by applying quantum gates, and determining their state. A control and measurement system for superconducting qubits is being developed to conduct qubit characterization experiments, and execute high-fidelity quantum gate operations. The controller is designed to support a diverse range of experiments, including the capability to perform resonator spectroscopy, qubit spectroscopy, Rabi experiment, XY gate operations, and measurements of qubit relaxation and de-phasing times.

Control and Measurement of State of a Qubit

A quantum bit or qubit is the fundamental unit of information in quantum computing, analogous to the classical bit [1]. A superconducting qubit is one of the many physical realizations possible for building a qubit [2]. It is built around a Josephson junction, which is formed by two superconductors separated by a thin insulating barrier. Its fabrication process aligns well with established semiconductor manufacturing techniques, making it conducive to scalability.

Controlling the state of a qubit involves manipulating its quantum state to perform desired operations. This manipulation typically involves applying sequence of quantum gates [3], which are analogous to classical logic gates but operate on quantum states [4]. These gates can deterministically change the state of qubits, allowing for the creation of superposition and entanglement, as well as other quantum operations required for computation. Measuring the state of a qubit involves determining its quantum state at a specific moment in time. Qubits are coupled to microwave resonators located in close physical proximity to them. It is through these resonators that qubit state is determined or “readout”. One common technique for determining the state of a qubit is the dispersive readout method [5]. This method utilizes the fact that the state of a qubit has a direct influence on certain macroscopic parameter of the readout resonator such as its resonant frequency.

Qubit Control and Measurement System

Architecture of the qubit controller

The qubit controller consists of an FPGA, a microprocessor, and data converters, and provides precise control and fast data acquisition essential for quantum state manipulation and measurement.

Fig.1 depicts the architecture of the qubit controller. The controller consists of an arbitrary waveform generator and a data acquisition block implemented in the FPGA. The arbitrary waveform generator utilizes digital up-conversion and interpolation operations to synthesize microwave pulses of specified frequency, shape and duration for both control and readout operations. The output of the generator connects to a DAC. During the measurement of the qubit state, the data acquisition block acquires samples from the ADC and performs digital down-conversion, decimation, and averaging operations. The microprocessor oversees overall operations, while the FPGA-based sequencer manages data acquisition and pulse generation, and is programmed to execute specific experiments.

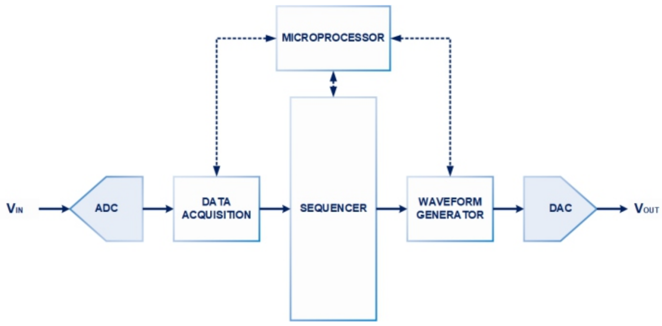

Fig.1: Architecture of Qubit controller.

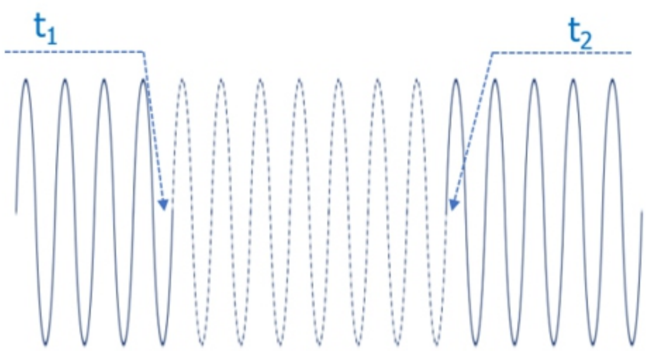

Fig.2: A continuous sinusoidal waveform depicting phase coherence.

Both digital up-conversion and digital down-conversion operations utilize a common time base to preserve phase coherence. Fig.2 illustrates the concept of phase coherency using a continuous sinusoidal waveform. This continuous sinusoid can be conceptualized as two pulsed sinusoids separated in time, with the first one ceasing at time ‘t1’ and the second one commencing at time ‘t2’. The initial phase of the second pulsed sinusoid matches the phase of the continuous sinusoid at time ‘t2’. Phase coherence in control and measurement signals ensures accurate qubit manipulation.

Application software

An application software, which enables performing a set of experiments, namely, resonator spectroscopy, qubit spectroscopy, Rabi experiment, decoherence time and dephasing time measurements, has been developed and deployed on the qubit controller.

Additionally, a graphical-user-interface (GUI) has been created to facilitate user interaction, allowing for configuration settings, experiment monitoring, and result analysis, thus enhancing the overall user experience. Fig.3 provides a screenshot of the GUI of the control and measurement system.

Experimental Results

Resonator spectroscopy

Resonator spectroscopy was performed to find out the resonant frequency of the readout resonator coupled to the qubit. A microwave signal with sweeping frequency was sent to the readout resonator, & the magnitude and phase responses of reflected signal were measured. At the point of resonance, two distinct features become evident: a reduction in signal magnitude and a sharp change in phase as depicted in Fig.4. The resonant frequency was measured to be 7.13416 GHz.

Qubit spectroscopy

Two-tone qubit spectroscopy experiment was performed to determine the qubit frequency. A low power, resonant signal was sent to the readout resonator, and the reflections were probed. Simultaneously, another tone with a sweeping frequency was sent to the resonator. When frequency of the second tone matches the qubit frequency, it excites the qubit

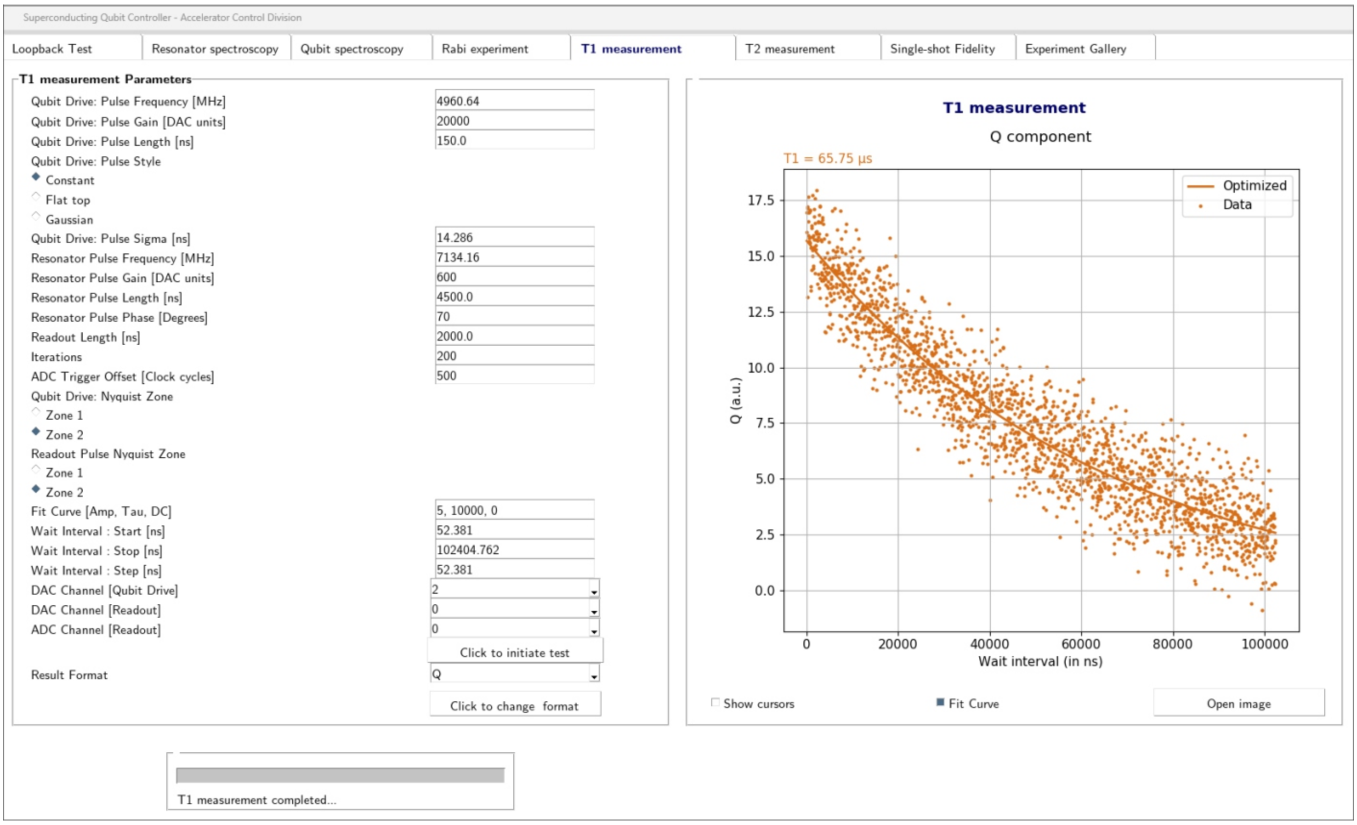

Fig.3: A snapshot of application software of the prototype qubit control and measurement system.

from its ground state, and causes a shift in the resonator's resonant frequency. The frequency of the sweeping tone at which this shift occurs is the frequency of the qubit. Fig.5 (a) displays the result of the qubit spectroscopy experiment. The qubit frequency was measured to be 4.96064 GHz.

Rabi experiment

In this experiment, a qubit drive signal was applied to the qubit, immediately followed by a measurement of its state. The length of the qubit drive signal was systematically varied, and the state of the qubit was measured. The probability of qubit being in excited/ground state varies sinusoidally with the length of the qubit drive signal. The frequency of the Rabi oscillations depends on the power level of the qubit drive signal. The experiment was conducted with various power levels for the qubit drive. For one of these power levels, the π

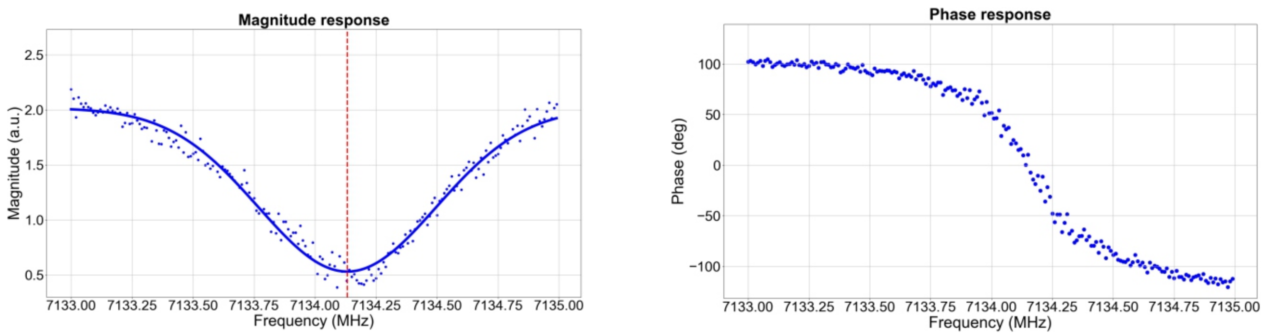

Fig.4: Resonator spectroscopy result.

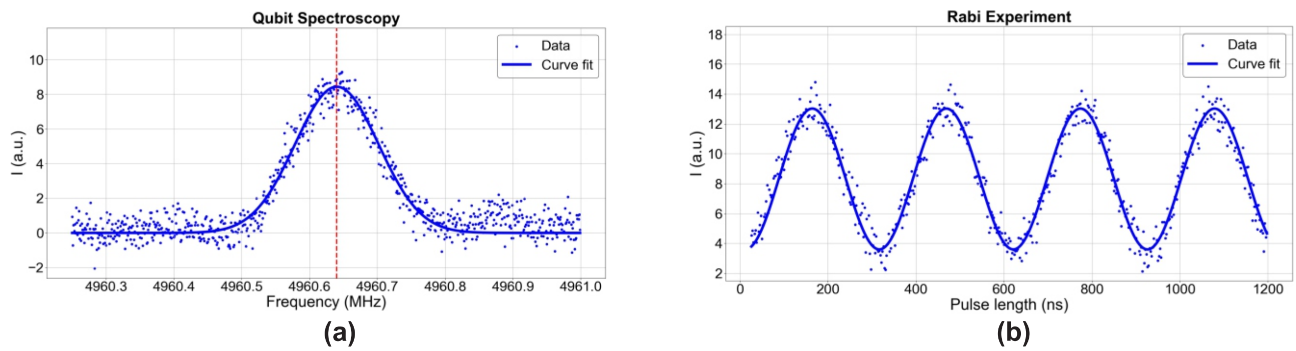

Fig.5: (a) Qubit spectroscopy result. (b) Rabi experiment result.

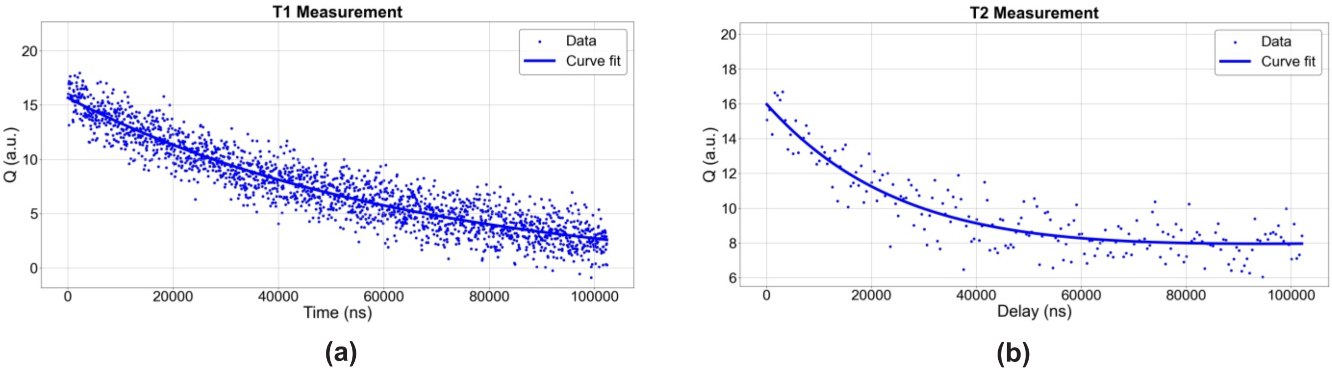

Fig.6: (a) T1 measurement result. (b) T2 measurement result.

length duration was measured to be 152.34 ns, as shown in Fig.5 (b).

T1 measurement

To measure the qubit relaxation time, also known as T1 time, the qubit was first transferred from the ground state to the excited state by sending a Π pulse. Subsequently, the state of the qubit was measured at various time intervals to determine the rate of decay. The result of the T1 measurement is shown in Fig.6 (a). The T1 time was measured to be 65.75 μs.

Ramsey experiment

The Ramsey experiment is a fundamental technique used to determine the qubit dephasing time, often referred to as T2 time. In this experiment, the qubit was subjected to two Π/2 pulses with a variable time delay between the pulses. Subsequently, an immediate measurement was performed to assess the state of the qubit. The result of the T2 measurement is shown in Fig.6 (b). The T2 time was measured to be 37.14 μs.

Readout Fidelity

A quantum system is inherently sensitive to external disturbances. Therefore, an ideal control and measurement system should introduce minimal or no additional noise, ensuring that the predominant source of noise remains the intrinsic noise of qubit. Achieving this requires a low-noise driving source and readout signal processing chain. Additionally, low-jitter sampling clocks for the data-converters become essential to fulfil this objective.

Readout fidelity in quantum computing is a measure of how accurately a system can distinguish between different quantum states, such as the excited state and ground state of a qubit. Higher readout fidelity means the system can determine the state of the qubit more accurately.

The readout fidelity of the prototype controller was measured to be 75.85% with no parametric amplification. Fig.7 depicts the result of the readout fidelity measurements.

Conclusion

A high-quality classical control is needed for initialization, manipulation, and readout of quantum states. A room-temperature qubit control and readout system for superconducting qubits is being developed that can conduct qubit characterization experiments, and implement high fidelity quantum gates. The performance of the qubit controller was evaluated by characterizing a superconducting qubit. Our future work will focus on optimizing the controller's performance and expanding its capability to manage a greater number of qubits. This system is believed to offer itself as a cost-effective solution for rapidly prototyping control electronics for multi-qubit systems and executing quantum algorithms in a seamless and user-friendly manner.

Acknowledgment

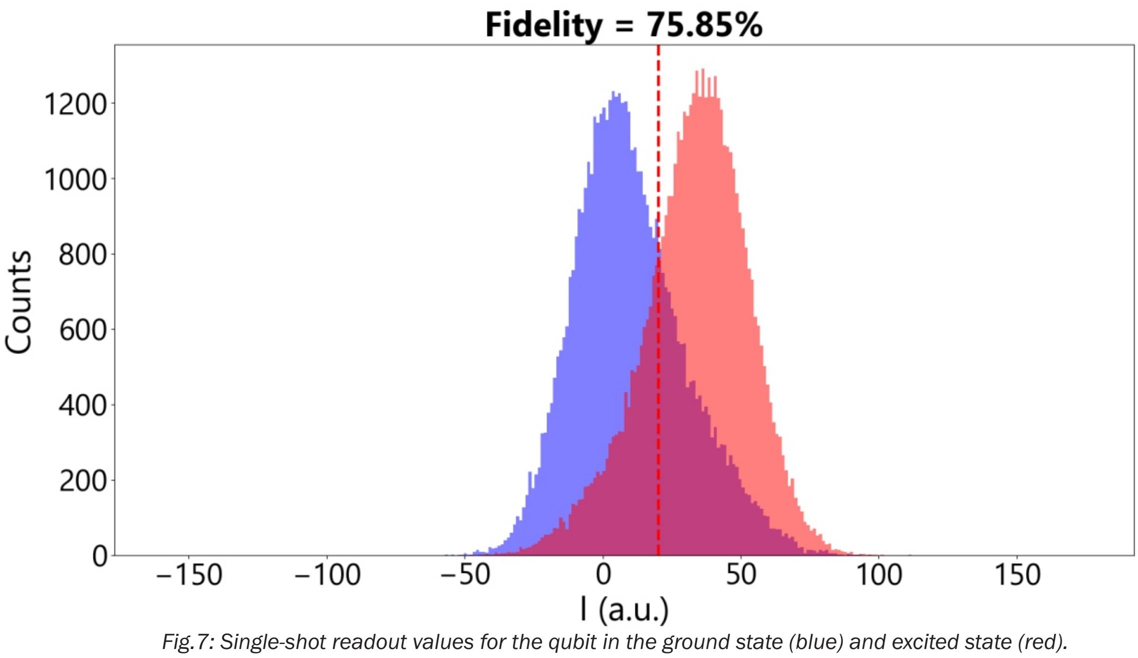

Fig.7: Single-shot readout values for the qubit in the ground state (blue) and excited state (red).

The authors sincerely appreciate the QuMaC team and the colleagues from ACnD who generously dedicated their time and resources to this endeavour, despite their busy schedules.

References

[1] M. A. Nielsen and I. L. Chuang, Quantum Computation and Quantum Information. Cambridge University Press, Cambridge, 2000.

[2] J. C. Bardin, D. H. Slichter and D. J. Reilly, "Microwaves in Quantum Computing". IEEE Journal of Microwaves, vol. 1, no. 1, pp. 403-427, Jan. 2021.

[3] P. Krantz, M. Kjaergaard, F. Yan, T. P. Orlando, S. Gustavsson, and W. D. Oliver, “A quantum engineer's guide to superconducting qubits”, Applied Physics Reviews 6, 021318 (2019).

[4] J. C. Bardin, D. Sank, O. Naaman and E. Jeffrey, "Quantum Computing: An Introduction for Microwave Engineers". IEEE Microwave Magazine, vol. 21, no. 8, pp. 24-44, Aug. 2020

[5] M. Naghiloo, “Introduction to Experimental Quantum Measurement with Superconducting Qubits,” Murch Lab, Washington University, St. Louis, MO, USA, April 2019.

क्वांटम कंट्रोल

15

क्यूबिट अंशांकन और गेट प्रचालन हेतु क्वांटम सॉफ्टवेयर स्टैक किस्किट का प्रयोक्तानुकूल तरंगरूप जनित्र के साथ समाकलन

*राधिका नासेरी[1], संदीप भराडे[1], एम. वाई. दीक्षित[1], गोपाल जोशी[1] और आर. विजयराघवन[2]

[1]*त्वरक नियंत्रण प्रभाग, भाभा परमाणु अनुसंधान केंद्र (भापअ केंद्र), ट्रांबे-400085, भारत*

[2]*क्वांटम मापन और नियंत्रण (क्यूएमएसी) पसंघनित पदार्थ भौतिकी और सामग्री विज्ञान विभाग, टाटा मूलभूत अनुसंधान संस्थान (टीआईएफआर), मुंबई*

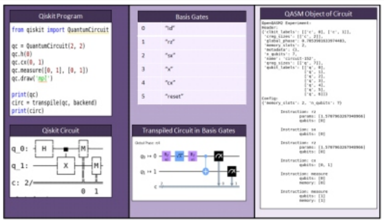

कम्पाइलेशन पाइपलाइन

सारांश

क्वांटम सॉफ्टवेयर स्टैक का एक आर्बिट्ररी वेवफॉर्म जेनरेटर (एडब्ल्यूजी) के साथ एकीकरण भौतिक क्वैबिट पर क्वांटम एल्गोरिदमऔर क्वांटम प्रयोगोंको निष्पादित करने के लिए महत्वपूर्ण है। यह आलेख ओपन सोर्स किस्किट क्वांटम सॉफ्टवेयर स्टैक को एडब्ल्यूजी के साथ सफलतापूर्वक एकीकृत करने को दर्शाता है, जिसमें किस्किट के विकास के माध्यम से यह हासिल किया गया है।

Quantum Control

15

Integration of Quantum Software Stack Qiskit to Custom Arbitrary Waveform Generator for Qubit Calibration and Gate Operations

***Radhika Nasery[1], Sandeep Bharade[1], M. Y. Dixit[1], Gopal Joshi[1] and R. Vijayaraghavan[2]**

[1]*Accelerator Control Division, Bhabha Atomic Research Centre (BARC), Trombay-400085, INDIA*

[2]*Quantum Measurement and Control (QuMaC) Laboratory,Department of Condensed Matter Physics and Materials Science, Tata Institute of Fundamental Research (TIFR), Mumbai*

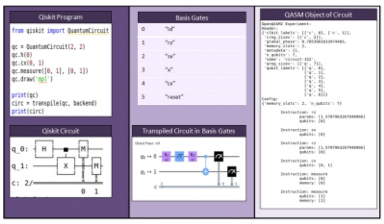

Compilation Pipeline

ABSTRACT

Quantum Software Stack integration with a Arbitrary Waveform Generator (AWG) is important for executing quantum algorithms and quantum experiments on physical qubits. This article demonstrates successful integration of Qiskit Quantum Software Stack with AWG through development of Qiskit Backend.

KEYWORDS: *Quantum software stack, Arbitrary waveform generator, Qiskit*

**Author for Correspondence: Radhika Nasery*
E-mail: radhikan@barc.gov.in

Introduction

Quantum computing is rapidly progressing, demanding sophisticated control mechanisms for precise manipulation of quantum bits - qubits. Qubits are the fundamental units of quantum information in quantum computing, and precise control over their states is crucial for implementing quantum gates and executing quantum algorithms. Arbitrary Waveform Generators (AWG) are used to produce user defined, precise and tailored RF waveforms to manipulate the state of qubits. Quantum algorithms are implemented using sequences of quantum gates. AWG support the creation of customizable pulse sequences, enabling the implementation of qubit calibration, quantum experiments and implementation of quantum circuits. To make quantum computers accessible to users and enable the development of quantum applications, a quantum software stack is required. This article presents integration of Qiskit quantum stack with AWG.

Quantum Software Stack

A quantum stack is the hierarchy of components, from the high-level algorithms down to the physical qubits that abstracts away the complexity of the underlying quantum hardware [1]. It typically consists of layers (Fig.1) like a quantum algorithm layer, an intermediate representation layer and a quantum control and readout electronics interface layer. The quantum algorithm layer is where quantum algorithms are implemented using high-level quantum programming languages and software development kits (SDKs). This layer is also used to define qubit calibration experiments. The quantum compilers convert the algorithms written in high level language to a format known as Intermediate Representation (IR). IR layer provides a hardware-agnostic representation of quantum circuits that are compiled and optimized for different target qubit architectures. OpenQASM [2] is an example of a popular IR for quantum circuits. The compiler optimization performs circuit rewriting, transformation, and optimization techniques to map logical qubits in the quantum circuit to the physical qubits of the hardware (as shown in Fig.2), while minimizing circuit depth and gate count. It also synthesizes gates into the native gate set supported by the target hardware. The quantum analog-digital interface layer is responsible for converting the digital gate-level instructions to analog waveforms that control the qubits. This layer handles tasks like frequency control, qubit initialization, gate application, and measurement. A micro-architecture is typically implemented to translate IR for arbitrary waveform generation. This is where arbitrary waveform generators play a key role in precisely shaping the control pulses. The physical qubit control layer

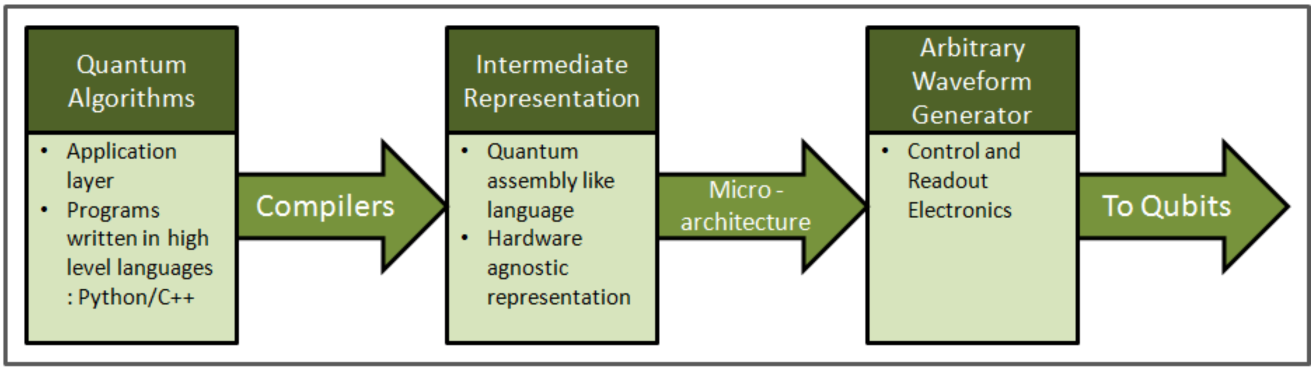

Fig.1: Quantum Software Stack

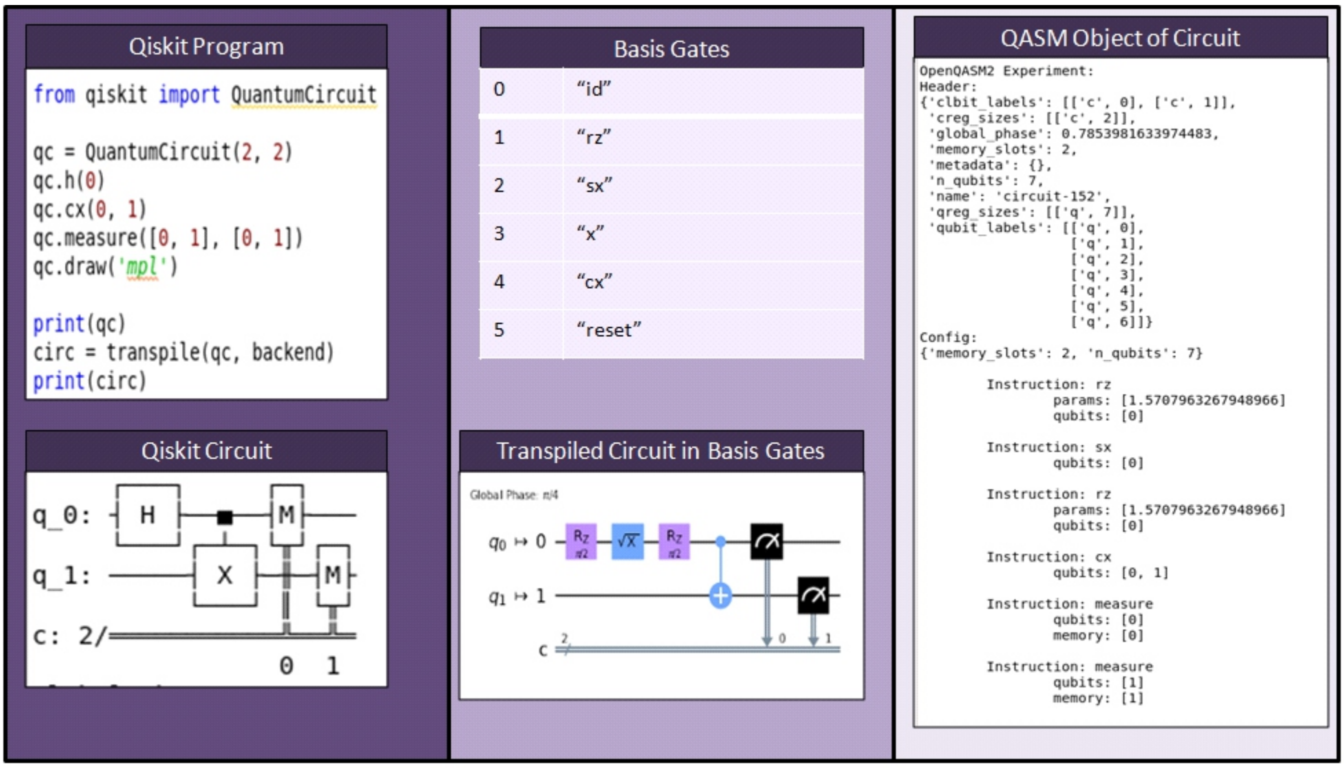

Fig.2: Qiskit Compilation Pipeline.

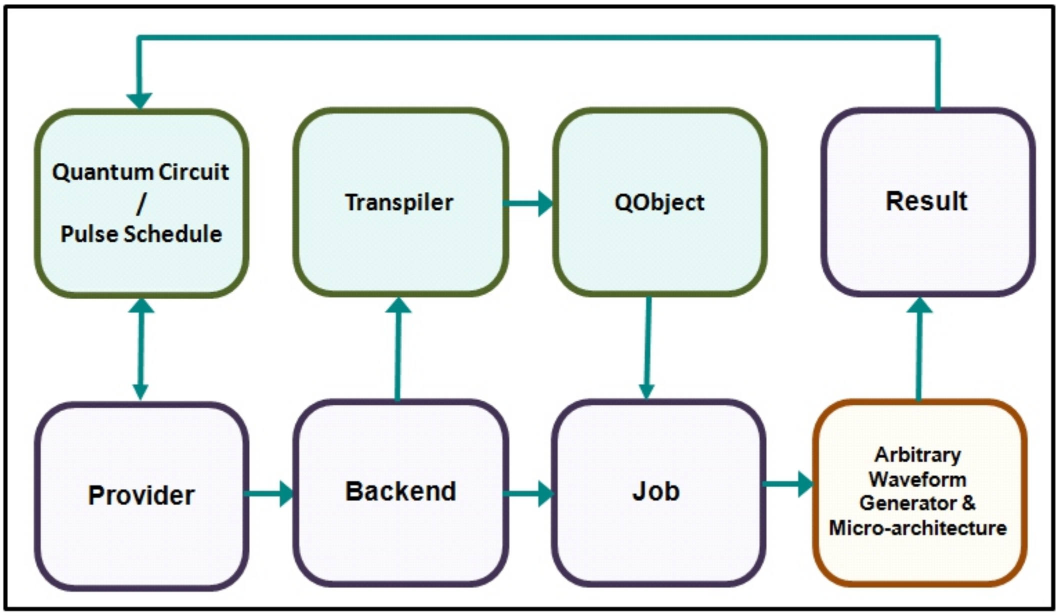

Fig.3: Qiskit Backend Integration.

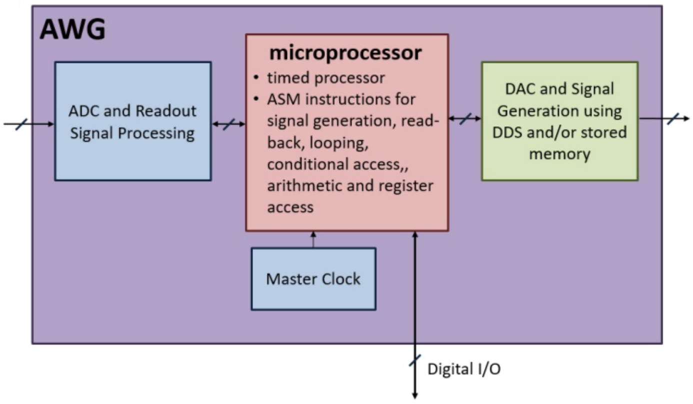

Fig.4: AWG Architecture

interacts directly with the qubits to apply the required operations.

Some of the leading quantum software stacks are Qiskit[3] (IBM), Cirq[4] (Google), Q# [5] (Microsoft), Forest (Rigetti) [6], and Ocean (D-Wave)[7]. While they share many similarities in terms of the overall architecture, they differ in aspects like the supported quantum hardware, programming languages and feature set. Qiskit has emerged as one of the most popular quantum software stacks due to its comprehensive feature set, extensibility, and strong community support. It is an open-source SDK that supports multiple programming languages (Python, Java, Swift, JavaScript), simulators, and quantum hardware backends (IBM, IonQ, Honeywell). Qiskit also provides higher-level abstractions and applications for domains like optimization, machine learning, finance, and chemistry. Therefore, open source Qiskit quantum software stack was selected for integration with AWG. Fig.2 shows the Qiskit compilation pipeline. A quantum circuit is defined in python high level language and submitted for compilation. The compiler transpiles the circuit into basis gates of the quantum hardware and a IR representation in form of OpenQASM2 object is generated.

Development of Qiskit Backend

The Qiskit backend [8] is the interface between the quantum circuits defined in the quantum algorithm layer and the underlying quantum hardware or simulator. It provides a

```
provider = BARCProviderInterface()
print("*****          Initialized the provider interface from user.py        **********")
```

Pulse Configuration	Meaning
n_qubits	Number of qubits
basis_gates	Basis gate set of the target device
gates	Gate name and Qasm def
open_pulse	If pulse library is supported
coupling_map	Physical qubit coupling map
qubit_freq_est	Estimated Qubit Frequency
meas_freq_est	Estimated Readout Resonator Frequecy
meas_levels	RAW, AVERAGE
pulse_library	Raw I,Q data samples for sequence

Backend Configuration	Meaning
dt	Sampling time
ch_name_idx	Qubit, readout and acquire channels
ch_idx_rdds	ADC to DAC readout mapping
ch_idx_page	Proc page corresponding to DAC, ADC channel
ch_idx_reg	Proc registers corresponding to freq, gain, mode, phase
misc_page, misc_reg	Misc pages and registers for shots
initial_cycle_offset	Initial offset of sync of proc
adc_trig_offset	Trig offset of DAC for acq
Acquire_pad	Time offset for ADC acq

Fig.5: BARCPoviderInterface and Backend Properties for custom AWG.

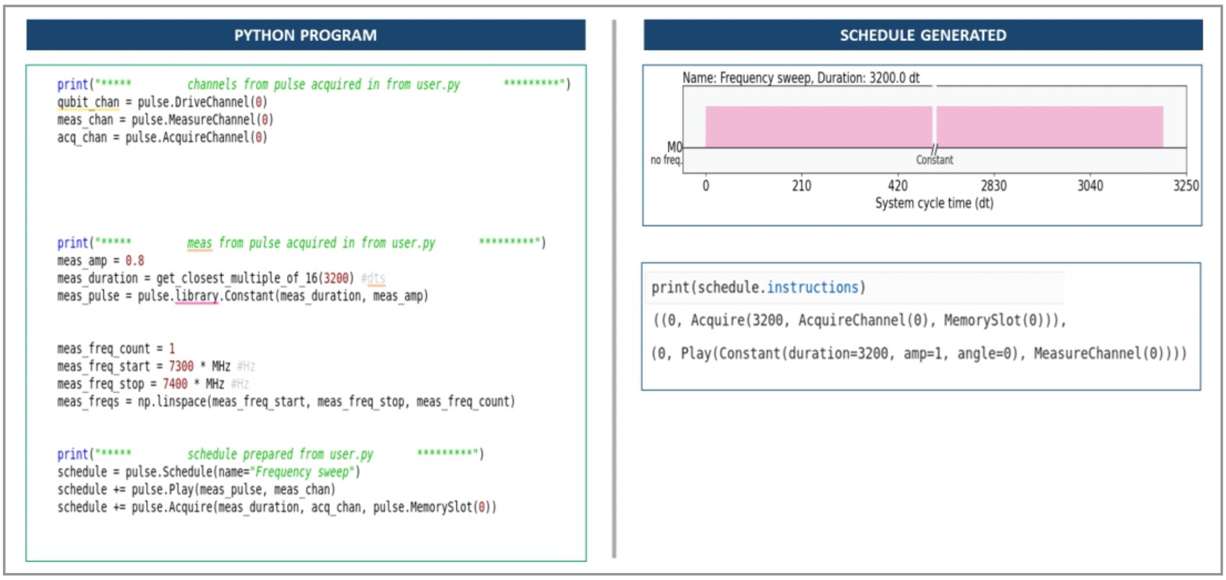

Fig.6: Python Program to provide schedule for single frequency Loopback Testing

unified API for running quantum circuits on different targets and returning the measurement results. To integrate a AWG into the Qiskit backend, a new (as shown in Fig. 3) backend provider, backend, job and result classes are implemented that conform to the Qiskit backend interface specifications. Quantum circuits are transpiled i.e. optimized by a compiler and then give the output in format of Quantum Object- Qobj. Backends take in a Qobj as input, which is a QASM - IR representation and a Job object is returned. Job instances can be thought of as the "ID" for a submitted job. They find out the execution's state at a given point in time (for example, if the job is queued, running, or has failed) and also allow control over the execution of the job on the AWG. The raw data sample stream from measurement operation of the qubit from the AWG is routed to Result class and then back to the higher level Quantum Circuit/ Pulse Schedule program.

Integration with AWG

The AWG has 3 main parts (Fig.4): micro-processor, readout processing block and signal generating block. The micro-processor with has added timed Assembly Language (ASM) instructions to generate RF pulses. RF pulses are generated for control and readout of qubits. The key aspect of the integration is mapping the quantum gates in the circuit to the corresponding analog waveforms generated by the AWG. This requires a gate-to-pulse mapping given by Fig.5 that translates each quantum gate to a sequence of control pulses with specific amplitudes, frequencies, and durations. The backend provider will use this mapping to convert the quantum circuit into a series of AWG instructions that generate the required pulses. The AWG integration also needs to handle aspects like synchronization, measurement, and feedback between the quantum and classical systems. Fig.5 also shows the python program invoking the implemented "BARCProviderInterface".

Results

Fig.6 shows the Qiskit python program describing the schedule of pulses to be run for a single frequency, constant amplitude loopback testing and corresponding schedule

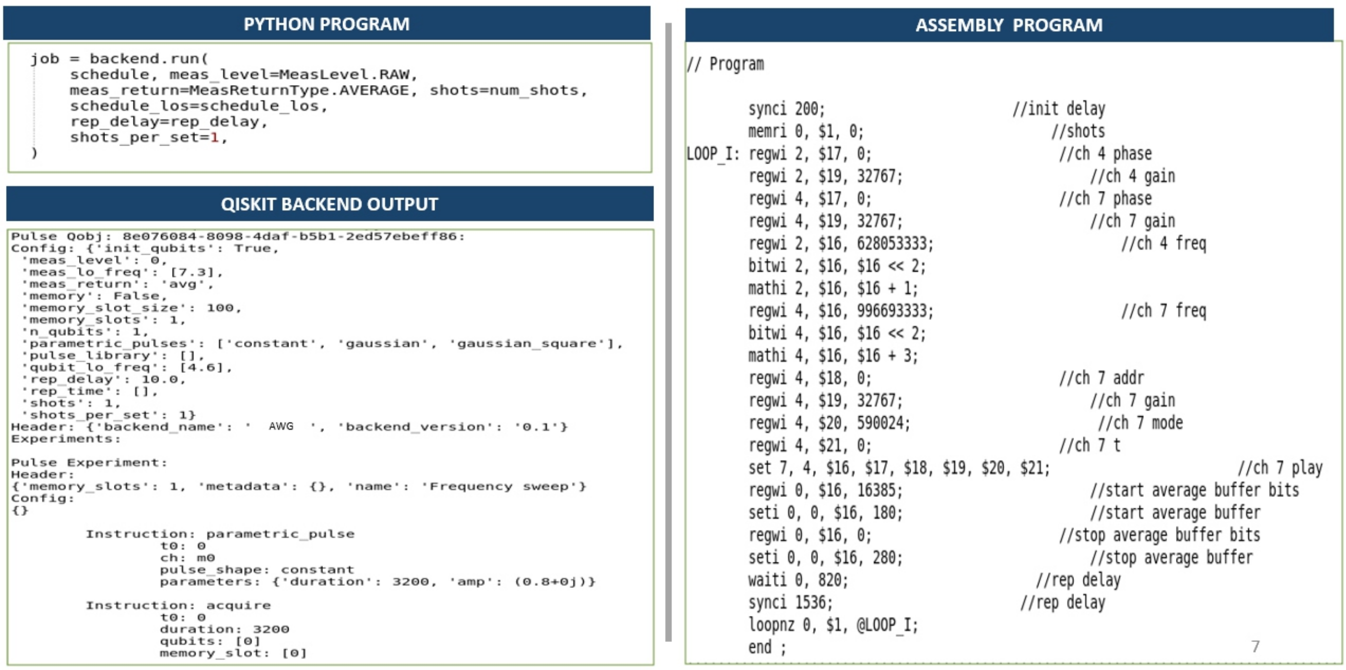

Fig.7: Python Program to run a pulse schedule and ASM output for AWG.

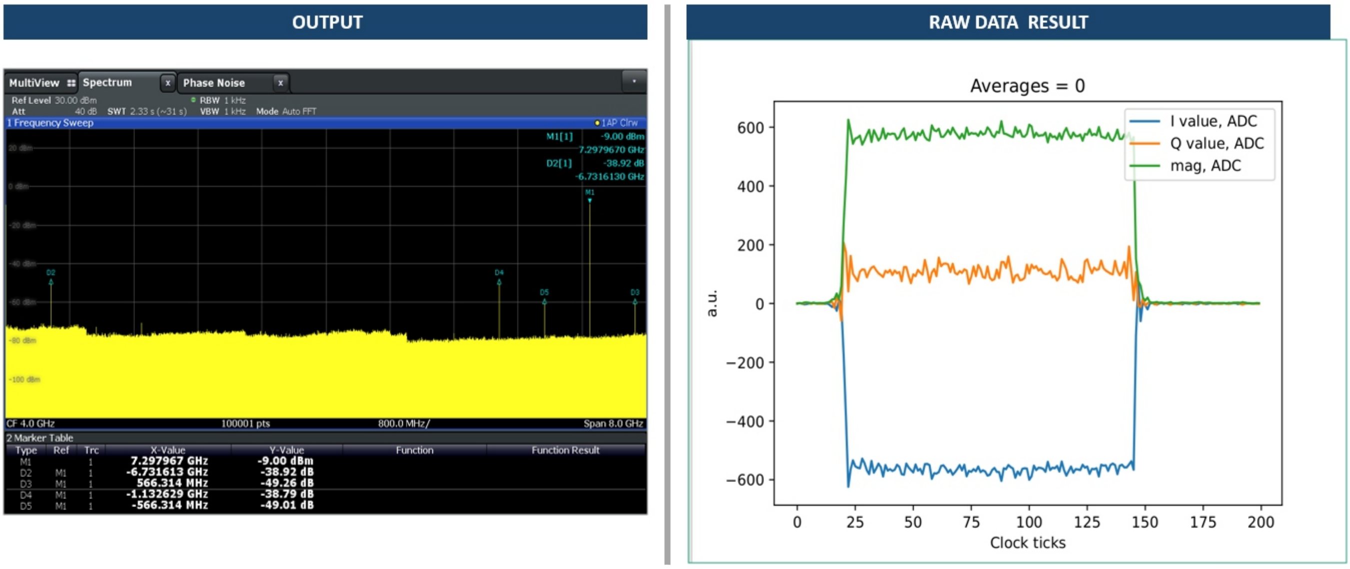

Fig.8: RF Frequency Spectrum Output and Results of Loopback Testing in Qiskit Python Program.

generated. Qubit channel is the channel for qubit state manipulation. Measure Channel is the channel for readout resonator pulse generation and Acquire Channel is the waveform acquisition channel for Qubit state measurement.

Fig.7 shows this Schedule running as a job on the Backend. The Backend compiles this Schedule as a Qiskit Backend Object and generates ASM language program to be run on the AWG using language to language parser. Generated ASM program is executed on micro-processor. The DAC and ADC are loop-backed.

Fig.8 shows the generated frequency of 7.3GHz as seen on Spectrum Analyzer. The tproc reads the ADC measurement channel and this data is displayed as Qiskit Result.

Conclusion

Qiskit Backend is successfully developed for AWG. The Backend integrates the Qiskit stack with the analog RF pulse generation. Python program generating a Qiskit pulse schedule of a single frequency loopback testing is successfully demonstrated on the backend. Future work involves integration of Qiskit experiment library with Backend. The AWG Backend for Qiskit software stack can be installed at intranet facility so that users across organization can avail this facility for quantum experiment.

Acknowledgments

We sincerely appreciate QuMaC Lab, TIFR, for their critical role in advancing this research. Their exceptional support and expertise have significantly contributed to the outcomes of this study.

References

[1] Frederic T. Chong, Diana Franklin & Margaret Martonosi, “Programming languages and compiler design for realistic quantum hardware”, Nature 549, 180–187 (2017). https://doi.org/10.1038/nature23459

[2] Andrew W. Cross, Lev S. Bishop, John A. Smolin, Jay M. Gambetta, “Open Quantum Assembly Language”, arXiv:1707.03429v2[quant-ph], 13 Jul 2017

[3] Gadi Aleksandrowicz, et al. “Qiskit: An Open-source Framework for Quantum Computing. 0.7.2” , Zenodo, 23 Jan. 2019, doi:10.5281/zenodo.2562111.

[4] Cirq Developers, “Cirq”. Zenodo, Dec. 01, 2023. doi: 10.5281/zenodo.10247207.

[5] A. S. Tolba, M. Z. Rashad, and Mohammed A. El-Dosuky. 2013 “Q#, a quantum computation package for the .NET platform”. arXiv preprint arXiv:1302.5133

[6] Peter J. Karalekas, et al. “Pyquil: Quantum Programming in Python. v2.17.0 ”, Zenodo, 30 Jan. 2020, doi:10.5281/zenodo.3631770.

[7] “D-Wave's Ocean Software,” http://ocean.dwavesys.com (2020)

[8] IBM Quantum Documentation, API Reference, Providers Interface, https://docs.quantum.ibm.com/api/qiskit/qiskit.providers.Backend.

Championing Health Equity

Insights from renowned former WHO Chief Scientist Dr. Soumya Swaminathan

In a recent talk at Trombay Colloquium, her maiden visit to Bhabha Atomic Research Centre, prominent pediatrician and tuberculosis (TB) and HIV researcher, Dr. Soumya Swaminathan, who served as the chief scientist at the World Health Organization (WHO), delivered an inspiring message about the critical role of countries like India in combating Tuberculosis and emerging global pandemics. Drawing from her frontline experience during the severe global COVID-19 pandemic, she emphasized the importance of innovative approaches in public health in her talk titled 'My Journey as a Physician Scientist and Researcher'.

1 A Call for Vaccine Leadership...

Dr. Soumya Swaminathan urged India to take a leadership role in developing new vaccines, highlighting the country's potential to leverage its scientific resources and expertise. She stressed that innovative vaccine development is essential not only for TB but for addressing broader public health challenges, especially in the context of lessons learned from the COVID-19 pandemic.

2 Strengthening Primary Health Centres...

A key component of her talk focused on the need to bolster the infrastructure of Primary Health Centres (PHCs). She strongly professed that enhancing these facilities is vital for effective disease management and prevention, particularly in rural and underserved areas. Improved PHC infrastructure would ensure better healthcare delivery, including enhanced surveillance and treatment of communicable diseases.

3 The Importance of Science Communication...

Dr. Soumya Swaminathan also addressed the necessity for scientists to develop strong communication networks. By becoming effective communicators, scientists can make their research more accessible to the public and policymakers, fostering greater science literacy. This, she asserted, is crucial for generating support for drug discovery, research and public health initiatives, particularly in the wake of the pandemic.

Dr. Soumya Swaminathan

4 Mentorship and Gender Balance...

During the Q&A session, Dr. Soumya Swaminathan reflected on her journey, acknowledging the mentors who guided her throughout her career. She emphasized the significant role mentorship plays in shaping future scientists, particularly for women in the field. Addressing gender imbalance in advanced scientific research, she called for more initiatives to support women scientists and ensure diverse representation in research roles.

5 Community Outreach at MSSRF...

When asked about outreach activities at the social foundation, the M.S. Swaminathan Research Foundation (MSSRF), she elaborated on the "Every Child is a Scientist" program. Tailored for students from government schools in underprivileged communities, this initiative, she said aims to spark scientific curiosity and provide hands-on learning experiences. By empowering these students, the program seeks to inspire the next generation of scientists, regardless of their socio-economic background.

Finally, the talk served as a powerful reminder of the multifaceted approach required to tackle tuberculosis and other public health challenges. By advocating for vaccine innovation, strengthening healthcare systems, enhancing science communication, and promoting diversity in research, the speaker outlined a hopeful vision for the future. Her insights resonate as a call to action for scientists, educators, and policymakers to collaborate in the pursuit of a healthier world.

Photo Courtesy @PIB Govt.of India.

Leading researchers from the ranks of Department of Atomic Energy (DAE) received top honors from the Government of India at the inaugural edition of national science awards (Rashtriya Vigyan Puraskar) in recognition of their outstanding work that contributed to the growth of science, technology and innovation in the country.

Dr. Avesh Kumar Tyagi (Distinguished Scientist & Former Director, Chemistry Group, Bhabha Atomic Research Centre, Mumbai), Professor Naba Kumar Mondal (INSA Senior Scientist, Saha Institute of Nuclear Physics, Kolkata) received Vigyan Shri awards in recognition of their outstanding work in the fields of Atomic Energy and Physics. Professor Vivek Polshettiwar (Professor (H), Division of Chemical Sciences, TIFR, Mumbai) secured Vigyan Yuva-Shanti Swarup Bhatnagar Award given for researchers under 45.

In the inaugural edition of the Rashtriya Vigyan Puraskar (RVP) 2024, 33 awards were presented to distinguished scientists from across the country in four different categories - Vigyan Ratna, Vigyan Shri, Vigyan Yuva, and Vigyan Team. The President of India, Smt. Droupadi Murmu, presented the Rashtriya Vigyan Puraskar-2024 awards at a ceremony held at Gantantra Mandap, Rashtrapati Bhavan on August 22, 2024.

The primary objective of the RVP is to recognize and celebrate the outstanding work of individuals and teams in various fields of science, technology, and innovation. This prestigious award is open to scientists, technologists, and innovators working in government and private sectors, as well as independent researchers and Indian-origin professionals abroad. The award seeks to acknowledge those who have made exceptional contributions in their respective fields, particularly those whose work has a significant impact on Indian society and the global scientific community, stated Government of India in a release.

The awards cover a wide range of scientific fields, including Physics, Chemistry, Biological Sciences, Mathematics & Computer Science, Earth Science, Medicine, Engineering Sciences, Agricultural Science, Environmental Science, Technology & Innovation, Atomic Energy, and Space Science and Technology. The nominations will be invited from January 14 to February 28 every year.

Captions to pictures in this page

1. Group Photograph of Rashtriya Vigyan Puraskar-2024 awardees.
2. President of India handing over the award to Dr. Avesh Kumar Tyagi.
3. Professor Naba Kumar Mondal receiving the award from the President of India.
4. President of India handing over the award to Professor Vivek Polshettiwar.

Dr. V. K. Iya
Champion of Radioisotope Program in India

Dr. V.K. Iya with Dr. Hemchandra Gupte (centre), Mayor of Bombay (now Mumbai) during his visit to BARC on September 2, 1971. Photo courtesy SIRD Archives.

Dr. Vasudeva Kilara Iya, an eminent Indian nuclear scientist and key figure in the country's radioisotope and radiation technology program, passed away on August 10, 2024, at age 96. His pioneering contributions have significantly shaped nuclear science in India.

Born on September 16, 1927, in Vadodara, Gujarat, Dr. Iya excelled academically, graduating in Chemistry from the University of Pune and earning a gold medal for his M.Sc. at Central College, Bangalore. He pursued his doctorate at Sorbonne University, completing his D.Sc. under Felix Trombe. In 1955, Dr. Iya was recruited by Dr. Homi J. Bhabha for the Indian Atomic Energy Programme, gaining experience at the French Nuclear Laboratories at Saclay. Returning to India in 1957, he joined the Atomic Energy Establishment, Trombay (AEET), now known as Bhabha Atomic Research Centre (BARC).

Dr. Iya took over the radioisotope program in AEET after C.B.G. Taylor's departure and led the Isotope Division by 1963. He was appointed Director of the Isotope Group in 1974, overseeing significant advancements in radioisotopes, radiopharmaceuticals, and radiation processing technologies. He played a crucial role in the work on preparing isotopes for India's first peaceful nuclear explosion in 1974, popularly known as " Operation Smiling Buddha". Beyond BARC, Dr. Iya established the Board of Radiation and Isotope Technology (BRIT) in 1987 and chaired the Experts Committee for the Performance Related Incentive Scheme for DAE units. He represented India in the Regional Cooperation Agreement for Nuclear Science and Technology in Asia and the Pacific since its inception in 1972. As an educator, Dr. Iya mentored many who became leaders in nuclear science. He was the Founder President of the National Association for Applications of Radioisotopes and Radiation in Industry and served as President of the Association of Medical Physicists of India from 1985 to 1987.

Dr. Iya received numerous accolades, including the DAE Homi Bhabha Lifetime Achievement Award in 2009 and the NAARRI Lifetime Achievement Award in 1995. His legacy as the "Pitamahah of Isotopes," aptly described by Dr. Anil Kakodkar (Former Chairman, AEC) in the book *The Renaissance Man*, authored by his daughters Vidya and Rekha published in 2010, is a testament to his profound impact on the field and his inspiring journey. Dr. Iya held significant positions at institutions such as Tata Memorial Hospital and the Bangalore Cancer Hospital, contributing to advancements in nuclear medicine. Dr. Iya is survived by his family, colleagues, and many inspired by his contributions to science. His passing marks the end of an era in nuclear science, but his legacy will continue to inspire future generations.

(Compilation by Shri Madhav N., of Public Awareness and Foreign Languages Section, SIRD, BARC).

Industry

BARC's Nuclear

By TT&CD and SIRD Editorial Team

The spinoff technologies developed through nuclear energy research and development at BARC are regularly transferred to industry for commercialization. BARC provides comprehensive support to licensees by offering technology training, field demonstrations, consultancy, and detailed documentation that includes procedures, flowcharts, diagrams, troubleshooting guides, and lists of raw materials, equipment, and suppliers. During the period from July to August 2024, BARC transferred eight technologies to various industries.

Technology Transfers

BARC has transferred the technology of Bio sensor Kit (BioKit) for detecting organophosphate and organocarbamate pesticides, which was transferred to M/s. Duke Thomson's India Pvt. Ltd. in Indore. BARC has also transferred the technology of Teletherapy Source Transportation Flask to M/s. Panacea Medical Technologies Pvt. Ltd. in Karnataka.

Technology Overview: Organophosphate and organocarbamate pesticides are commonly used in agriculture and domestic applications, often contaminating soil, water, and food commodities (such as vegetables, fruits, and spices). A simple visual detection method for these pesticides in food samples would greatly benefit farmers, traders, and consumers. BARC has developed a colorimetric visual biosensor kit capable of detecting safe levels of organophosphate (including Methyl parathion, Parathion, Monocrotophos, Chlorpyrifos, Phorate, Profenfos, Quinalphos, and Dichlorvos) and organocarbamate pesticides (including Aldicarb, Carbaryl, Carbofuran, and Carbosulfan).

Technology Overview: A qualified source transportation cask is essential for shipping Cobalt-60 teletherapy source capsules between the manufacturer and the teletherapy unit (usually a cancer hospital). To protect people and the environment from harmful radiation, this package must meet stringent safety requirements for both normal and accident transport conditions, in accordance with national and IAEA safety guidelines. As part of the Indigenous Teletherapy Programme, BARC has developed a Cobalt-60 Teletherapy Source Transportation Flask, which has been approved by the AERB as Type B(U).

Other key technologies transferred to industry include

Technology for Assessing Bioavailability of Nutrients in Soil (Code AB54NABTD): Transferred to M/s. W.S. Telematics Pvt. Ltd., New Delhi, using a universal multi-nutrient soil extractant.

Rapid Composting Technology (Code AB25NABTD): For decomposing dry leaves, kitchen waste, and temple waste, transferred to M/s. Swayambhar Producer Company Ltd., Birbhum, West Bengal.

Indigenous Cold Atmospheric Pressure Plasma System - 10 MHz (ICAPPS-10) (Code EG46L&PTD): Transferred to M/s. IEEC Power Electronics Pvt. Ltd., Mumbai.

Low Carbon Ferro Alloys (Code CH21MP&CED): Transferred to M/s. Synergy Steels Ltd., New Delhi.

Compact Helical Biodegradable Waste Converter SHESHA [Code EV07NABTD]: Transferred to M/s. Eshika Engineering, Palghar, Maharashtra.

NISARGRUNA Biogas Plant for Processing Biodegradable Waste [Code EV01NABTD]: Technology transferred to M/s. Hariom Electricals, Navi Mumbai, Maharashtra.

Startup Incubation

The Atal Incubation Centre (AIC) at BARC successfully launched its first 6-week pre-incubation program for aspiring entrepreneurs from May 30 to July 4, 2024, conducted entirely online. The program welcomed twelve participants and aimed to equip them with the principles of idea validation prior to launching their

beckons

Spin-off technologies

Signing of Incubation Extension Agreement with M/s. Pratishna Engineer for BARC's Alkaline Water Electrolyzer technology.

startups. Sessions were designed to provide a framework for making informed decisions about the viability of their products, businesses, or services.

Throughout the program, teams concentrated on developing initial proposals based on their submitted technical ideas. They collaborated to build teams, create product requirement documents, and conduct customer discovery research. The program culminated in a pitching session on August 9, 2024, where teams presented their proposals to a jury panel from BARC. The best-pitched team received a cash prize of Rs.5,000, while all participating teams were awarded digital certificates of appreciation.

From June to August 2024, several agreements were established under the AIC-BARC arrangement to support startup business incubation and collaborative activities:

Startup Business Incubation Agreement: This was signed for two BARC technologies—NISARGRUNA and SHESHA .

In-house Technology Incubation Agreement: An agreement was made for the Nisarguna Biogas Plant with M/s. Gir Gau Jatan Sansthan in Rajkot, Gujarat, as well as with ONGC Energy Centre in Delhi for a process system designed to clean up dissolved oil and salt-contaminated wastewater for beneficial utilization.

Collaborative Technology Incubation: This involved the Nisarguna Biogas Plant technology in partnership with the Department of Chemistry at Raipur Institute of Technology, Raipur.

Extension of Incubation Agreements: Continued support was provided for Alkaline Water Electrolyzer technology with M/s. Pratishna Engineers, and X-band LINAC technology with M/s. Panacea Medical Technologies Pvt. Ltd. in Karnataka.

Extension of incubation agreement with M/s. Panacea for BARC's X band LINAC technology.

The signing of agreement for transfer of Teletherapy Source Transportation Flask technology in presence of (Right to left): Shri Daniel Babu P., Head, TT&CD, BARC; Dr. S. Adhikari, Director, KMG, BARC; Mr. Animesh, Senior Vice President, M/s. Panacea Medical Technologies; Dr. D. C. Kar, Head, DRHR, BARC and Shri Chandan Dey, Scientific Officer, DRHR, BARC.

Project Phoenix completes Six Decades: Dr. Homi J. Bhabha addressing the dignitaries present at the program for the dedication of Trombay Fuel Reprocessing Facility to the nation. Prime Minister Shri Lal Bahadur Shastri dedicated the facility to the nation in 1965. The decision to construct the plant was proposed by Atomic Energy Commission headed by Dr. Bhabha in 1958 as part of 'Project Phoenix', and the maiden Reprocessing facility was commissioned in Trombay in 1964. The Diamond Jubilee of this prestigious facility was celebrated by organizing a special program under the auspices of the Nuclear Recycle Group, BARC, on August 17, 2024.

Edited & Published by

Scientific Information Resource Division

Bhabha Atomic Research Centre, Trombay, Mumbai-400 085, India

BARC Newsletter is also available at URL:https://www.barc.gov.in